

### 342 Ocular angiography and oxymetry

Tuesday, May 05, 2015 11:00 AM–12:45 PM

Exhibit Hall Poster Session

**Program #/Board # Range:** 3306–3365/B0089–B0148

**Organizing Section:** Multidisciplinary Ophthalmic Imaging Group

**Contributing Section(s):** Clinical/Epidemiologic Research, Physiology/Pharmacology, Retinal Cell Biology, Retina

**Program Number:** 3306 **Poster Board Number:** B0089

**Presentation Time:** 11:00 AM–12:45 PM

#### Can OCT be accurate in quantifying retinal oxygen metabolism?

Hao F. Zhang, Ji Yi, Siyu Chen, wenzhong Liu. Biomedical Engineering, Northwestern University, Evanston, IL.

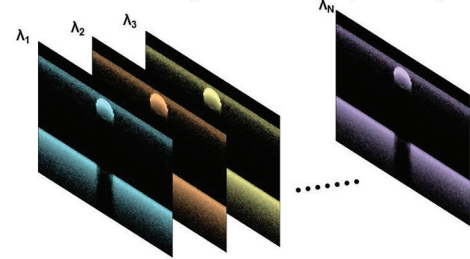
**Purpose:** To explore whether OCT can be a potential candidate for accurate measurement of retinal oxygen metabolism towards early diagnosis of ischemic retinal diseases.

**Methods:** We first used statistical methods to numerically simulate photon transport in the retina to mimic OCT working under different spectral ranges. Then we analyze accuracy of OCT oximetry subject to parameter variations such as vessel size, pigmentation, and oxygenation. We then developed an experimental OCT system based on the spectral range identified by our simulation work. We applied the newly developed OCT to measure both retinal hemoglobin oxygen saturation ( $sO_2$ ) and retinal retinal flow. To measure blood flow, we performed double-circular-trajectory scans around the optic disk to obtain the absolute blood velocity. After obtaining the retinal  $sO_2$  and blood velocity, we further measured retinal vessel diameter and calculated the retinal oxygen metabolism rate ( $MRO_2$ ). To test the capability of our OCT, we imaged wild-type Long-Evans rats ventilated with both normal air and air mixtures with various oxygen concentrations.

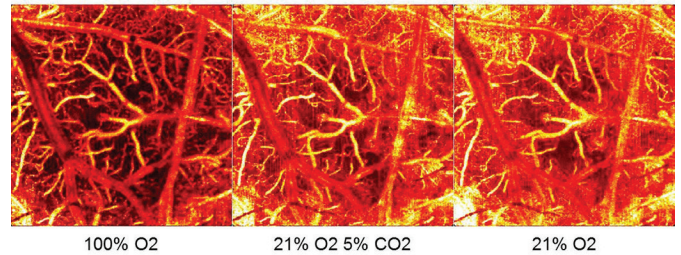
**Results:** Our simulation suggested that OCT working within visible spectral range is able to provide accurate measurement of retinal  $MRO_2$  using inverse Fourier spectral reconstruction. We refer our newly developed OCT as vis-OCT, and showed that vis-OCT was able to measure the  $sO_2$  value in every single major retinal vessel around the optical disk as well as in micro retinal vessels as shown in Figure 1. When breathing normal air, the averaged  $sO_2$  in arterial and venous blood in Long-Evans rats was measured to be 95% and 72%, respectively. When we challenge rats using air mixtures with different oxygen concentrations, vis-OCT measurement follows analytical models of retinal oxygen diffusion and pulse oximeter well.

**Conclusions:** Vis-OCT is a sensitive tool to measure retinal  $MRO_2$  with a high repeatability. It opens up a new window to investigate several significant blinding diseases, such as diabetic retinopathy and glaucoma, which strongly associate with retinal oxygen metabolic disorders.

Simulated OCT images under different spectral ranges



Microvascular system imaged by vis-OCT under oxygen challenge



**Commercial Relationships:** Hao F. Zhang, Opticent Health (I); Ji Yi, None; Siyu Chen, None; wenzhong Liu, None

**Support:** NIH 1R01EY019951, 1R24EY022883, and NSF CBET-1055379

**Program Number:** 3307 **Poster Board Number:** B0090

**Presentation Time:** 11:00 AM–12:45 PM

#### Error analysis of two-wavelength algorithms for retinal oximetry

J.C. Ramella-Roman<sup>1,2</sup>, Daniel Rodriguez<sup>2</sup>, Quanzeng Wang<sup>3</sup>, Joshua Pfefer<sup>3</sup>. <sup>1</sup>BME and Herbert Wertheim College of Medi, Florida International University, Miami, FL; <sup>2</sup>Biomedical Engineering Department, Florida International University, Miami, FL; <sup>3</sup>Center for Devices & Radiological Health, Food and Drug Administration, Silver Spring, MD.

**Purpose:** A new imaging technique for the assessment of retinal vascular oximetry has been introduced recently. The technique utilizes two-wavelength illumination of the fundus for the estimation of oxygen saturation in the retina. Utilizing a well-calibrated, three-dimensional stochastic model of light transport, we have examined the error associated with the two-wavelength technique (570 nm, 600 nm). We analyzed the error produced when the analyzing algorithm calibration assumptions are incorrect, vessel diameter varies, choroidal melanin concentration varies, and when there is vascular crosstalk from the choroid.

**Methods:** The voxel-based Monte Carlo code used is capable of handling heterogeneous tissue structures, such as a vessel embedded in a stratified medium with different optical properties. A simplified tissue geometry comprised of four layers was used: retina, RPE, choroid, and sclera. A vessel embedded within the retina was also implemented. Two hundred million photons were launched in each simulation. Photons back-reflected by the layers were used to create images of fundus vasculature and then analyzed using the standard two wavelength algorithm approach. This included the calibration mechanism where a representative artery and a vein were selected and their values were fixed to 96% and 54% respectively.

**Results:** Under ideal conditions, two-wavelength retinal oximetry estimates compare well with true oxygen saturation levels of the vessel of interest. When the assumed values of calibrating arteries or veins do not correspond to true values, errors as high as 20% in veins and 10% in arteries may occur. When vessel size is increased, the optical density ratio (ODR) decreases and the assessed oxygen

saturation error can be as high as 15% of its true value. Similar trends were found when analyzing the effect of melanin in the choroid and choroidal vessel crosstalk.

**Conclusions:** Two-wavelength retinal oximetry is a popular technique because of its simplicity, however, it may be prone to significant error. An advanced light-tissue interaction modeling approach was effective in quantifying and elucidating key sources of error. Although some have attempted to correct oxygen saturation measurements for differences in pigmentation or vessel size, there are still many confounding variables that may degrade accuracy; this may lead to misdiagnosis of a range of retinal pathologies.

**Commercial Relationships:** J. C. Ramella-Roman, None; Daniel Rodriguez, None; Quanzeng Wang, None; Joshua Pfefer, None

**Program Number:** 3308 **Poster Board Number:** B0091

**Presentation Time:** 11:00 AM–12:45 PM

**Dynamically measuring retinal oxygen saturation at microvascular level using visible-light OCT angiograph**

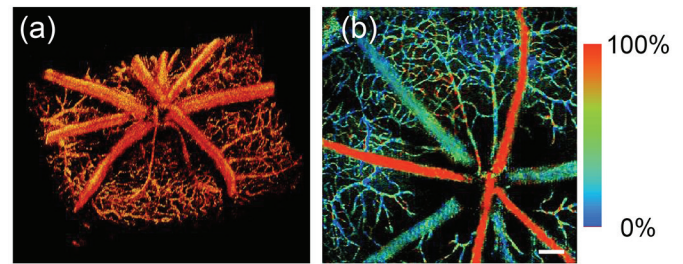
Siyu Chen<sup>1</sup>, Ji Yi<sup>1</sup>, Hao F. Zhang<sup>1,2</sup>. <sup>1</sup>Department of Biomedical Engineering, Northwestern University, Evanston, IL; <sup>2</sup>Department of Ophthalmology, Northwestern University, Chicago, IL.

**Purpose:** Although hemoglobin oxygen saturation ( $sO_2$ ) is a vital physiological indicator for the functionality of retina tissues, accurate measurement of ocular microvasculature  $sO_2$  remains challenging. Here we propose to use optical coherence tomography based angiography working within visible-light spectral range (Vis-OCT) to measure absolute retina  $sO_2$ .

**Methods:** We developed a Vis-OCT system working from 520 nm to 630 nm to image rodent retina *in vivo*. Long Evans rats were anesthetized using Ketamine/Xylazine cocktail. Once the animal stabilized, it was ventilated normal air (21%  $O_2$ ) and a reference image was taken. Then we supplied the following inhalation gas mixtures in random order: (1) pure oxygen; (2) carbon dioxide oxygen mixture (21%  $O_2$ , 5%  $CO_2$ ); and (3) low oxygen air (10%  $O_2$ ). For each inhalation gas, the animal was allowed to stabilize for 3 minutes, and normal air was supplied for at least 3 minutes between changes. We took one additional measurement after the sequence with normal air ventilation. During the experiment, a pulse oximeter was attached to the hind limb to monitor the peripheral capillary oxygen saturation ( $spO_2$ ). The acquired OCT images were processed using phase-sensitive decorrelation algorithm. A series of short time Fourier transform allowed the extraction of the  $sO_2$  encoded spectral information. We calculated the first derivative of the wavelength-dependent angiography intensity ( $A'$ ) around 574 nm. The value was then calibrated into absolute  $sO_2$  percentage using  $spO_2$  readings.

**Results:** A linear regression showed strong positive correlation between  $A'$  and  $spO_2$  readings ( $R^2 = 0.98$ ). When inhaling normal air, the  $sO_2$  was  $80.6 \pm 7.4\%$  for arteries and  $65.2 \pm 4.9\%$  for veins ( $n = 8$ ). During inhalation of gas 1 and 2, both artery and veins showed significant increase in  $sO_2$  (A:  $p < 0.05$ ; V:  $p < 0.01$ ). The increase was more dramatic in veins and when gas 1 was inhaled. We also observed a significant decrease in  $sO_2$  when gas 3 was supplied ( $p < 0.01$ ). When normal air was supplied again,  $sO_2$  return to its original value for both arteries ( $p = 0.65$ ) and veins ( $p = 0.10$ ).

**Conclusions:** Our results demonstrated that Vis-OCT angiography can accurately measure retinal  $sO_2$  and its variations, which can be invaluable for the early diagnosis of several retinal metabolic diseases.



a) Three dimensional view of retina angiography. b) *En face* view of  $sO_2$  mapping. Scale: 200  $\mu m$ .

**Commercial Relationships:** Siyu Chen, None; Ji Yi, None; Hao F. Zhang, None

**Support:** NIH Grant 1R01EY019951, NIH Grant 1R24EY022883, NSF Grant CBET-1055379, NSF Grant CBET-1066776, NSF Grant DBI-1353952

**Program Number:** 3309 **Poster Board Number:** B0092

**Presentation Time:** 11:00 AM–12:45 PM

**Fluorescein Angiography and Retinal Vessel Oxygen Saturation in Patients with Proliferative Diabetic Retinopathy**

Nicole K. Sripsema, Chavakij Bhoombunchoo, Paul Whitten, Robert Masini, Richard B. Rosen. Ophthalmology, The New York Eye and Ear Infirmary of Mount Sinai, New York, NY.

**Purpose:** To determine oxygen saturation differences between areas of active versus inactive Proliferative Diabetic Retinopathy (PDR) using the Oxymap Retinal Oximeter.

**Methods:** Following a previous study which demonstrated increased oxygen saturation in retinal vessels proportional to the severity of Diabetic Retinopathy<sup>1</sup>, a retrospective review of diabetic patients with PDR was performed. Patients imaged using both fluorescein angiography (FA, Topcon, USA) and Oxymap T1 (Reykjavik, Iceland) were included. Relative oxygen saturation of retinal vessels was analyzed with the Oxymap. Retinal vessels associated with areas of neovascularization on FA were compared to areas of inactive disease. Paired t-tests were used to compare oxygen saturations.

**Results:** 48 eyes of 29 patients were included. 10 eyes were excluded due to inadequate image quality. Mean age was  $53.83 \pm 9.11$  yrs. 62% were female, 38% male. 44% were Hispanic, 26% African American, 11% Asian, 10% Caucasian, and 9% Other. Mean duration of diabetes (DM) was  $19.85 \pm 8.83$  yrs. Mean hemoglobin A1c was  $9.47 \pm 3.81\%$ . A majority of patients were initially diagnosed with Type II DM (82.8%), now requiring both insulin and oral hypoglycemics for glycemic control (84.6%). Mean relative arterial oxygen saturation was higher in vessels associated with neovascularization when compared to vessels in regions with no active disease ( $107.93 \pm 13.85\%$ ,  $104.87 \pm 14.25\%$ ,  $p = 0.14$ ). Mean relative venous oxygen saturation was significantly lower in vessels associated with neovascularization when compared to vessels in regions with no active disease ( $66.05 \pm 11.87\%$ ,  $69.57 \pm 9.19\%$ ,  $p = 0.02$ ).

**Conclusions:** These results suggest oxygen saturation in retinal vessels associated with neovascularization varies from areas of inactive disease. Our findings of higher arterial oxygen saturation are consistent with a previous study that reported increased oxygen saturation proportional to the severity of retinopathy. The lower venous oxygen saturation in vessels associated with neovascularization could be related increased leakage in areas of angiogenesis. Initial data suggests the Oxymap could serve as a clinically useful non-invasive imaging method for monitoring disease progression. Further studies are needed to unravel the correlation between Oxymap results and FA findings.

**Reference:**

1. Jørgensen CM et al. Acta Ophthalmol. 2014 Feb;92(1):34-9.

**Commercial Relationships:** Nicole K. Scripsema, None; Chavakij Bhoomibunchoo, None; Paul Whitten, None; Robert Masini, None; Richard B. Rosen, Advanced Cellulat Technologies (C), Allergan (C), Carl Zeiss Meditech (C), Clarity (C), OD-OS (C), Opticology (I), Optovue (C)

**Support:** The Bendheim-Lowenstein Retina Center Fund of the New York Eye and Ear Infirmary

**Program Number:** 3310 **Poster Board Number:** B0093

**Presentation Time:** 11:00 AM–12:45 PM

**Oxygen Metabolism of the Inner Retina in the 50/10 Rat Model of Retinopathy of Prematurity**

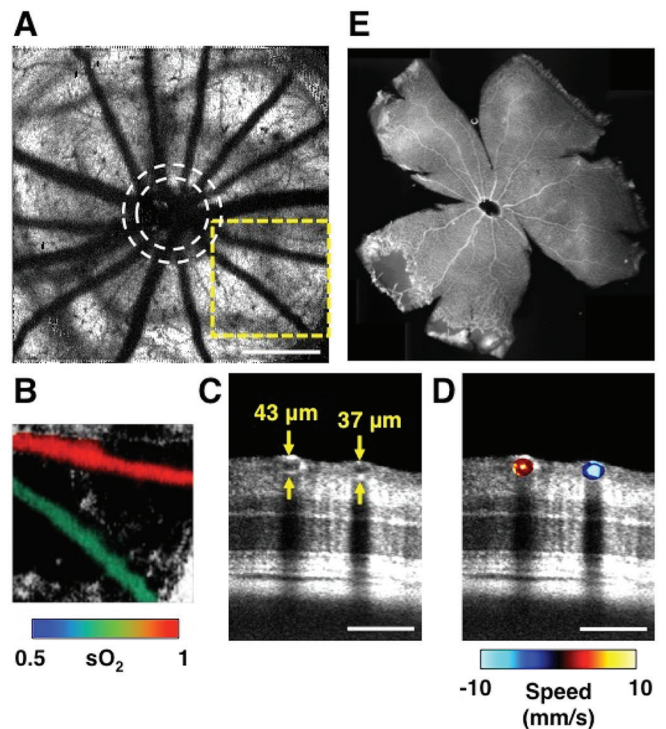
Brian Soetikno<sup>1,2</sup>, Ji Yi<sup>2</sup>, Patryk Purta<sup>1</sup>, wenzhong Liu<sup>2</sup>, Ronil S. Shah<sup>1</sup>, Hao F. Zhang<sup>2</sup>, Amani A. Fawzi<sup>1</sup>. <sup>1</sup>Department of Ophthalmology, Northwestern University Feinberg School of Medicine, Chicago, IL; <sup>2</sup>Department of Biomedical Engineering, Northwestern University, Functional Optical Imaging Laboratory, Evanston, IL.

**Purpose:** To compare the inner retinal metabolic rate of oxygen (rMRO<sub>2</sub>) in normal rats and rats with 50/10 oxygen-induced retinopathy (OIR) using visible-light optical coherence tomography (vis-OCT) at P18.

**Methods:** Beginning at birth, four Sprague-Dawley rat pups were exposed to alternating hyperoxia (50% O<sub>2</sub>) and hypoxia (10% O<sub>2</sub>) every 24 hours for 14 days (OIR group), while six rat pups were allowed to grow at room air (control group). On P14, the OIR pups were returned to room air. On P18, imaging was performed to measure the oxygen saturation of hemoglobin (sO<sub>2</sub>) of the inner retinal arterioles and venules for both control and OIR groups [A, B]. These experiments used a vis-OCT system, which incorporated a supercontinuum source with wavelengths from 500 nm to 620 nm. A dual-circle scanning protocol implemented on the same OCT system enabled the measurement of vessel diameter, blood velocity, and volumetric blood flow [C, D]. Using the sO<sub>2</sub> measurements, we calculated the oxygen extraction fraction (OEF) of the inner retina. Combining the OEF with the total blood flow permitted the calculation of the rMRO<sub>2</sub>. Following the imaging experiments on P18, the retinas were harvested, immunostained with Alexa Fluor 594 isolectin, and imaged using fluorescence microscopy [E]. We quantified the percentage of vaso-obliteration and counted the number of clock-hours with neovascularization in the OIR retinas. An unpaired Student's t-test was used to compare the measurements between control and OIR groups.

**Results:** There was no significant difference in the OEF between the control and OIR groups (0.231 ± 0.037 vs. 0.262 ± 0.054; p=0.3550). The average total estimated blood flow was significantly lower in OIR versus control groups (2.74 ± 0.58 μl/min vs. 7.37 ± 2.96 μl/min; p=0.003). Additionally, rMRO<sub>2</sub> was significantly decreased in OIR versus control groups (128 ± 32 nl min<sup>-1</sup> vs. 338 ± 138 nl min<sup>-1</sup>; p = 0.0108). For the OIR group, the average vasoobliteration was 10.92 ± 3.50% and the average number of clock hours with neovascularization was 4.25 ± 2.25 clock hours.

**Conclusions:** We observed a 59% reduction in the rMRO<sub>2</sub> in the OIR group as compared with that of control group, suggesting that the metabolism of the inner retina is markedly reduced at P18 in the 50/10 OIR rat model.



**Commercial Relationships:** Brian Soetikno, None; Ji Yi, None; Patryk Purta, None; wenzhong Liu, None; Ronil S. Shah, None; Hao F. Zhang, None; Amani A. Fawzi, None  
**Support:** R01EY019951 (AAF, HFZ) and R21HD077336 (AAF), Research to Prevent Blindness, NY (Department of Ophthalmology, Northwestern University)

**Program Number:** 3311 **Poster Board Number:** B0094

**Presentation Time:** 11:00 AM–12:45 PM

**Oxygen saturation profiles in Asian Indian eyes with central retinal artery occlusion (CRAO)**

Ashwin Mohan<sup>1</sup>, Priya Srinivasan<sup>1</sup>, Supriya Dabir<sup>1</sup>, Rajani Battu<sup>1</sup>, Naresh K. Yadav<sup>1</sup>, Rohit Shetty<sup>2</sup>. <sup>1</sup>Retina, Narayana Nethralaya, Bangalore, India; <sup>2</sup>Vice-Chairman, Narayana Nethralaya, Bangalore, India.

**Purpose:** To study the oxygen saturation profiles in Asian Indian eyes with central retinal artery occlusion (CRAO)

**Methods:** This is a retrospective review of 10 patients presenting to our hospital in the last 6 months with a history of sudden painless loss of vision and diagnosed as CRAO on clinical examination. In addition to a comprehensive ophthalmic examination, they underwent retinal oximetry (Oxymap T1, Oxymap hf, Reykjavik, Iceland). 2 patients had oximetry pre and post anterior chamber paracentesis and 3 patients had a follow up Oximetry at monthly intervals. Optic disc centered images taken after dilatation were analysed by selecting the thickest arteriole and venule per quadrant for saturation and diameter.

**Results:** The oxygen saturation was decreased in both the arterioles (86%) and venules (50%). The arteriolar and venous diameters and the arterio-venous saturation difference did not vary significantly between the groups. In the 3 patients on follow up we saw an improvement of arteriolar saturations in all and venous values in 2 of them. Two patients who underwent anterior chamber paracentesis showed an improvement of both arteriolar and venous saturation values after paracentesis.

**Conclusions:** Oximetry in CRAO shows an initial fall in saturations with an increase over time or after paracentesis.

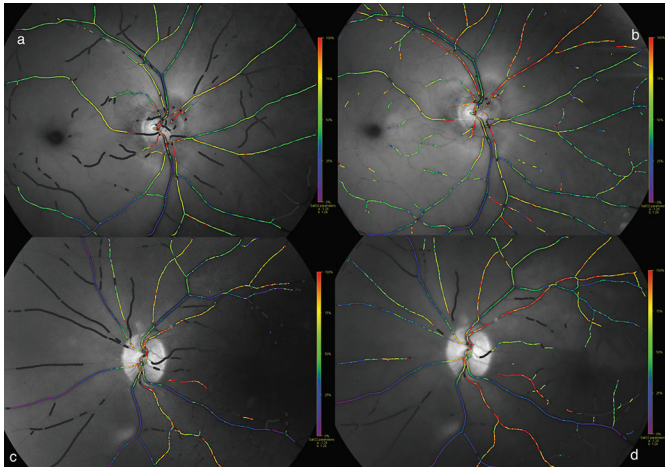


Figure a & b of Patient 1 and c & d of Patient 2 at presentation and immediately after paracentesis respectively

**Commercial Relationships:** Ashwin Mohan, None; Priya Srinivasan, None; Supriya Dabir, None; Rajani Battu, None; Naresh K. Yadav, None; Rohit Shetty, None

**Program Number:** 3312 **Poster Board Number:** B0095

**Presentation Time:** 11:00 AM–12:45 PM

**Retinal oximetry as a novel parameter in the non-invasive assessment of cerebral oxygenation**

Karel Van Keer<sup>1</sup>, Cathy De Deyne<sup>2,3</sup>, Cornelia Genbrugge<sup>2,3</sup>, Luis Pinto<sup>4</sup>, Evelien Vandewalle<sup>1</sup>, Ingeborg Stalmans<sup>1,5</sup>. <sup>1</sup>Department of Ophthalmology, University Hospitals Leuven, Leuven, Belgium; <sup>2</sup>Department of Anesthesiology, Intensive Care, Emergency Medicine and Pain Therapy, Ziekenhuis Oost-Limburg ZOL, Genk, Belgium; <sup>3</sup>Faculty of Medicine and Life Sciences, Biomedical Research Institute, Hasselt University, Diepenbeek, Belgium; <sup>4</sup>Department of Ophthalmology, Faculty of Medicine of Lisbon, Lisbon, Portugal; <sup>5</sup>Department of Ophthalmology Neurosciences, Laboratory of Ophthalmology, KU Leuven, Leuven, Belgium.

**Purpose:** To investigate the relation between retinal and cerebral oximetry, as measured by non-invasive spectroscopy and to establish the relative partition of arterial and venous retinal oxygen saturation to the measured cerebral oxygen saturation.

**Methods:** In this observational, cross-sectional study we performed peripheral, retinal and cerebral oxygen saturation measurements in healthy volunteers during steady state conditions. Peripheral oxygen saturation was measured on the left index finger by pulse oximetry (Ohmeda TruSat Pulse Oximeter, GE Healthcare, Finland). Arterial and venous retinal oxygen saturation and vessel diameter were measured in the left eye using a noninvasive spectrophotometric retinal oximeter (Oxymap T1, Oxymap ehf., Reykjavik, Iceland). Cerebral oxygen saturation was measured over the left cerebral cortex using cerebral near-infrared spectroscopy (NIRS) (FORE-SIGHT technology, CAS Medical Systems, Branford, CT). Correlations between the parameters were assessed using Pearson correlation coefficients. The relative arterial and venous partition was determined.

**Results:** 21 young healthy individuals aged 26.4±2.2 years were analyzed. Cerebral oxygen saturation values showed a significant positive correlation with both arterial and venous retinal vessel oxygen saturation values ( $r = 0.442$ ,  $P=0.045$  and  $r = 0.434$   $P=0.049$  respectively) and a significant negative correlation with retinal

venous diameter (Pearson correlation coefficient = -0.513,  $P=0.017$ ). The relative partition of arterial and venous retinal oxygen saturation to the cerebral oxygen saturation value was 31.5% and 68.5% respectively.

Peripheral oxygen saturation was correlated neither with cerebral nor with retinal oxygen saturation.

**Conclusions:** This is the first study to show a correlation between retinal and cerebral oximetry, as measured by non-invasive spectroscopy.

The observed relative partition of arterial and venous retinal oxygen saturation is very close to the established calibration of FORE-SIGHT NIRS technology to a weighted average of 30% arterial and 70% venous contribution. Therefore, our first findings support a promising role for retinal oximetry as a non-invasive reliable tool in evaluating cerebral oxygenation in health and disease.

**Commercial Relationships:** Karel Van Keer, None; Cathy De Deyne, None; Cornelia Genbrugge, None; Luis Pinto, None; Evelien Vandewalle, None; Ingeborg Stalmans, None

**Program Number:** 3313 **Poster Board Number:** B0096

**Presentation Time:** 11:00 AM–12:45 PM

**Retinal Blood Oxygen Saturation and Aqueous Humor Biomarkers in Early Diabetic Retinopathy**

Faryan Tayyari<sup>1</sup>, Lee-Anne Khuu<sup>2</sup>, Jeremy M. Sivak<sup>2</sup>, Shaun Singer<sup>2</sup>, Michael H. Brent<sup>2</sup>, John G. Flanagan<sup>1,2</sup>, Christopher Hudson<sup>1,2</sup>.

<sup>1</sup>Optometry and Vision Science, University of Waterloo, Waterloo, ON, Canada; <sup>2</sup>Ophthalmology and Vision Sciences, University of Toronto, Toronto, ON, Canada.

**Purpose:** To investigate the relationship between retinal blood oxygen saturation (SO<sub>2</sub>) and aqueous humor (AH) concentrations of protein biomarkers in diabetic patients with non-proliferative diabetic retinopathy (NPDR) and to compare them with those of control subjects.

**Methods:** The sample comprised 14 participants with mild-to-moderate NPDR (66.3 ± 9.1 years) and 17 age-matched controls (69.1 ± 5.7 years); all participants were previously scheduled for routine cataract extraction with intraocular lens implantation. At the start of surgery, AH was collected using a Sautter hydrodissection cannula (27G, 0.4x22mm; Geuder, Heidelberg, Germany). Multiplex cytokine analyses of 26 biomarkers, including Angiopoietin 2 (Ang 2), Epidermal Growth Factor (EGF), Hepatocyte Growth Factor (HGF) and Interleukin-8 (IL-8) were performed by BioPlex 200 system (Bio-Rad Laboratories, Inc., Hercules, CA, USA). Four weeks after uncomplicated surgery and 2 weeks after cessation of any anti-inflammatory eyedrops, non-invasive hyperspectral retinal (HR) imaging (prototype H-8.5 HR Camera, Optina, QC, Canada) was undertaken. Six repeated retinal images were acquired centered on the optic nerve head at wavelengths of 586 and 605nm using the HR camera for each subject.

**Results:** Mean venular retinal blood oxygen saturation ( $p<0.001$ ) and AH levels of HGF ( $p=0.018$ ), Ang 2 ( $p=0.005$ ), EGF ( $p=0.030$ ) and IL-8 ( $p=0.034$ ) were significantly higher in NDPR when compared to controls. This study demonstrated a correlation between venular retinal blood oxygen saturation and pro-angiogenic factors HGF ( $r=0.584$ ,  $p=0.030$ ), Ang 2 ( $r=0.592$ ,  $p=0.026$ ), and EGF ( $r=0.523$ ,  $p=0.050$ ), but did not find any correlation for IL-8 ( $r=0.435$ ,  $p=0.120$ ) even though this biomarker was significantly higher in the diabetic group.

**Conclusions:** The results of this study revealed a direct relationship between retinal blood SO<sub>2</sub> and Ang 2, EGF and HGF but not IL-8.

**Commercial Relationships:** Faryan Tayyari, None; Lee-Anne Khuu, None; Jeremy M. Sivak, None; Shaun Singer, None;

**Michael H. Brent**, None; **John G. Flanagan**, None; **Christopher Hudson**, Optina (F)  
**Support:** Ontario Research Fund for Research Excellence

**Program Number:** 3314 **Poster Board Number:** B0097

**Presentation Time:** 11:00 AM–12:45 PM

**Computer-based quantification of acellular capillaries to assess experimental diabetic retinopathy**

*Craig Schebler<sup>1,2</sup>, Mihran Tuceryan<sup>1</sup>, Jiang-Yu Zheng<sup>1</sup>, Ashay D. Bhatwadekar<sup>2</sup>.* <sup>1</sup>Department of Computer and Information Science, Indiana University Purdue University Indianapolis, Indianapolis, IN; <sup>2</sup>Department of Ophthalmology, Indiana University, Indianapolis, IN.

**Purpose:** Increase in acellular capillary numbers is the pathologic hallmark of diabetic retinopathy. Traditionally, the acellular capillaries are enumerated by blinded investigators either directly through a microscope or via manual counting of captured images. However, this system is laborious, time consuming, and often shows inconsistency amongst researchers. The purpose of this study is to create a computer based algorithm that will assess the acellular capillaries of the retina, consistently reducing the human error and time.

**Methods:** The retinas of control and diabetic mice were processed using trypsin digestion and the high resolution .tiff images of retinal quadrants. We used the Python programming language using assorted open source package to write a custom-designed code. The images underwent a Gaussian blur and noise reduction to clean up the imperfections of the image. We used a purpose-built *k*-means clustering algorithm to group similar parts of the image together. We generated the paths in each image by converting all non-white elements to black. These images were then processed for Medial Access Transform (MAT) to create the skeleton as well as to find the distance from the skeleton to the edges formed in the above steps. The colors represent the distance from the edges, in which red is the largest distance and purple is the shortest distance. Then the locations where the skeleton is purple and connects to another color on both ends were counted. This count is the number of acellular capillaries.

**Results:** We have developed a precise algorithm with improved accuracy to enumerate the numbers of acellular capillaries. This algorithm can be used to quickly count the acellular capillaries in diabetic retinas and to create a standard for retinopathy assessment. Moreover, this algorithm is compatible with open source image analysis programs, enabling ease of access to the users.

**Conclusions:** We have designed an automated computer-based system to enumerate the acellular capillaries in diabetic retina. This computer based automated system will enhance consistency in retinopathy assessment and reduce time for analysis.

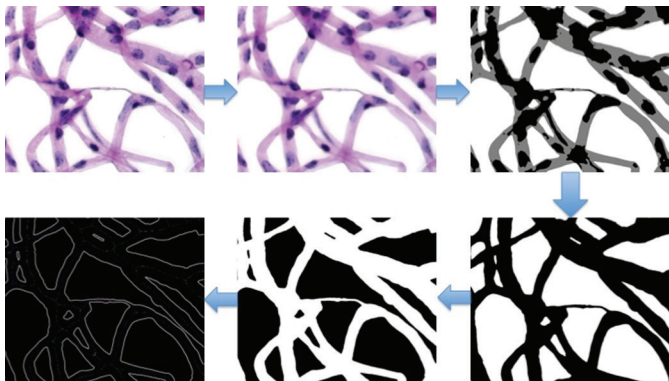


Figure 1 Schematics of serial image processing as described in methods.



Figure 2 Identification of acellular capillaries (blue arrow & purple area in inset) after MAT.

**Commercial Relationships:** **Craig Schebler**, None; **Mihran Tuceryan**, None; **Jiang-Yu Zheng**, None; **Ashay D. Bhatwadekar**, None

**Support:** LHSI Internship and Glick Eye Institute Foundation

**Program Number:** 3315 **Poster Board Number:** B0098

**Presentation Time:** 11:00 AM–12:45 PM

**The Association of Retinal Blood Flow and Retinal Blood Oxygen Saturation in Mild-to-Moderate Diabetic Retinopathy**

*Christopher Hudson<sup>1,2</sup>, Faryan Teyyari<sup>1</sup>, Lee-Anne Khuu<sup>2</sup>, Shaun Singer<sup>2</sup>, John G. Flanagan<sup>1,2</sup>, Michael H. Brent<sup>2</sup>.* <sup>1</sup>School of Optometry, University of Waterloo, Waterloo, ON, Canada; <sup>2</sup>Ophthalmology and Vision Sciences, University of Toronto, Toronto, ON, Canada.

**Purpose:** The aim of this study was to evaluate the relationship between retinal blood flow (RBF) and retinal oxygen saturation (SO<sub>2</sub>) in mild-to-moderate non-proliferative diabetic retinopathy (NPDR) and in age-matched controls.

**Methods:** One eye of each of 15 healthy subjects (68.1 ± 6.0 years) and 13 subjects with mild-to-moderate NPDR (67.3 ± 10.2 years) was dilated. None of the patients with NPDR had received treatment for their retinopathic changes or had any evidence of sight-threatening characteristics. Doppler FD-OCT blood flow was measured using the prototype RTVue system (Optovue Inc., USA); six separate measurements each comprising an upper and a lower, nasal pupil scan were acquired. Non-invasive hyperspectral retinal (HR) imaging (prototype H-8.5 HR Camera, Optina, QC, Canada) was also undertaken to measure retinal blood oxygen saturation; six HR camera (including the 586 to 605nm wavelengths) measurements were acquired.

**Results:** Total retinal blood flow was significantly lower in NPDR when compared to controls (42.66 ± 7.5 vs 33.73 ± 9.13; p=0.004). Mean retinal venular blood oxygen saturation was higher in NPDR than in the healthy controls (62.55 ± 5.7% vs 56.29 ± 4.7%; p=0.003). However, there was no correlation between venular retinal blood flow and venular oxygen saturation in controls (r=0.243, p=0.34) or in DR (r=0.228, p=0.45).

**Conclusions:** There was no correlation between venular retinal blood flow and retinal blood oxygen saturation. Given that there was no correlation between SO<sub>2</sub> and RBF, the results of this study suggest that there is a need to measure both SO<sub>2</sub> and RBF in order to calculate retinal oxygen utilization.

**Commercial Relationships:** Christopher Hudson, Optina (F), Optovue Inc (F); Faryan Tayyari, None; Lee-Anne Khuu, None; Shaun Singer, None; John G. Flanagan, None; Michael H. Brent, None

**Support:** Ontario Research Fund for Research Excellence

**Program Number:** 3316 **Poster Board Number:** B0099

**Presentation Time:** 11:00 AM–12:45 PM

**Image Quality Affects Measurements of Retinal Vessel Oxygen Saturation**

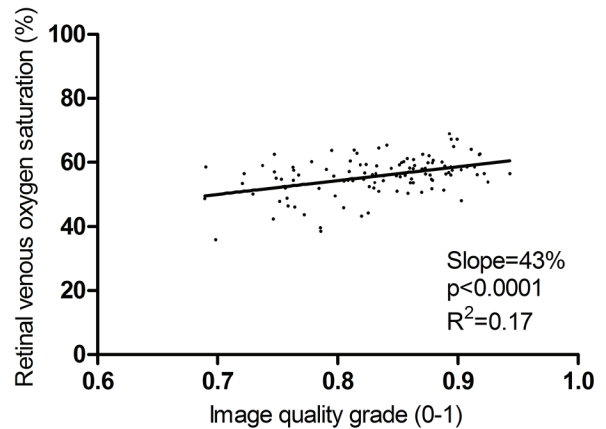
Sveinn H. Hardarson<sup>1</sup>, Benedikt A. Jonsson<sup>2</sup>, Robert A. Karlsson<sup>3</sup>, Asbjorg Geirsdottir<sup>4</sup>, David Bragason<sup>1</sup>, Thor Eysteinnsson<sup>1,5</sup>, Olof B. Olafsdottir<sup>1</sup>, Jona V. Kristjansdottir<sup>1</sup>, Einar Stefansson<sup>1</sup>.  
<sup>1</sup>Ophthalmology, University of Iceland / Landspítali University Hospital, Reykjavik, Iceland; <sup>2</sup>Electrical- and Computer Engineering, University of Iceland, Reykjavik, Iceland; <sup>3</sup>Oxymap ehf., Reykjavik, Iceland; <sup>4</sup>St. Eriks Eye Hospital, Stockholm, Sweden; <sup>5</sup>Physiology, University of Iceland, Reykjavik, Iceland.

**Purpose:** Non-invasive measurements of oxygen saturation in retinal vessels are based on retinal images, taken at two wavelengths of light. The purpose of the study was to test if and how image quality affects measurements of retinal vessel oxygen saturation.

**Methods:** The retinal oximeter (Oxymap ehf., Iceland) simultaneously acquires images of the retina at 570nm and 600nm. Software automatically measures light absorbance of retinal vessels and calculates oxygen saturation. A newly developed software tool automatically grades the images on the scale of 0 to 1 according to quality of the images. The quality grade is composed of assessment of focus and contrast. Oximetry images of 108 healthy individuals (age 18-77) and 17 individuals, scheduled for cataract surgery were analyzed for quality.

**Results:** In the healthy individuals, measured venous oxygen saturation decreased with worsening image quality ( $p < 0.0001$ ,  $R^2 = 0.17$ ) but measured arteriolar oxygen saturation was not significantly affected ( $p = 0.79$ ). A linear model indicated that the relationship between quality and measured venous saturation was not due to age:  $\text{VenousSaturation} = 26 - 0.043 * \text{Age} + 37 * \text{ImageQualityGrade}$ ,  $p = 0.29$  for age and  $p = 0.0008$  for image quality. Further analysis showed that the effect of image quality was due to contrast ( $p = 0.0002$ ) rather than focus ( $p = 0.36$ ). In individuals scheduled for cataract surgery, image quality correlated positively with measured oxygen saturation in both arterioles ( $p = 0.0079$ ,  $R^2 = 0.38$ ) and venules ( $p = 0.0034$ ,  $R^2 = 0.45$ ).

**Conclusions:** Poor image quality leads to lower measured venous oxygen saturation and, in more extreme cases, also affects measurements of arterioles. This may explain why measured oxygen saturation has previously been found to decrease with age. The new tool for image quality assessment allows quality control of retinal oximetry measurements and may potentially be used to apply correction factors.



The figure shows that measured retinal venous oxygen saturation increases with improved image quality as assessed by an automatic image quality tool. The results of simple linear regression are shown (not corrected for age).

**Commercial Relationships:** Sveinn H. Hardarson, Oxymap ehf. (C), Oxymap ehf. (I), Oxymap ehf. (P); Benedikt A. Jonsson, Oxymap ehf. (F); Robert A. Karlsson, Oxymap ehf. (E), Oxymap ehf. (I), Oxymap ehf. (P); Asbjorg Geirsdottir, None; David Bragason, None; Thor Eysteinnsson, Oxymap ehf. (I), Oxymap ehf. (P); Olof B. Olafsdottir, None; Jona V. Kristjansdottir, None; Einar Stefansson, Oxymap ehf. (I), Oxymap ehf. (P), Oxymap ehf. (S)

**Support:** The Icelandic Center for Research (Rannis), University of Iceland Research Funds, The Landspítali University Hospital Research Fund, Helga Jónsdóttir and Sigurliði Kristjánsson Memorial Fund

**Program Number:** 3317 **Poster Board Number:** B0100

**Presentation Time:** 11:00 AM–12:45 PM

**Validation of model based hyperspectral retinal oximetry algorithms using systemic gas provocations in healthy individuals**

Susith Kulasekara<sup>1</sup>, Kalpana Rose<sup>2</sup>, Michèle Desjardins<sup>4</sup>, Reza Jafari<sup>3</sup>, J Daniel Arbou<sup>5,3</sup>, Frédéric Lesage<sup>4</sup>, Jean-Philippe Sylvestre<sup>3</sup>, Christopher Hudson<sup>1,2</sup>.  
<sup>1</sup>Ophthalmology & Vision Sciences, University of Toronto, Toronto, ON, Canada; <sup>2</sup>School of Optometry and Vision Science, University of Waterloo, Waterloo, ON, Canada; <sup>3</sup>Optina Diagnostics, Montreal, QC, Canada; <sup>4</sup>Institut de génie biomédical, École Polytechnique de Montréal, Montréal, QC, Canada; <sup>5</sup>Department of Ophthalmology, University of Montreal, Montreal, QC, Canada.

**Purpose:** Retina is a highly metabolically active tissue with a very high demand for oxygen. Dysregulation of retinal oxygen supply and demand is associated with many ocular and systemic diseases. Changes in retinal tissue oxygen tension may take place before these changes are reflected in retinal vessels. The purpose of this study is to validate the use of a model based on a hyperspectral algorithm for measuring retinal tissue oxygen saturation ( $t\text{SO}_2$ ).

**Methods:** One eye of 12 healthy non-smoking volunteers was chosen for the study. End-tidal  $\text{O}_2$  concentration ( $P_{\text{ET}}\text{O}_2$ ) was adjusted using a model based prospective targeting device (RespirAct) to induce normoxia ( $P_{\text{ET}}\text{O}_2 = 100\text{mmHg}$ ), hypoxia ( $P_{\text{ET}}\text{O}_2 = 50\text{mmHg}$ ) and hyperoxia ( $P_{\text{ET}}\text{O}_2 = 300\text{mmHg}$ ), while maintaining normocarbina. The order of hyperoxia and hypoxia was randomized between subjects. Heart rate, blood pressure, and finger pulse oximetry were monitored throughout. A prototype metabolic hyperspectral retinal camera

(MHRC, Optina Diagnostics) was used to image the fundus from 500-600nm in 5nm steps (3 repeats per condition) after stabilization of finger pulse oximetry for over 3 min. The reflectance intensity data was fit in MATLAB to a model where oxy- and deoxyhemoglobin are the main absorbers and scattering is modeled by a  $\log(1/\text{wavelength})$  term. The fitted parameters were used to extract an estimation of  $t\text{SO}_2$  and total hemoglobin content (HbT) in each pixel of the images and values obtained in the different  $P_{\text{ET}}\text{O}_2$  conditions were compared for a region of the retina, free of any visible blood vessels, at a half disc diameter distance from the disc margin.

**Results:** The preliminary results show that as the breathing air  $P_{\text{ET}}\text{O}_2$  was increased from normoxia to hyperoxia  $t\text{SO}_2$  significantly increased ( $p=0.001$ ) from 41%( $\pm 11$ ) to 53%( $\pm 10$ ). Lowering the  $P_{\text{ET}}\text{O}_2$  from normoxia to hypoxia significantly decreased ( $p=0.001$ )  $t\text{SO}_2$  from 41%( $\pm 11$ ) to 34%( $\pm 14$ ). The mean HbT at hypoxia, normoxia, and hyperoxia, were not significantly different ( $p=0.3$ ) from each other: 2.8( $\pm 0.7$ ); 2.5( $\pm 0.6$ ); 2.4( $\pm 0.8$ ). However, there was a trend towards an increase in HbT in hypoxia.

**Conclusions:** As the breathing air oxygen composition ( $P_{\text{ET}}\text{O}_2$ ) is changed from normoxia to hypoxia and hyperoxia, retinal tissue oxygen saturation ( $t\text{SO}_2$ ) measurements, based on a hyperspectral algorithm, showed parallel changes, suggesting that the method could be used to monitor the health of the retina.

**Commercial Relationships:** Susith Kulasekara, None; Kalpana Rose, None; Michèle Desjardins, None; Reza Jafari, Optina Diagnostics (E); J Daniel Arbour, Optina Diagnostics (I); Frédéric Lesage, None; Jean-Philippe Sylvestre, Optina Diagnostics (E), Optina Diagnostics (I); Christopher Hudson, Optina Diagnostics (F), Thornhill Research Inc. (P)

**Support:** Vision Science Research Program (VSRP) Award, Department of Ophthalmology, University of Toronto, Canada; Ontario Research Fund – Research Excellence (ORF-RE); Dalton Whitebread Scholarship Fund, Faculty of Medicine, University of Toronto.

**Program Number:** 3318 **Poster Board Number:** B0101

**Presentation Time:** 11:00 AM–12:45 PM

#### OCT Angiography (OCTA) in Healthy Human Subjects

Jack Yi<sup>1</sup>, Douglas Matsunaga<sup>1</sup>, John E. Legarreta<sup>2</sup>, Andrew D. Legarreta<sup>2</sup>, Giovanni Gregori<sup>2</sup>, Mary K. Durbin<sup>3</sup>, Utkarsh Sharma<sup>3</sup>, Philip J. Rosenfeld<sup>2</sup>, Carmen A. Puliafito<sup>1</sup>, Amir H. Kashani<sup>1</sup>. <sup>1</sup>USC Eye Institute, Keck School of Medicine of USC, Los Angeles, CA; <sup>2</sup>Bascom Palmer Eye Institute, University of Miami Miller School of Medicine, Miami, FL; <sup>3</sup>Advanced Development, Carl Zeiss Meditec, Inc., Dublin, CA.

**Purpose:** To evaluate the feasibility of noninvasive retinal angiography using a prototype using swept-source (SS) and spectral-domain (SD) optical coherence tomography (OCT) angiography.

**Methods:** Data was acquired using a Cirrus (Carl Zeiss Meditec, Dublin, CA) SS-OCT and SD-OCT prototype angiography systems. Five healthy subjects (nine eyes) with no past ophthalmologic history were recruited. 3x3mm regions centered on the fovea, nasal macula, and temporal macula were imaged. Retinal vasculature was assessed in three horizontal slabs consisting of the inner, middle, and outer retina. The vasculature was reconstructed using an intensity-based algorithm into separate en face images. Post-processed en face OCT angiograms were analyzed with ImageJ (NIH, Bethesda, MD) to quantify the density of retinal microvasculature using the “Auto Local Threshold” plug-in (Landini G. v1.5).

**Results:** OCTA in healthy subjects resembled fine capillary networks that have been demonstrated in previous histological studies of human cadaver eyes. Retinal vessels were not visualized in the outer retina. Within the central macula and temporal macula, the

inner retina displayed continuous capillaries traveling in the same retinal plane while the middle retinal slab contained a lattice pattern of vessels. The nasal macular region showed capillary segments radiating out from the optic disc in the inner retina while the middle retinal slab featured a lattice pattern of discontinuous vessel segments. Vessel density analyses using ImageJ are shown in Figures 1 and 2.

**Conclusions:** Noninvasive, high-resolution angiograms produced by OCTA show qualitatively similar vascular patterns to previous histological images of the retina. OCTA angiography can reliably and reproducibly image the fine capillary networks of the retina and may have a role in assessing the retinal microvasculature when conventional fluorescein angiography cannot be performed.

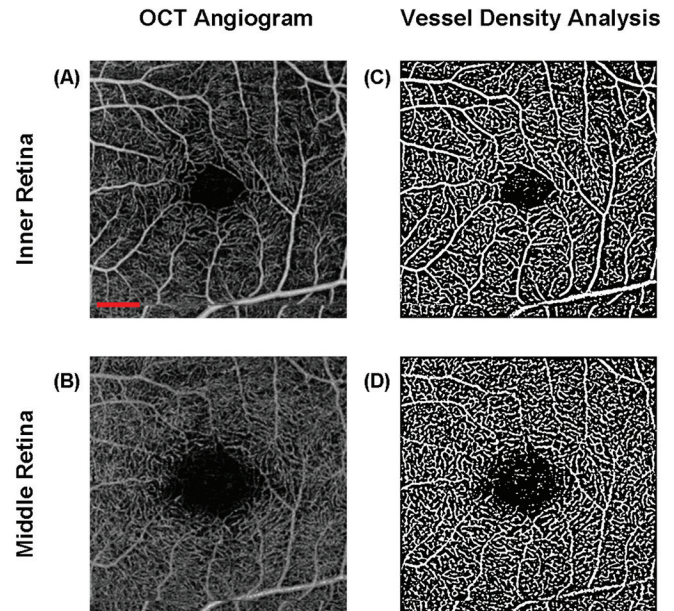


**Fig. 1.** Vessel density analysis of the central macular region of a healthy subject yielded an average total density of 31.68%  $\pm$  1.15% in the inner retina and a density of 30.86%  $\pm$  1.20% in the middle retina.

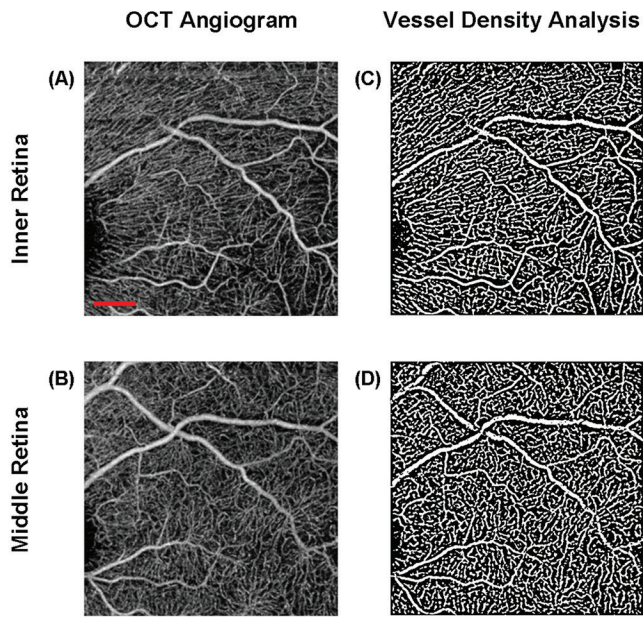


**Fig. 2.** Vessel density analysis of the nasal macular region of a healthy subject yielded an average total density of  $31.59\% \pm 1.40\%$  in the inner retina and a density of  $31.47\% \pm 1.62\%$  in the middle retina.

**Commercial Relationships:** Jack Yi, Carl Zeiss Meditec (F); Douglas Matsunaga, Carl Zeiss Meditec (F); John E. Legarreta, Carl Zeiss Meditec (F); Andrew D. Legarreta, Carl Zeiss Meditec (F); Giovanni Gregori, Carl Zeiss Meditec (F); Mary K. Durbin, Carl Zeiss Meditec (E); Utkarsh Sharma, Carl Zeiss Meditec (E); Philip J. Rosenfeld, Carl Zeiss Meditec (F); Carmen A. Puliafito, Carl Zeiss Meditec (F); Amir H. Kashani, Carl Zeiss Meditec (F)  
**Support:** An Unrestricted grant from Research to Prevent Blindness, New York, NY 10022

**Program Number:** 3319 **Poster Board Number:** B0102

**Presentation Time:** 11:00 AM–12:45 PM

#### Comparison of Swept Source Versus Spectral Domain Optical Coherence Tomography Angiography (OCTA) in Chorioretinal Diseases

Lauren Branchini<sup>1</sup>, Talisa de Carlo<sup>1</sup>, Eric Moul<sup>2</sup>, Nadia K. Waheed<sup>1</sup>, Andre Witkin<sup>1</sup>, Caroline R. Bauman<sup>1</sup>, James G. Fujimoto<sup>2</sup>, Jay S. Duker<sup>1</sup>. <sup>1</sup>Tufts New England Eye Center, Boston, MA; <sup>2</sup>Massachusetts Institute of Technology, Cambridge, MA.

**Purpose:** Optical coherence tomography angiography (OCTA) to visualize chorioretinal vasculature can be performed using both 840 nm wavelength spectral domain (SD) as well as 1060 nm swept source (SS) systems. This cross sectional, observational case series compares and contrasts the imaging capabilities of SS-OCTA to SD-OCTA in a variety of cases.

**Methods:** 9 subjects underwent sequential same-day SD-OCTA and SS-OCTA at the New England Eye Center between 8/2014 and 11/2014. These subjects included 1 normal control and 8 with a variety of chorioretinal diseases including wet age-related macular degeneration, central serous chorioretinopathy, central retinal vein occlusion, diabetic retinopathy, birdshot chorioretinopathy, Best's disease and retinitis pigmentosa. All subjects were imaged on a prototype SS-OCTA system featuring an imaging speed of 400 kHz, with an axial resolution of 7-10  $\mu\text{m}$  and 5 repeated B-scans per position. All subjects were also imaged with the AngioVue OCTA system on the commercially available Avanti SD-OCT (Optovue, Inc,

Fremont, CA) operating at 70 kHz with an axial resolution of 5  $\mu\text{m}$  using 2 repeated B-scans. An investigational OCTA software program was used to evaluate the images. Images were compared qualitatively. When available, OCTA was also compared with corresponding fluorescein angiography (FA).

**Results:** High quality images were obtained on both systems in all subjects. All data sets were segmented and vascular layers in the retina and choroid were identified. Pathologic features of disease were identified in images from both systems. These pathologic features, including choroidal neovascular membranes (Figure 1), retinal microaneurysms and vessel dropout were correlated between scanning systems and with FA. Better quality images of the choroidal vasculature were obtained with the SS-OCTA especially in patients with ocular opacities including subretinal lipofuscin deposits. No retinal vascular pathology could not be identified on both systems.  
**Conclusions:** Both SS-OCTA and SD-OCTA have a role in evaluating chorioretinal vasculature and demonstrate consistent findings.

**Commercial Relationships:** Lauren Branchini, None; Talisa de Carlo, None; Eric Moul, None; Nadia K. Waheed, Iconic Therapeutics (C); Andre Witkin, None; Caroline R. Bauman, None; James G. Fujimoto, Carl Zeiss Meditec, Inc. (P), Optovue (C); Jay S. Duker, Carl Zeiss Meditec Inc. (P), EyeNetra (I), Hemera Biosciences (I), Ophthotech Corp. (I)

**Support:** This work was supported in part by a Research to Prevent Blindness Unrestricted grant to the New England Eye Center/ Department of Ophthalmology, Tufts University School of Medicine, National Institutes of Health (NIH) contracts R01-EY011289-28, R01-EY013178-12, R01-CA075289-16, Air Force Office of Scientific Research contracts FA9550-10-1-0551 and FA9550-12-1-0499, DFG contracts DFG-HO-1791/11-1, DFG Training Group 1773, DFG-GSC80-SAOT, and Massachusetts Lions Club.

**Program Number:** 3320 **Poster Board Number:** B0103

**Presentation Time:** 11:00 AM–12:45 PM

#### Comparison of two free retinal vascular measurement software packages: IVAN and VAMPIRE

Elaine Downie<sup>1</sup>, Julian Tokarev<sup>1</sup>, Afshin Divani<sup>3</sup>, Dara D. Koozekanani<sup>2</sup>. <sup>1</sup>University of Minnesota Medical School, Minneapolis, MN; <sup>2</sup>Department of Ophthalmology, University of Minnesota, Minneapolis, MN; <sup>3</sup>Department of Neurology, University of Minnesota, Minneapolis, MN.

**Purpose:** Retinal image analysis can be used to quantify retinal vascular changes due to hypertensive retinopathy, changes shown to be predictive of stroke risk. A number of software packages are available for this, and each utilizes different techniques for detection and measurement of retinal vascular features. Here, we compared the performance of a well known package, IVAN, with a newly available tool, VAMPIRE.

**Methods:** 50 degree color fundus images obtained with a Topcon TRC 50DX camera (Topcon Medical Systems, Oakland, NJ) were graded using IVAN (Interactive Vessel ANalyzer), v1.3 (courtesy of Dr. Nicola Ferrier of the UW Madison School of Engineering and the Dept. of Ophthalmology and Visual Sciences) and VAMPIRE (Vascular Assessment and Measurement Platform for Images of the Retina, available at vampire.computing.dundee.ac.uk). Both are available free of charge. Both were used to calculate central retinal artery equivalents (CRAE), central retinal vein equivalents (CRVE), and arteriolar:venular ratio (AVR) for each eye.

**Results:** 21 patients, 42 eyes, were analyzed. CRAE, CRVE, and AVR values were obtained for 41 eyes, one eye was ungradeable. The values were plotted and a correlation coefficient between the IVAN and VAMPIRE values was calculated and tested for significance



using the Pearson Product-Moment Significance Test. For CRVE, the  $R^2=0.7032$ , the Pearson correlation coefficient (R)=0.839,  $p<0.001$ . For CRAE, the  $R^2=0.2604$ , the Pearson correlation coefficient (R)=0.510,  $p=0.001$ . For AVR, the  $R^2=0.5747$ , the Pearson correlation coefficient (R)=0.758,  $p<0.001$ .

**Conclusions:** The CRAE, CRVE, and AVR values measured with the newer VAMPIRE software package corresponded with those obtained using IVAN. While the two packages use different methods and have different degrees of automaticity, this suggests both can be valuable tools in the investigation of hypertensive retinopathy and other retinal vascular conditions for which CRAE, CRVE, and AVR are relevant.

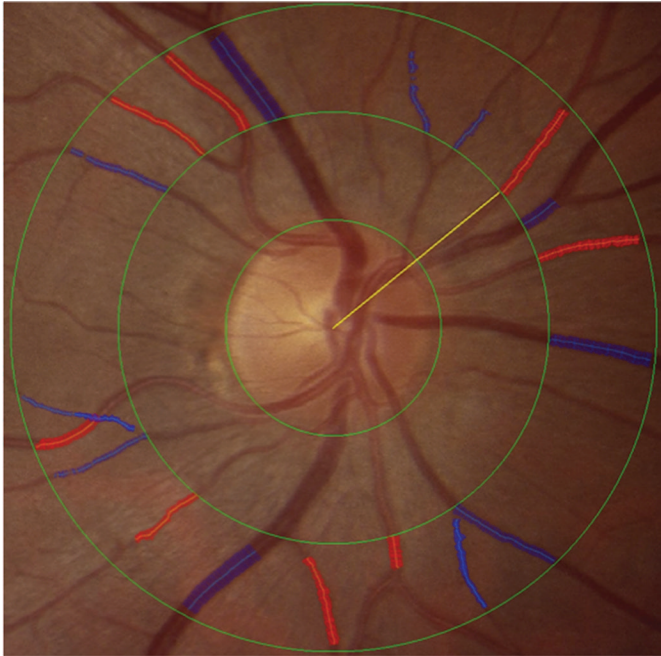


Figure 1. IVAN segments vessels within a ring between 0.5 and 1 disc diameters from the disc center. The grader verifies correct vessel identification and revises the segmentations. CRAE, CRVE, and AVR are calculated using the Parr-Hubbard-Knudtson equation.

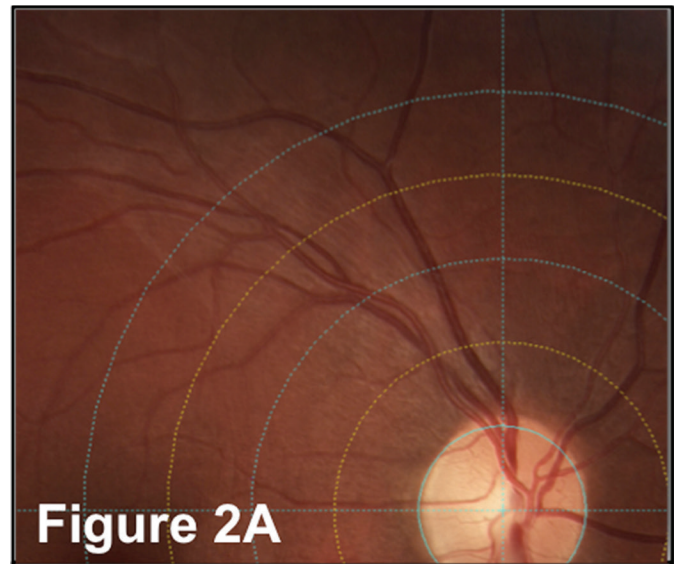


Figure 2A

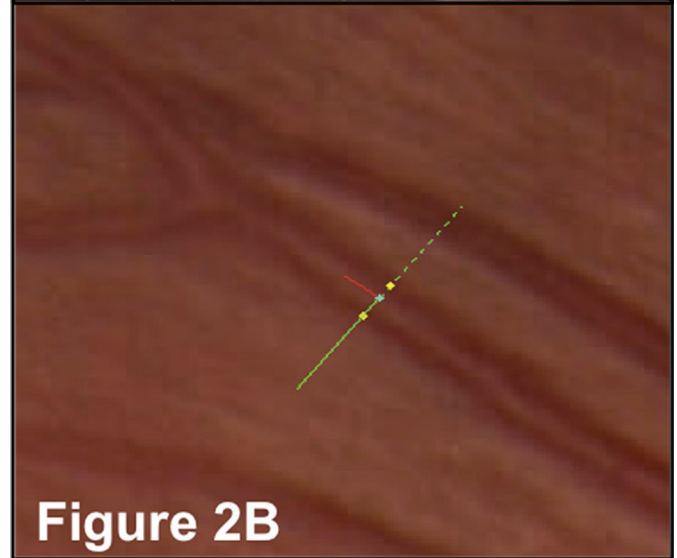


Figure 2B

**Figure. 2A** VAMPIRE displays concentric rings and allows the user to designate points for vascular measurement.

**Figure. 2B** Vascular measurement is made manually with a measuring tool.

**Commercial Relationships:** Elaine Downie, None; Julian Tokarev, None; Afshin Divani, None; Dara D. Koozekanani, None

**Program Number:** 3321 **Poster Board Number:** B0104

**Presentation Time:** 11:00 AM–12:45 PM

**An improved semi-automatic method to measure retinal vessel caliber from fundus photographs and measurement results in normal Japanese**

*Makoto Araie<sup>1</sup>, Aiko Iwase<sup>2</sup>, Ryo Kawasaki<sup>3</sup>, Jun Suehiro<sup>4</sup>, Akihiko Sekine<sup>4</sup>.* <sup>1</sup>Kanto Central Hospitals, Mutual Aid Assoc of Public Sch Teachers, Setagaya-Ku, Japan; <sup>2</sup>Ophthalmology, Tajimi Iwase Eye Clinic, Tajimi, Japan; <sup>3</sup>Yamagata Univ, Yamagata, Japan; <sup>4</sup>Topcon, Tokyo, Japan.

**Purpose:** Retinal vessel caliber (RVC) changes are associated with various systemic and ocular abnormalities. Accurate magnification correction in each eye is indispensable for measuring RVC from fundus photographs, but currently available semi-automatic methods to determine RVD are not necessarily satisfactory in this respect.

**Methods:** In addition to Littmann's correction, ray-tracing algorithm was applied to optical system of Topcon non-mydiatic fundus camera (TRC-NW7, Topcon, Tokyo) and magnification was corrected using corneal curvature, axial length (AL) and refraction of each subject eye. RVC was always determined in an annular area between 1.8 and 2.7 mm from the disc center. Measurement reproducibility was checked in 20 normal eyes by 4 independent examiners, and the results with the current method were compared to those with Interactive Vessel Analysis System (IVAN) in other 180 normal eyes of 99 subjects with mean age of 52 yrs. Factors relating to central retinal arteriolar equivalent (CRAE) were studied in 793 right eyes with AL less than 26 mm of 793 normal Kumejima Study participants with average age of 50 yrs. The Ethic Committee of Kumejima Town approved the study.

**Results:** Intra-individual ICC was 0.921-0.993 and 0.995-0.999, and Inter-individual ICC 0.998 and 0.996 for CRAE and central retinal venular equivalent (CRVE), respectively. The current method yielded CRAE and CRVE values 1.8 % smaller and .4.3% greater than those with IVAN ( $P < 0.017$ ), and the difference between the results with the two methods was AL-dependent. In normal Japanese, CRAE was  $162.5 \pm 9.3$  (SD) and CRVE  $232.9 \pm 16.1$   $\mu\text{m}$ . A multiple regression analysis revealed that female gender ( $P = 0.002$ ), older age ( $P = 0.000$ ), higher blood pressure ( $P = 0.014$ ), longer AL ( $P = 0.000$ ) and larger beta-peripapillary atrophy (beta-PPA) ( $P = 0.000$ ) were correlated with CRAE in this population.

**Conclusions:** An improved method to measure RVC from fundus photographs with reasonable measurement reproducibility was developed. In normal Japanese, two ocular factors, axial length and beta-PPA area, were newly found to significantly correlate with CRAE beside systemic factors well known to affect it.

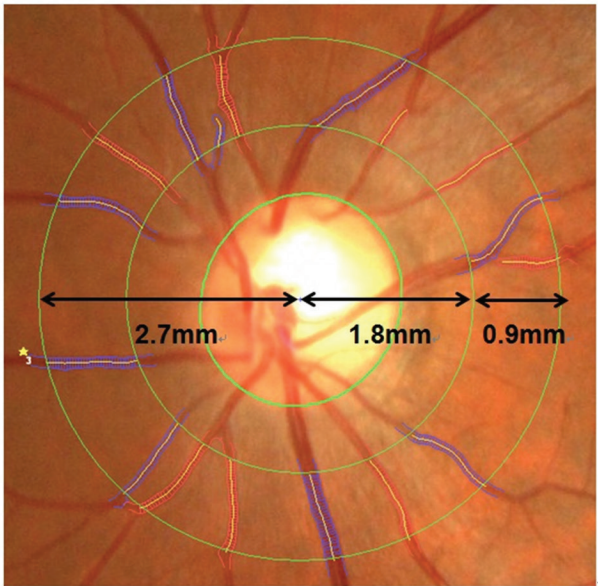


Figure showing the annular area for measurement of retinal vessel caliber

**Commercial Relationships:** Makoto Araie, Topcon (P); Aiko Iwase, Topcon (P); Ryo Kawasaki, None; Jun Suehiro, Topcon (E); Akihiko Sekine, Topcon (E)

**Program Number:** 3322 **Poster Board Number:** B0105

**Presentation Time:** 11:00 AM–12:45 PM

**Total retinal blood flow measurement in the human eye with 3-Beam Doppler Optical Coherence Tomography**

Richard Haindl<sup>1,2</sup>, Wolfgang Trasischker<sup>1,2</sup>, Bernhard Baumann<sup>1,2</sup>, Andreas Wartak<sup>1,2</sup>, Michael Pircher<sup>1,2</sup>, Christoph K. Hitzenberger<sup>1,2</sup>. <sup>1</sup>Center for Medical Physics and Biomedical Engineering, Medical University of Vienna, Vienna, Austria; <sup>2</sup>Medical Imaging Cluster, Medical University of Vienna, Vienna, Austria.

**Purpose:** To measure the total retinal blood flow and obtain flow/velocity profiles within all major retinal vessels originating from the optic nerve head (ONH) using an improved three-beam Doppler OCT (D-)OCT technique.

**Methods:** The three beam D-OCT consists of three independent superluminescent diode (SLD) sources with a central wavelength of 840 nm and a spectral bandwidth of 50 nm. The collimated exiting beams share a common bulk optics Michelson interferometer. A well-defined beam geometry enables the full reconstruction of the three dimensional velocity vector, without prior knowledge on the vessel geometry, which is normally required for D-OCT systems with less than three beams.

In the sample arm a custom made facet prism telescope allows for variable beam separation adjustment without alteration of the beam diameter. In conjunction with a normal telescope a transversal resolution of approximately 30  $\mu\text{m}$  is achieved.

A two axis gimbal less MEMS mirror allows raster, circular and resonant scan patterns, which are not practical with a classical 2 axis galvo scanner, because of heavy beam movement at the pupil of the eye, caused by off-pivot point scanning.

Eyes of healthy subjects were imaged and the mean total retinal blood flow as well as the velocity profiles inside all major retinal vessels emerging from the ONH were extracted.

**Results:** Figure 1 shows an example of a circular scan around the ONH of a healthy human subject. The velocity profiles of all major vessels are visible. Furthermore 3 beam D-OCT allows the reconstruction of the vessel geometry, showing excellent agreement between the actual and calculated vessel orientation as well as the flow direction. The total venous mean flow was 54.7  $\mu\text{l}/\text{min}$ , while the total arterial flow was 47.8  $\mu\text{l}/\text{min}$ .

**Conclusions:** The improved three beam D-OCT technique allows the direct measurement of total retinal blood flow as well as velocity vector determination with various scan patterns independent from any a-priori knowledge on the vessel geometry. With further development the technique may aid the early diagnosis of eye diseases like glaucoma.

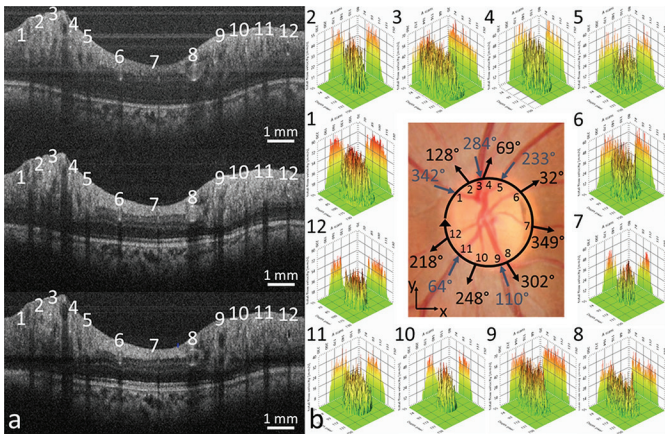


Figure 1: a) single circular B-scan for every channel, consisting of 4096 A-scans each. White numbers, vessel numbering. b) Middle: Color fundus photo. Black circular arrow indicates the direction and path of the circular scan. Black inner numbers: Vessel numbering. Arrows with numbers: calculated vessel orientation from the 3 beam D-OCT data. Surrounding: Reconstructed velocity profiles for the corresponding vessels around the ONH after phase offset subtraction, phase unwrapping and averaging over 10 B-scans. X-Axis: A-scans, Y-Axis: Depth pixel, Z-Axis: Velocity (mm/s).

**Commercial Relationships:** Richard Haindl, None; Wolfgang Trasischker, None; Bernhard Baumann, None; Andreas Wartak, None; Michael Pircher, None; Christoph K. Hitzenberger, None  
**Support:** Austrian Science Fund Grant Number P26553-N20

**Program Number:** 3323 **Poster Board Number:** B0106

**Presentation Time:** 11:00 AM–12:45 PM

**Measurement of blood flow in the largest vessels and smallest capillaries in the living mouse retina using an adaptive optics scanning light ophthalmoscope**

Aby Joseph<sup>2,1</sup>, Andres Guevara-Torres<sup>2,1</sup>, David R. Williams<sup>2,1</sup>, Jesse B. Schallek<sup>2</sup>. <sup>1</sup>Institute of Optics, University of Rochester, Rochester, NY; <sup>2</sup>Center for Visual Science, University of Rochester, Rochester, NY.

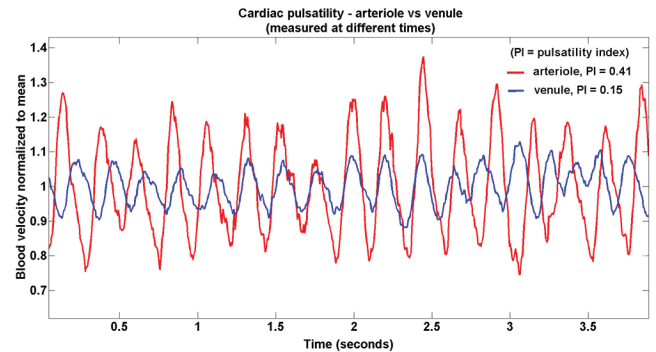
**Purpose:** Blood cell velocities in the mammalian retina range from  $\mu\text{m/s}$  to  $\text{cm/s}$ , depending on vessel size and health. Here we automate blood flow (BF) measurement from the full spectrum of vessels using an adaptive optics scanning light ophthalmoscope (AOSLO).

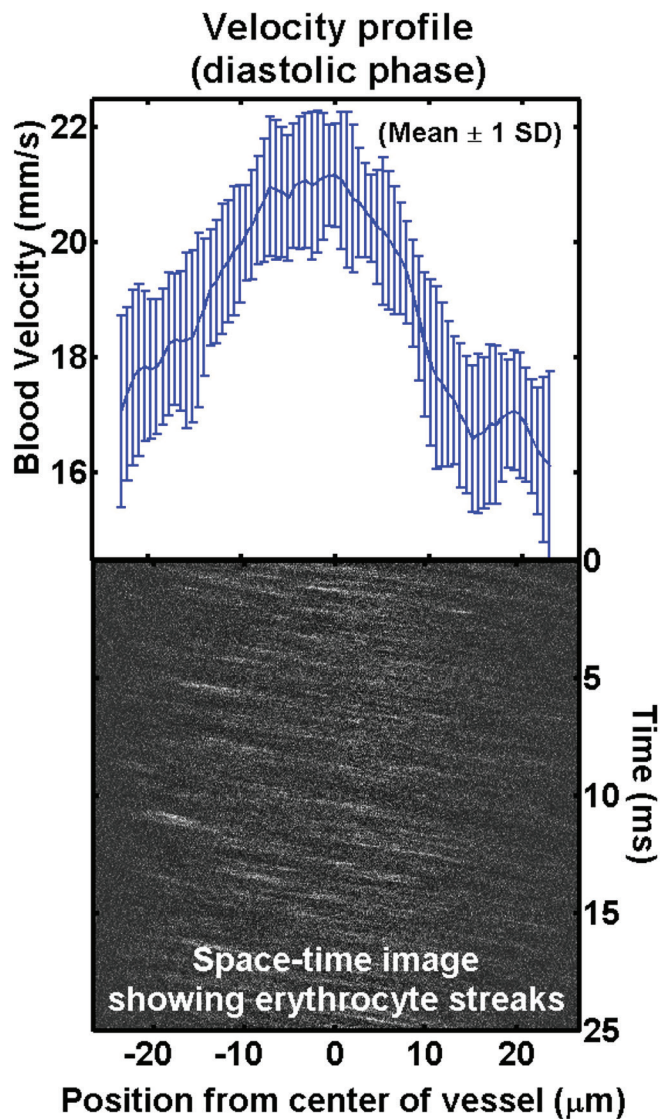
**Methods:** Anesthetized C57BL/6J mice were imaged with an AOSLO using near infrared light. Vessel lumen diameters were measured in raster mode using sodium fluorescein contrast. Additionally, single blood cells were imaged as they passed through a one dimensional 31 kHz scanning beam (Zhong et al 2008). Images of cell position as a function of time were captured; cells manifest as bright streaks. Streak slope was automatically determined using the Radon transform, which can measure cell velocities up to 1 m/s. BF in each vessel was calculated assuming laminar flow and cylindrically shaped vessels.

**Results:** Measured inner lumen diameters ranged from 4.5  $\mu\text{m}$  in the capillaries to 53  $\mu\text{m}$  in the largest vessels near the disc. Measured erythrocyte velocities ranged from stopped flow in capillaries to 35  $\text{mm/s}$  in large vessels. Temporal variations in velocity, measured in both arterioles and venules, corresponded to heart rates of 202–280 bpm, that matched well with simultaneous measurements with a pulse oximeter.

The velocity signal was robust in vessels that intersected the scanning beam at less than 40° (45% of vessels), the contrast between erythrocyte streaks being insufficient for remaining vessels. BF in the remaining vessels was estimated by scaling the measured BF in other vessels by the fourth power of the ratio of the widths of each vessel (Poiseuille's Law). Averaging across time, total retinal BF values ranging from 3.76–4.79  $\mu\text{L}/\text{min}$  in arterioles and 3.85–4.78  $\mu\text{L}/\text{min}$  in venules were calculated.

**Conclusions:** We quantified BF in the largest vessels and the smallest capillaries in the mouse retina, which has been challenging for other approaches that may lack the necessary spatial and temporal resolution. The rapid rate of acquisition allowed precise measurements of fast blood velocity fluctuations associated with the mouse cardiac cycle, in arterioles, venules and capillaries. This method can provide a complete analysis of hemodynamics throughout retinal circulation, which is important to study ocular diseases that disturb regional and global BF, such as diabetic retinopathy and glaucoma.





**Purpose:** Geometric changes of the retinal vasculature may precede or form part of the pathophysiology of eye diseases such as diabetic retinopathy or retinal vascular occlusion. Quantitative vasculature parameters are used clinically and in research for risk assessment, disease monitoring and as markers of therapeutic efficacy. This study describes a new method for rapid automated measurement of vascular geometric parameters within a selectable region. Baseline measurements for the adult C57BL/6J mouse retina are defined.

**Methods:** Retinal flat-mounts were prepared from adult C57BL/6 mice, stained with fluorophore-conjugated isolectin B4, and imaged by confocal microscopy. Animal care guidelines of the ARVO Statement for the Use of Animals in Ophthalmic and Vision Research were followed and all procedures were approved by the institutional animal care and use committee (St Vincent's AEC protocol SABC001). 8 retinal flat-mounts 4900 $\times$ 5800 pixels were obtained and corrected for uneven illumination. Images were binarized using an SVM classifier. Vessel bifurcations and crossover points were automatically detected using a novel backward morphological shrinking operation as shown in Figure 1. Flat-mount images were partitioned into 5 non-overlapping regions 1200 $\times$ 1200 pixels centred on the optic disc (OD) and each retinal quadrant (RQ). Vascular parameters including the branching angles (value and count), vessel to background (V/B) ratio and fractal dimension (FD), were obtained for each region.

**Results:** FDs for OD (mean $\pm$ SD=1.522  $\pm$  0.012) and RQ (1.526  $\pm$  0.021) regions were similar. Similarity was also found in V/B ratio (OD=18.86  $\pm$  1.54 %, RQ= 18.80  $\pm$  2.83%). However, OD had fewer branch points (bp) (255 $\pm$  39.55) and acute angle(aa) (88.64 $\pm$  24.08 degrees) compared to RQ (bp=355.5 $\pm$ 97.71, aa =92.16  $\pm$  21.09).

**Conclusions:** This novel technique provides a fast, automated and reliable method for quantification of vascular parameters including estimates of the mean and variance of branching angles which is not feasible manually or by other software modules such as VESGEN (VESSEL GENeration Analysis). Also unlike VESGEN, our method does not require a binary vascular image as the input and works with any grayscale image format. The reliable quantification of retinal vascular parameters is likely to be of value to studies of retinal vascular disease, including angiogenesis, and putative therapies for these disorders.

**Commercial Relationships:** Aby Joseph, None; Andres Guevara-Torres, Canon, Inc. (F), University of Rochester (P); David R. Williams, Canon, Inc. (F), Canon, Inc. (R), Polgenix, Inc. (F), University of Rochester (P); Jesse B. Schallek, University of Rochester (P)

**Support:** Research reported in this publication was supported by the National Eye Institute of the National Institutes of Health under Award No. P30 EY001319 and F32 EY023496. The content is solely the responsibility of the authors and does not necessarily represent the official views of the National Institute of Health.

**Program Number:** 3324 **Poster Board Number:** B0107

**Presentation Time:** 11:00 AM–12:45 PM

**Automated measurement of vascular parameters in mouse retinal flat-mounts**

Behzad Aliahmad<sup>1</sup>, Dinesh K. Kumar<sup>1</sup>, Marc Sarossy<sup>2</sup>, Elsa Chan<sup>3</sup>, Peter V. Wijngaarden<sup>3</sup>. <sup>1</sup>RMIT University, Melbourne, VIC, Australia; <sup>2</sup>Royal Victorian Eye and Ear Hospital, Melbourne, VIC, Australia; <sup>3</sup>Centre for Eye Research Australia & Department of Ophthalmology, The University of Melbourne, Melbourne, VIC, Australia.

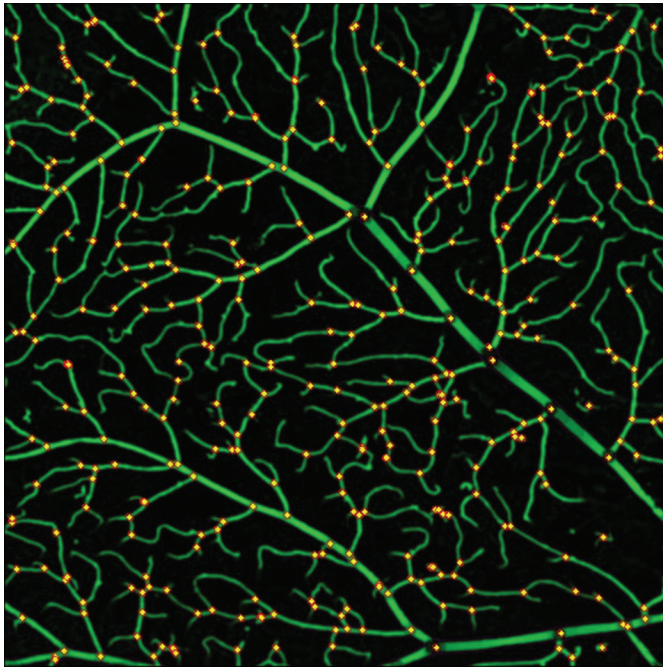


Figure 1

**Commercial Relationships:** Behzad Aliahmad, None; Dinesh K. Kumar, None; Marc Sarossy, None; Elsa Chan, None; Peter V. Wijnngaarden, None

**Program Number:** 3325 **Poster Board Number:** B0108

**Presentation Time:** 11:00 AM–12:45 PM

**Conventional Multimodal Imaging Versus “En-Face” OCT2 Angiography: deep inside the chorioretinal vascular tissue**

Marco Lupidi<sup>1,2</sup>, Gabriel J. Coscas<sup>2</sup>, Florence Coscas<sup>2</sup>. <sup>1</sup>S.Maria Della Misericordia Hospital, Eye Clinic, Perugia, Italy; <sup>2</sup>Centre Ophtalmologique De L'Odeon, Paris, France.

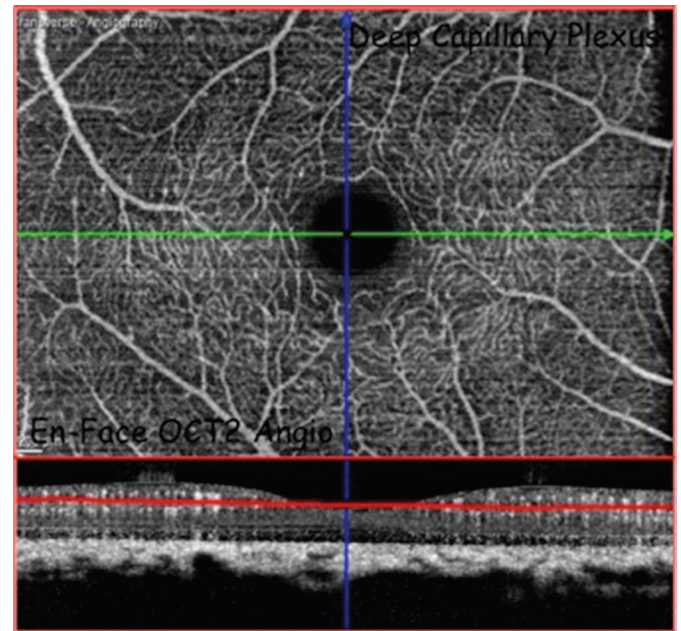
**Purpose:** To describe and compare the conventional multimodal imaging findings to the images of all the retinal and choroidal vascular layers obtained with the Spectralis “En-Face” OCT2-ANGIOGRAPHY in healthy subjects without dye injection.

**Methods:** Prospective case series of 10 eyes of 10 consecutive asymptomatic patients (7 females, mean age  $34 \pm 15$ ) were evaluated by the use of a conventional multimodal protocol including Fluorescein Angiography (FA) and Enhanced Depth Imaging (EDI) B-Scan Spectral Domain Optical Coherence Tomography (OCT) and by a new multimodal approach based on the “En-Face” visualization of the macular area obtained with a Spectralis OCT2-ANGIOGRAPHY (Heidelberg Engineering, Heidelberg, Germany). A macro-structural and micro-structural analysis (on a  $15 \times 10^\circ$  area) was performed to achieve the difference in detecting capability between the two diagnostic protocols. In order to obtain the best En-Face OCT2-ANGIOGRAPHY images a 25  $\mu\text{m}$  thickness C-scan section was shaped on the ILM profile till the end depth of the foveal depression and then modeled to the BM shape from this level to the Haller’s layer.

**Results:** The visualization of the superficial retinal vascular layers was appreciable with both protocols, but the En-Face OCT2-ANGIOGRAPHY offered the possibility to study in detail the deep capillary plexus (in its two components) and the connections with the superficial one. Moreover the En-Face and the OCT2-ANGIOGRAPHY allowed us to distinguish different choroidal

vascular layers, including Choriocapillaris and often to highlight the connections between these layers.

**Conclusions:** Our study shows the capability of the Spectralis OCT2-ANGIOGRAPHY system to analyze in detail the whole retinal and choroidal vascular tissue in order to be a useful reference in case of pathological conditions.



**Commercial Relationships:** Marco Lupidi, None; Gabriel J. Coscas, None; Florence Coscas, None

**Program Number:** 3326 **Poster Board Number:** B0109

**Presentation Time:** 11:00 AM–12:45 PM

**Characterizing the Effect of Anti-VEGF Injection on Choroidal Neovascularization Using Optical Coherence Tomography Angiography**

Nora W. Muakkassa, Adam T. Chin, Talisa de Carlo, Caroline R. Baumal, Andre Witkin, Jay S. Duker, Nadia K. Waheed. Ophthalmology, New England Eye Center/Tufts Medical Center, Boston, MA.

**Purpose:** To measure the change in size of choroidal neovascularization (CNV) in response to anti-vascular endothelial growth factor (VEGF) treatment measured using a spectral domain optical coherence tomography angiography (SD-OCTA) system.

**Methods:** Eight eyes from eight patients diagnosed with CNV who underwent OCTA pre and post-treatment with anti-VEGF agents were enrolled. One eye was treatment-naïve. Each eye was imaged prior to treatment and scanned at multiple follow up visits using the prototype AngioVue OCTA system applying a split-spectrum amplitude decorrelation angiography (SSADA) algorithm on a SD-OCT device (Optovue Inc, Fremont, CA). The system operated at 70,000 A-scans per second to acquire OCTA volumes of  $304 \times 304$  A-scans. Orthogonal registration and merging of two consecutive image sets were used to obtain OCT angiograms. OCTA volumes were segmented into 30-50 micrometer-thick en-face segments demonstrating the dimensions of the CNV. Trained readers at the Boston Image Reading Center measured the greatest linear dimension and the area of the CNV in the pre-treatment and post-treatment images. The primary outcomes of the study were greatest linear dimension and area of the CNV. Secondary outcomes included the appearance of CNV (well-circumscribed versus poorly

circumscribed), the presence of subretinal and/or intraretinal fluid on OCT B-scan, and visual acuity.

**Results:** Eight eyes of eight patients with CNV were scanned with the OCTA system. Ages ranged from 31 – 85 and included four males and four females. Etiology of CNV included age-related macular degeneration, multifocal choroiditis and central serous chorioretinopathy. 50 % of eyes had significant reduction in the length and area of the CNV after treatment as well as resolution of subretinal fluid. 25 % had no change in the size of the CNV and no change in amount of subretinal fluid present.

**Conclusions:** CNV size measured using OCTA may decrease after successful anti-VEGF treatment. No change in the size of the CNV may suggest resistance to anti-VEGF agents. Optical coherence tomography angiography may be a useful tool for monitoring and quantifying the response of choroidal neovascularization to treatment.

**Commercial Relationships:** **Nora W. Muakkassa**, None; **Adam T. Chin**, None; **Talisa de Carlo**, None; **Caroline R. Baumal**, None; **Andre Witkin**, None; **Jay S. Duker**, Carl Zeiss Meditec Inc. (C), Carl Zeiss Meditec Inc. (F), EyeNetra (I), Hamera Biosciences Inc. (I), Ophthotech Corp (I), Optovue (C), Optovue (F); **Nadia K. Waheed**, None

**Support:** This work was supported in part by a Research to Prevent Blindness Unrestricted grant to the New England Eye Center/ Department of Ophthalmology, Tufts University School of Medicine, and Massachusetts Lions Club.

**Program Number:** 3327 **Poster Board Number:** B0110

**Presentation Time:** 11:00 AM–12:45 PM

**Methodology for visualization of reduced choriocapillaris density using optical coherence tomography angiography**

*Simon S. Gao, Yali Jia, Nieraj Jain, Mark E. Pennesi, David Huang.* Ophthalmology, Oregon Health & Science University, Portland, OR.

**Purpose:** To develop a method of visualizing reduced choriocapillaris density using optical coherence tomography (OCT) angiography.

**Methods:** Macular scans of a participant with a clinical diagnosis of choroideremia were taken using a spectral OCT system (RTVue-XR) and compared with normal participants. The split-spectrum amplitude-decorrelation angiography algorithm was used to detect flow. The inner retinal layer from the internal limiting membrane to 90  $\mu\text{m}$  below showed the retinal circulation. The choriocapillaris layer was defined to be 10  $\mu\text{m}$  below Bruch's membrane to 20  $\mu\text{m}$  below. Flow projections from retinal vessels were treated as null in the choriocapillaris layer. The choriocapillaris angiogram was then split into 8x8 superpixels, and the vessel density was calculated for each superpixel. This vessel density map was then smoothed using linear interpolation.

**Results:** In the choroideremia case, *en face* OCT angiogram of the retinal circulation appeared normal (Fig. 1A). The *en face* structural OCT of the retinal pigment epithelium (RPE) showed hyporeflexive regions indicating RPE loss (Fig. 1B). The choriocapillaris angiogram and vessel density map showed distinct areas of reduced flow (Fig. 1C-E). Overlay (Fig. 1F) showed patches of reduced choriocapillaris vessel density within regions of RPE loss.

**Conclusions:** We have developed a method to visualize reduced choriocapillaris density. This method may be useful in the assessment of diseases such as choroideremia and age-related macular degeneration.

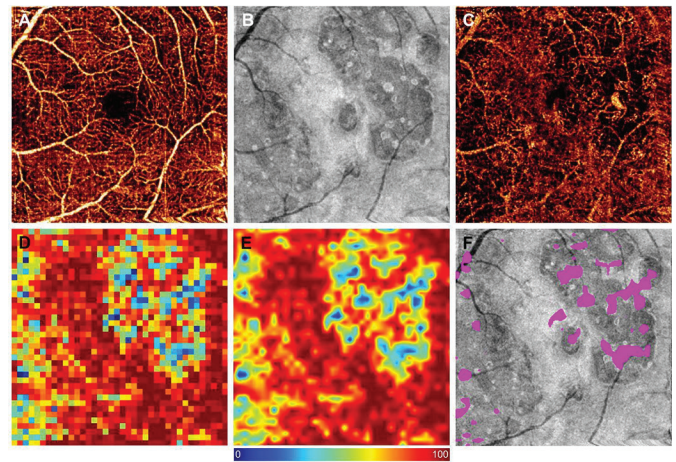


**Figure 1.** (A) *En face* OCT angiogram of the retinal circulation in a patient with choroideremia. (B) *En face* OCT structural image of the retinal pigment epithelium. (C) OCT angiogram of the choriocapillaris. (D) Vessel density map of the choriocapillaris. (E) Smoothed vessel density map. Scale bar shows vessel density from 0% (blue) to 100% (red). (F) Areas where the vessel density was less than 50% (pink-purple) overlaid on (B).

**Commercial Relationships:** **Simon S. Gao**, None; **Yali Jia**, Optovue, Inc. (F), Optovue, Inc. (P); **Nieraj Jain**, None; **Mark E. Pennesi**, Sucampo Pharmaceuticals (C); **David Huang**, Carl Zeiss Meditec, Inc. (P), Optovue, Inc. (F), Optovue, Inc. (I), Optovue, Inc. (P)

**Support:** NIH grants R01 EY023285, R01 EY024544, DP3 DK104397, K08 EY021186 and T32 EY23211; CTSA grant UL1TR000128; FBB grants CD-NMT-0914-0659-OHSU and CDA CF-CL-0614-0647-OHSU; Alcon Research Institute Young Investigator Grant; Career Development Award from RPB and an unrestricted grant from RPB

**Program Number:** 3328 **Poster Board Number:** B0111

**Presentation Time:** 11:00 AM–12:45 PM

**Longitudinal monitoring of choroidal neovascularization by OCT angiography in mice**

*wenzhong Liu<sup>1</sup>, Ji Yi<sup>1</sup>, Ronil S. Shah<sup>2</sup>, Brian Soetikno<sup>3</sup>, Amani A. Fawzi<sup>2</sup>, Hao F. Zhang<sup>1,2</sup>.* <sup>1</sup>Biomedical Engineering, Northwestern University, Evanston, IL; <sup>2</sup>Department of Ophthalmology, Northwestern University, Evanston, IL; <sup>3</sup>Feinberg School of Medicine, Northwestern University, Evanston, IL.

**Purpose:** Early detection of choroidal neovascularization (CNV) remains challenging in clinical practice by existing optical coherence tomography (OCT) and fluorescein angiography. Recently developed OCT angiography enhanced the blood flow contrast and suppressed the other static tissue signals, which allows us to visualize CNV directly. We hypothesize that OCT angiography can effectively detect CNV.

**Methods:** Adult pigmented mice were anesthetized by ketamine/xylene cocktail and subjected to laser treatment following established protocols of laser induced CNV around optic disc. Two OCT systems working in near infrared (NIR-OCT) and visible light range were used to provide complementary images for CNV characterization. A peripapillary area of 2x2mm<sup>2</sup> centering optic nerve disk was imaged with both OCT systems. The OCT angiography scanning protocol scanned the same B-scan location twice and took the difference to enhance the blood flow contrast. The choroidal vasculature was extracted from the three-dimensional OCT angiography. OCT

structural image and angiography were registered and compared between NIR and visible light OCT images. Four different CNV lesions were monitored longitudinally for 4 weeks after laser.

**Results:** NIR-OCT provides better penetration depth into choroidal layer (sample image can be found in Figure 1) and the visible light OCT provides superb axial resolution down to 1 micrometer. We quantified the CNV area/volume from 3D angiography. We observed the choroidal vascular remodeling on both NIR and visible light OCT, which started around 4 days and peaked one week after laser induction. The CNV lesion gradually regressed afterwards.

**Conclusions:** Compared to conventional OCT images, OCT angiography provides enhanced contrast from vasculature and can be used to detect and monitor the progression of CNV.

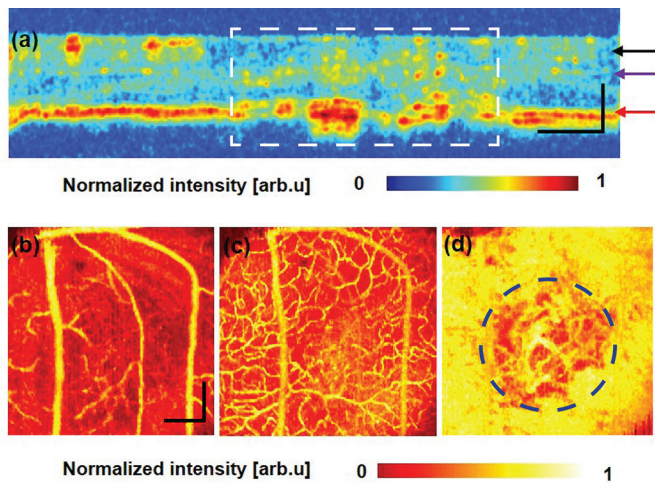


Figure 1. NIR OCT angiography of a CNV mouse. (a) Sample OCT angiography B-scan. The dash box indicates the CNV location. (b) OCT angiography of major retinal vessels from the layer indicated by black arrow in (a). (c) OCT angiography of retinal capillaries from the layer indicated by purple arrow in (a). (d) OCT angiography of choroidal vessels from the layer indicated by red arrow in (a). CNV position is circled by the dash ring. Bar: 100  $\mu$ m for (a) and 200  $\mu$ m for (b).

**Commercial Relationships:** wenzhong Liu, None; Ji Yi, None; Ronil S. Shah, None; Brian Soetikno, None; Amani A. Fawzi, None; Hao F. Zhang, None

**Support:** HHMI international student fellowship, NIH grants 1R01EY019951, NIH grants 1R24EY022883

**Program Number:** 3329 **Poster Board Number:** B0112

**Presentation Time:** 11:00 AM–12:45 PM

#### Detection of occult choroidal neovascularization in age-related macular degeneration with optical coherence tomography angiography

Steven T. Bailey<sup>1</sup>, Yali Jia<sup>1</sup>, Christina J. Flaxel<sup>1</sup>, Thomas S. Hwang<sup>1</sup>, Martin F. Kraus<sup>2</sup>, David Huang<sup>1</sup>. <sup>1</sup>Ophthalmology, Casey Eye Institute, OHSU, Portland, OR; <sup>2</sup>Advanced Optical Technologies, Pattern Recognition Lab, Erlangen-Nuremberg, Germany.

**Purpose:** To visualize occult choroidal neovascularization (CNV) in age-related macular degeneration using OCT angiography.

**Methods:** 15 eyes from 13 study participants with active occult CNV, as defined by fluorescein angiography (FA), were scanned with either a prototype (100 kHz A-scan repetition rate) swept-source OCT acquiring 3x3 mm scans or a commercially available high-speed spectral OCT (70 kHz, RTVue XR, Optovue, Inc.) acquiring both 3X3 and 6X6 mm scans. Flow was detected with the split-spectrum

amplitude decorrelation angiography (SSADA) algorithm and motion artifact was removed by 3D orthogonal registration and merging of 2 scans. The volumetric angiogram was segmented into inner retinal, outer retinal and choroidal layers to construct separate *en face* angiograms. CNV was identified as vessels above Bruch's Membrane in the outer retinal layer. CNV area was assessed by summing pixels with detectable flow in the *en face* outer retinal angiogram. Composite color-coded angiograms allowed for *en face* visualization of multiple vascular beds as well as representation of both flow and structure on cross sections.

**Results:** In 9 eyes with fibrovascular pigment epithelial detachment (PED), large CNV vessels with smaller vascular fronds were seen with OCT angiography; while FA revealed only large diffuse areas of staining and leakage (Fig 1). In 6 eyes with stippled hyperfluorescence from an undetermined source with FA, OCT angiography demonstrated a clearly defined vascular network in the outer retina (Fig. 2). CNV area could be assessed in all cases. Cross-sectional OCT angiograms demonstrated type 1 CNV in all cases. **Conclusions:** OCT angiography with SSADA improved visualization of occult CNV compared to FA. All cases were type 1 CNV. CNV were ill-defined with FA due to fluorescein leakage and from blockage from retinal pigment epithelial cells. CNV areas were quantified with OCT angiography, which may be useful barometer in assessing response to treatment.

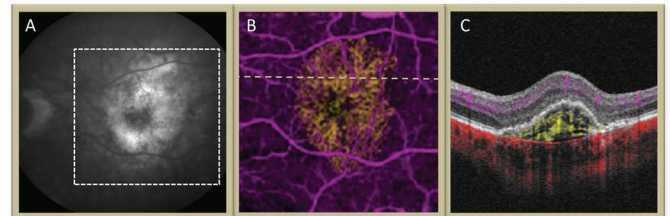


Fig 1. A, Late phase FA. B, 6X6 mm OCT angiogram: retinal vessels (purple) and CNV (yellow). C, Horizontal cross-sectional OCT angiogram (retinal vessels – purple; CNV – yellow; choroidal vessels – red) of type 1 CNV

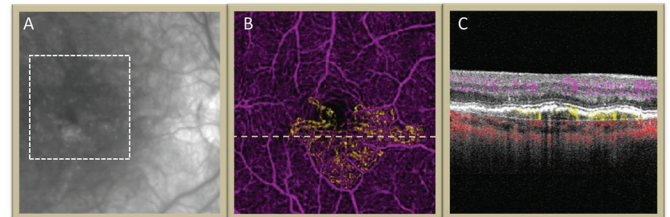


Fig 2. A, Late phase FA. B, 3X3 mm OCT angiogram: retinal vessels (purple) and CNV (yellow). C, Horizontal cross-sectional OCT angiogram of type 1 CNV

**Commercial Relationships:** Steven T. Bailey, None; Yali Jia, Optovue INC (P); Christina J. Flaxel, None; Thomas S. Hwang, None; Martin F. Kraus, Optovue Inc. (P); David Huang, Carl Zeiss Meditec, Inc. (P), Optovue, Inc. (C), Optovue, Inc. (F), Optovue, Inc. (I), Optovue, Inc. (P), Optovue, Inc. (R)

**Support:** R01 EY024544, RPB, CTSA grant (UL1TR000128)

**Program Number:** 3330 **Poster Board Number:** B0113  
**Presentation Time:** 11:00 AM–12:45 PM  
**Sensitivity and Specificity of Ultra-High Speed Optical Coherence Tomography Angiography in Detection of Choroidal Neovascularization in Neovascular Age-Related Macular Degeneration**

Anthony Joseph<sup>1</sup>, Talisa E. de Carlo<sup>1</sup>, Mehreen Adhi<sup>1</sup>, Eric Moul<sup>2</sup>, Nadia Waheed<sup>1</sup>, Caroline Baumal<sup>1</sup>, Woo Jhon Choi<sup>2</sup>, James G. Fujimoto<sup>2</sup>, Jay S. Duker<sup>1</sup>, Andre Witkin<sup>1</sup>. <sup>1</sup>New England Eye Center and Tufts Medical Center, Boston, MA; <sup>2</sup>Department of Electrical Engineering and Computer Science, Massachusetts Institute of Technology, Boston, MA.

**Purpose:** To estimate the sensitivity and specificity for the detection of choroidal neovascularization (CNV) using ultrahigh speed swept source optical coherence tomography angiography (SS-OCTA) in patients with neovascular age-related macular degeneration (AMD).

**Methods:** In this retrospective observational cross-sectional study, patients with a clinical diagnosis of neovascular AMD were evaluated at New England Eye Center between January 2014 and November 2014. 25 patients who received ultrahigh speed SS-OCTA (Massachusetts Institute of Technology, Cambridge MA) and 50-degree fluorescein angiography (FA) on the same day were evaluated. The SS-OCTA software co-registers the SS-OCTA en-face angiograms with SS-OCTA correlating b-scans allowing for visualization of structure and blood flow in tandem. FA, SS-OCTA angiograms, and SS-OCTA correlating b-scans were independently reviewed by two masked *Boston Image Reading Center* (BIRC) trained readers to identify CNV. Sensitivity and specificity of CNV detection using SS-OCTA were calculated using FA as the ground truth in three different ways: (1) SS-OCTA angiograms alone (2) SS-OCTA correlating b-scans alone (3) SS-OCTA angiograms and correlating b-scans.

**Results:** Sensitivity of CNV detection was moderate when using either SS-OCTA angiograms or SS-OCTA correlating b-scans alone. However, sensitivity improved when using the SS-OCTA images in tandem. Specificity was high in all three groups.

**Conclusions:** SS-OCTA is able to non-invasively visualize CNV which may provide a method for identifying and guiding treatment of CNV. The sensitivity and specificity of CNV detection on ultra-high SS-OCTA compared with FA appears high. Future studies with larger sample sizes are needed to better elaborate on the sensitivity and specificity of CNV detection and illustrate clinical utility.

**Commercial Relationships:** Anthony Joseph, None; Talisa E. de Carlo, None; Mehreen Adhi, None; Eric Moul, None; Nadia Waheed, None; Caroline Baumal, None; Woo Jhon Choi, None; James G. Fujimoto, Carl Zeiss Meditech Inc. (P), Optovue Inc. (I), Optovue Inc. (P); Jay S. Duker, Carl Zeiss Meditech Inc. (C), EyeNetra (I), Hemera Biosciences Inc. (I), Ophthotech Corp. (I), Optovue Inc. (C); Andre Witkin, None

**Support:** This work was supported by the National Institute of Health (NIH R01-EY011289-27, R44-EY022864-01, R44-EY022864-02, R01-CA075289-16), Air Force Office of Scientific Research (AFOSR FA9550-10-1-0551 and FA9550-12-1-0499), a Samsung Scholarship, and by a Natural Sciences and Engineering Research Council of Canada Scholarship.

**Program Number:** 3331 **Poster Board Number:** B0114  
**Presentation Time:** 11:00 AM–12:45 PM

**Histopathological correlation of optical coherence tomography angiography in laser-induced choroidal neovascularization**

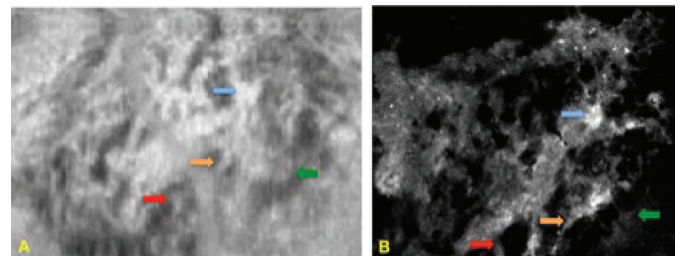
Ronil S. Shah<sup>2</sup>, Brian Soetikno<sup>2,1</sup>, wenzhong Liu<sup>1</sup>, Ji Yi<sup>1</sup>, Hao F. Zhang<sup>1</sup>, Amani A. Fawzi<sup>2</sup>. <sup>1</sup>Biomedical Engineering, Northwestern University, Evanston, IL; <sup>2</sup>Ophthalmology, Feinberg School of Medicine - Northwestern University, Chicago, IL.

**Purpose:** In-vivo assessment of choroidal neovascularization (CNV) is currently done via optical coherence tomography (OCT) and fluorescein/ICG angiography, and recently, the novel technology of OCT angiography (OCT-ang) - a system capable of measuring retinal blood flow. The purpose of this study is to explore whether OCT-ang accurately correlates with histological neovascularization in an experimental model of murine laser induced CNV.

**Methods:** Twenty adult pigmented mice of mixed background were anesthetized and subjected to laser induced CNV following pre-established protocols. Four laser lesions were applied around the optic nerve to induce rupture Bruch's membrane; laser applications that did not result in a bubble formation indicating rupture of Bruch's membrane were excluded from analysis. Animals were imaged with OCT-ang at varying intervals between 1 to 28 days post laser injury in order to visualize the development & regression of CNV. Histological samples were obtained at the corresponding intervals - eyes were paraformaldehyde-fixed and stored in phosphate buffered saline at 4°C. The choroid was dissected, stained with isolectin B4 and flat mounted to visualize the CNV. These images were compared to OCT-ang images obtained the same day.

**Results:** Comparing the images obtained from OCT-ang to the immunostained flat mount shows consistency between the two modalities. The vessels visualized by the OCT-ang are representative of the vessels visualized via immunostaining of the choroidal flat mount (see figure). We observed that the OCT-ang images have better contrast between background and neovascular images. Further analysis of the various time points is underway to identify the earliest detectable lesion on OCT-ang.

**Conclusions:** OCT angiography of CNV correlates well with the true choroidal morphology as viewed in choroidal vascular flat mount. Since the murine laser induced CNV model is a widely accepted model for human neovascular AMD, this technology holds promise for in vivo detection & management for neovascular AMD.



A) En face choroidal OCT-ang image of CNV lesion; B) Confocal microscopy of choroid flat mount of the same lesion obtained the same day - immunostained with isolectin B4 (stains vascular endothelium). Arrows highlight same areas on both images; slight disparity because OCT-ang image is a 20-micron thick slab compared to a 2-micron thick confocal slice.

**Commercial Relationships:** Ronil S. Shah, None; Brian Soetikno, None; wenzhong Liu, None; Ji Yi, None; Hao F. Zhang, None; Amani A. Fawzi, None

**Support:** Research to Preventing Blindness, NY (Department of Ophthalmology, Northwestern University); Macula Society Research Grant (AAF)



**Program Number:** 3332 **Poster Board Number:** B0115

**Presentation Time:** 11:00 AM–12:45 PM

**Fate of non-perfused vessels in ischemic retina**

Marcus Fruttiger<sup>1</sup>, Michael Pownier<sup>1</sup>, Ryan Jones<sup>1</sup>, Weijen Tan<sup>1</sup>, Meidong Zhu<sup>2</sup>, Andrew A. Chang<sup>3</sup>, Dawn A. Sim<sup>3</sup>, Pearse A. Keane<sup>4</sup>, Adnan Tufail<sup>5</sup>, Catherine A. Egan<sup>5</sup>. <sup>1</sup>UCL Institute of Ophthalmology, London, United Kingdom; <sup>2</sup>Save Sight Institute, Sydney, NSW, Australia; <sup>3</sup>Sydney Retina Clinic and Day Surgery, Sydney, NSW, Australia; <sup>4</sup>NIHR Biomedical Research Centre for Ophthalmology, Moorfields Eye Hospital, London, United Kingdom; <sup>5</sup>Moorfields Eye Hospital, London, United Kingdom.

**Purpose:** Ischemic retinopathy is associated with several vision threatening complications, such as neural atrophy, vascular leakage and neovascularisation. Traditionally ischemia has been assessed by fluorescein angiography, visualising perfused vessels. Although this method does not provide any information about non-perfused vessels, it is often assumed that vessels in ischemic areas regress. Here we aim to learn more about the longterm fate of non-perfused vessels in the retinal vasculature.

**Methods:** Optical coherence tomography (Avanti Angiovue SDOCT, Optovue, Inc. Fremont, CA, USA) was used to visualise perfusion as well as structural properties of the retinal vasculature in patients suffering from retinal vascular occlusions. In addition, post mortem tissue from a patient with long standing (6 years) central retinal vein occlusion (CRVO) was investigated, using immunohistochemistry on whole mount retina and paraffin sections to visualise blood vessel components and retinal cells.

**Results:** Comparing OCT angiography (based on speckle variance) with en-face OCT images from selected retinal layers revealed that in ischemic areas of the retina non-perfused, larger vessels could be detected as hyper reflective structures. Furthermore, analysis of the CRVO postmortem tissue revealed perfect preservation of the basement membrane from all retinal vessels, including capillaries. However, these non-perfused “vessels sleeves” did not contain endothelial cells or pericytes.

**Conclusions:** Our data suggests longterm preservation of vascular basement membrane in ischemic retina. This has implications for therapeutic approaches aiming to alleviate retinal ischemia via cell therapy.

**Commercial Relationships:** Marcus Fruttiger, Astra Zeneca (F), Novartis (F); Michael Pownier, None; Ryan Jones, None; Weijen Tan, None; Meidong Zhu, None; Andrew A. Chang, None; Dawn A. Sim, None; Pearse A. Keane, None; Adnan Tufail, Alergan (C), Bayer (C), GSK (C), Novartis (C), Pfizer (C), Thrombogenics (C); Catherine A. Egan, None

**Support:** Fight for Sight, Diabetes UK, NIHR Biomedical Research Centre at Moorfields Eye Hospital and UCL Institute of Ophthalmology, Moorfields Trustees, Lowy Medical Research Institute

**Program Number:** 3333 **Poster Board Number:** B0116

**Presentation Time:** 11:00 AM–12:45 PM

**Imaging of choroidal neovascularization by Angio-OCT: a comparison with indocyanine green angiography (ICGA)**

Vittoria Ravera, Marco Pellegrini, Marta Oldani, Matteo G. Cereda, Alessandra Acquistapace, Giovanni Staurenghi. Clinical Science “Luigi Sacco”, University of Milan, Milan, Italy.

**Purpose:** To evaluate the visibility of choroidal neovascularizations (CNVs) in patients affected by age related macular degeneration (ARMD) or inflammatory affections by Angio-OCT imaging and to compare findings with fluorescein and indocyanine green angiography (FA and ICGA)

**Methods:** Retrospective study. All the patients underwent a complete ophthalmological examination including blue autofluorescence (B-FAF), fluorescein (FA) and indocyanine green (ICGA) angiography, spectral domain optical coherence tomography (SD-OCT) (HRA + OCT Spectralis, Heidelberg Engineering, Heidelberg, Germany) and angio-OCT using AngioVue technologies (Optovue Inc.)

**Results:** 20 eyes of 20 patients with CNVs were included in the study: 19 secondary to exudative age-related macular degeneration and one inflammatory. FA was evaluated in order to classify CNVs and to define their activity. 13 eyes displayed CNV type 1 (occult), 4 CNV type 2 (classic), 2 presented a combination of the two (minimally or predominantly classic), and 1 was a CNV type 3 (retinal angiomatous proliferation). On ICGA, CNV complex was visible in 99% of cases, whereas the precise characterization of the vessels belonging to the lesion was possible only in 30% of cases. On Angio-OCT the visibility of the CNV complex was typically better compared with ICGA (100% of cases), particularly allowing a better identification of the neovascular network. On SD-OCT we determined the presence of subretinal fluid or blood and pigmented epithelium detachment (PED) to determine if they reduced the visibility of the net on SSADA. Imaging was not limited by either subretinal fluid or blood while PED produced mild masking

**Conclusions:** Angio-OCT represents a novel diagnostic technique capable to perform non-invasive high resolution imaging of the retina and choroid. Further studies are required to study its reproducibility and applications in the clinical scenario

**Commercial Relationships:** Vittoria Ravera, None; Marco Pellegrini, Bayer (S); Marta Oldani, None; Matteo G. Cereda, None; Alessandra Acquistapace, None; Giovanni Staurenghi, Alcon Laboratories, Inc. (C), Allergan, Inc. (C), Bayer (C), Boehringer (C), Genentech (C), GlaxoSmithKline (C), Heidelberg Engineering (C), Novartis Pharmaceuticals Corporation (C), Novartis Pharmaceuticals Corporation (S), Ocular instruments, Inc. (P), Optos, Inc. (C), Optovue (S), Roche (C), Zeiss (C), Zeiss (S)

**Program Number:** 3334 **Poster Board Number:** B0117

**Presentation Time:** 11:00 AM–12:45 PM

**OCT Angiography (OCTA) of Macular Neovascularization (MNV)**

Emeline R. Ramenaden<sup>1</sup>, John E. Legarreta<sup>1</sup>, Andrew D. Legarreta<sup>1</sup>, Douglas Matsunaga<sup>2</sup>, Amir H. Kashani<sup>2</sup>, Giovanni Gregori<sup>1</sup>, Qinqin Zhang<sup>3</sup>, Ruikang K. Wang<sup>3</sup>, Carmen A. Puliafito<sup>2</sup>, Philip J. Rosenfeld<sup>1</sup>. <sup>1</sup>Ophthalmology, Bascom Palmer Eye Institute, University of Miami Miller School of Medicine, Miami, FL; <sup>2</sup>USC Eye Center, Keck School of Medicine, University of Southern California, Los Angeles, CA; <sup>3</sup>Bioengineering, University of Washington, Seattle, WA.

**Purpose:** To evaluate the microvasculature of the central macula in eyes with macular neovascularization (MNV) using swept-source (SS) and spectral-domain (SD) optical coherence tomography (OCT) angiography.

**Methods:** Subjects were enrolled in a prospective, observational study and evaluated using a high-speed 1050 nm SS-OCT prototype system (100,000 kHz) and a 840 nm SD-OCT prototype system (68,000 kHz). SS-OCT angiography was performed using a 3X3mm raster scan pattern centered on the fovea. In the transverse scanning direction, a single B-scan was comprised of 300 A-scans. Four consecutive B-scans were performed at each fixed position before proceeding to the next transverse position on the retina. A total of 300 B-scan positions located 10 µm apart over a 3 mm distance were sampled. SD-OCT angiography was performed using a 3X3mm and 6X6mm raster scan pattern. In the 3X3 raster scan, four consecutive B-scans, each comprised of 245 A-scans, was performed in the

transverse scanning direction. In the 6X6 raster scan pattern, the transverse scanning direction was comprised of two consecutive B-scans, each of 350 A-scans. A total of 245 B-scan positions were located 12.4  $\mu\text{m}$  apart over the 3 mm distance, and a total of 350 B-scan positions were located 17.1  $\mu\text{m}$  apart over the 6 mm distance. Algorithms segmented the retina into three layers; an inner retinal layer, a middle retinal layer, and an outer retinal layer. The choriocapillaris and choroidal vasculature were further segmented. The vascular distribution in each layer was depicted as an *en face* image. *En face* OCT angiographic images were compared to early and late phase fluorescein angiography (FA) images.

**Results:** Imaging was performed using the SS-OCT and SD-OCT instruments. OCT angiography of MNV showed well-defined microvascular networks. Furthermore, imaging before and after treatment with aflibercept demonstrated a decrease in size of the microvascular network after therapy. The decreased size of the neovascular network exposed marked flow impairment in the underlying choriocapillaris. Images obtained with both the SS-OCT and SD-OCT instruments are being compared in this ongoing study.

**Conclusions:** OCTA, which can be performed with both SS-OCT and SD-OCT instruments, provides rapid, non-invasive, high-resolution, depth-resolved, images comparable to or even better than conventional fluorescein angiography in eyes with macular neovascularization.

**Commercial Relationships:** Emeline R. Ramenaden, Carl Zeiss Meditec, Inc (F); John E. Legarreta, Carl Zeiss Meditec, Inc (F); Andrew D. Legarreta, Carl Zeiss Meditec, Inc (F); Douglas Matsunaga, Carl Zeiss Meditec, Inc (F); Amir H. Kashani, Carl Zeiss Meditec, Inc (F); Giovanni Gregori, Carl Zeiss Meditec, Inc (F), Carl Zeiss Meditec, Inc (P); Qinqin Zhang, Carl Zeiss Meditec, Inc (F); Ruikang K. Wang, Carl Zeiss Meditec, Inc (F); Carmen A. Puliafito, Carl Zeiss Meditec, Inc (F); Philip J. Rosenfeld, Carl Zeiss Meditec, Inc (F)

**Support:** Research Support from Carl Zeiss Meditec, Inc

**Program Number:** 3335 **Poster Board Number:** B0118

**Presentation Time:** 11:00 AM–12:45 PM

#### **OCT Angiography (OCTA) of Diabetic Retinopathy**

Douglas Matsunaga<sup>1</sup>, Jack Yi<sup>1</sup>, Lisa C. Olmos<sup>1</sup>, John Legarreta<sup>3</sup>, Andrew D. Legarreta<sup>3</sup>, Giovanni Gregori<sup>3</sup>, Utkarsh Sharma<sup>2</sup>, Phillip J. Rosenfeld<sup>3</sup>, Carmen A. Puliafito<sup>1</sup>, Amir H. Kashani<sup>1</sup>. <sup>1</sup>USC Eye Center, Keck School of Medicine of USC, Los Angeles, CA; <sup>2</sup>Research and Development, Carl Zeiss Meditec, Dublin, CA; <sup>3</sup>Bascom Palmer Eye Institute, Miami, FL.

**Purpose:** To non-invasively evaluate the retinal microvasculature in diabetic human subjects with swept-source (SS) and spectral-domain (SD) optical coherence tomography (OCT) angiography.

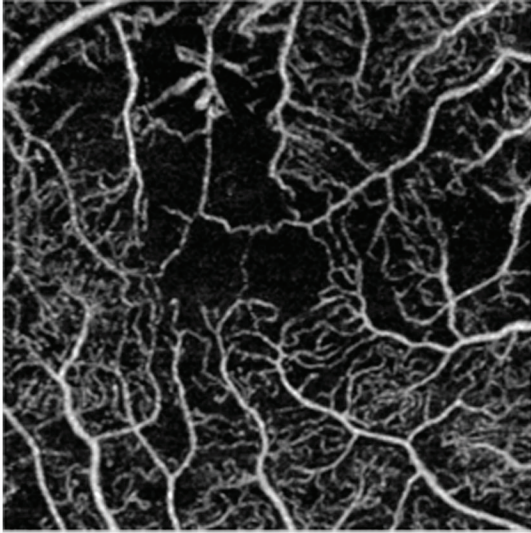
**Methods:** Ten subjects diagnosed with diabetes mellitus were enrolled in a cross-sectional, observational study and all underwent a complete ophthalmic examination. Subjects were evaluated using a high-speed 1050 nm SS-OCT prototype system (100,000 kHz) and a 840 nm SD-OCT prototype system (67,500 kHz). SD-OCT angiography was performed using a 3X3mm and 6X6mm raster scan pattern, which consisted in the transverse scanning direction of, respectively, four consecutive B-scans each comprised of 245 A-scans in the 3X3 raster scan and a pair of consecutive B-scans each comprised of 350 A-scans in the 6X6 raster scan pattern. A total of 245 B-scans positions located 12.4  $\mu\text{m}$  apart over the 3 mm distance and 350 B-scans positions located 17.1  $\mu\text{m}$  apart over the 6 mm distance were sampled. Retinal vasculature was assessed in three retinal slabs consisting of the superficial retina, middle retina and outer retina. The vasculature was reconstructed using an

intensity based algorithm and visualized *en face* for comparison with fluorescein angiograms (FA).

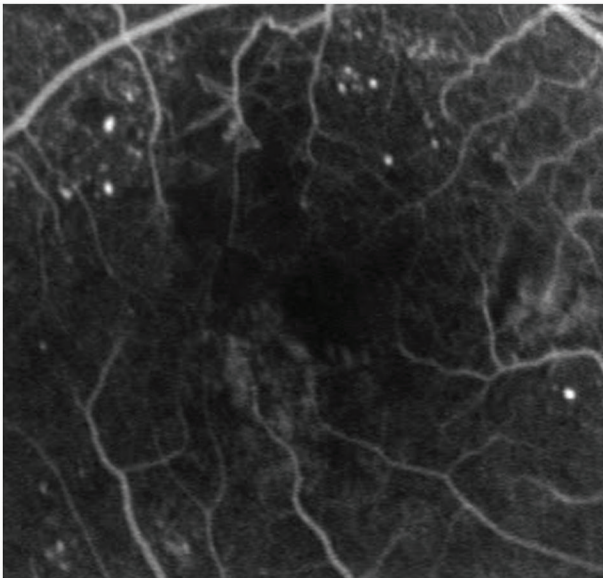
**Results:** OCTA in subjects with non-proliferative diabetic retinopathy (DR) or proliferative DR showed areas of non-perfusion, irregular capillaries, and microaneurysms that were qualitatively similar to findings on FA. However, capillary non-perfusion could be localized to either the superficial or middle retina in most cases using OCTA whereas this distinction could not be made with FA. Microaneurysms were observed in OCTA but their number, size and shape did not correspond to FA findings in some cases.

**Conclusions:** OCTA generates high-resolution images that are qualitatively similar to retinal vasculature imaged with conventional fluorescein angiography. While OCTA is completely non-invasive and may be performed with greater ease and frequency than conventional fluorescein angiography, some clinical findings, such as vascular leakage, cannot yet be assessed with OCTA. OCTA may serve as an alternative method of assessing retinal vascular changes when conventional fluorescein angiography cannot be performed.

OCT Angiogram

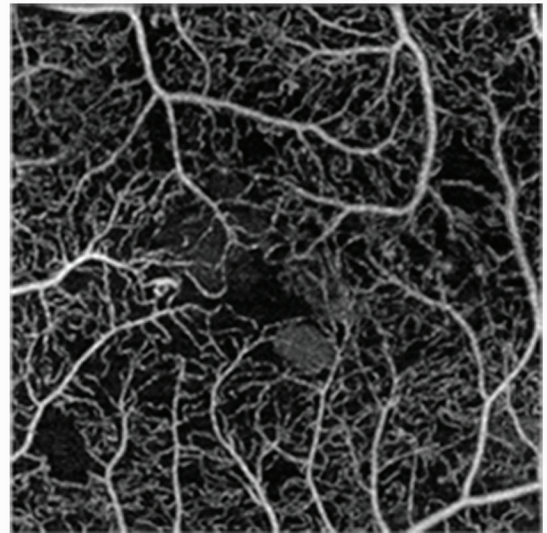


Fluorescein Angiogram

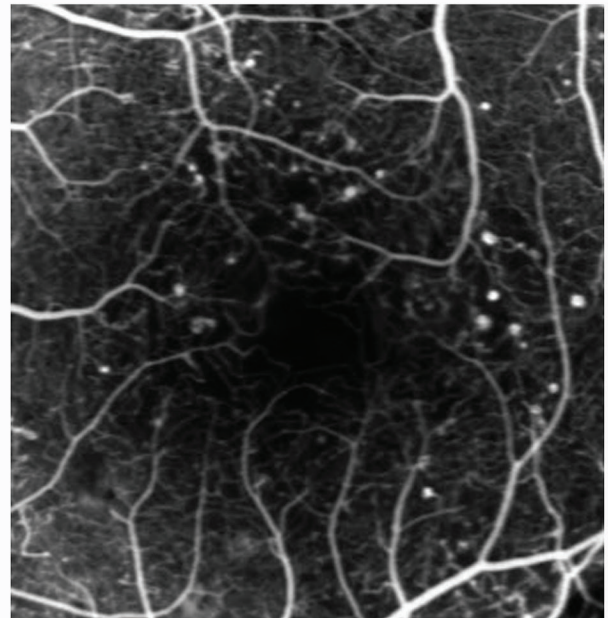


Inner retinal OCTA and FA of the fovea in a subject with severe non-proliferative diabetic retinopathy.

OCT Angiogram



Fluorescein Angiogram



Inner retinal OCTA and FA of the fovea in a subject with severe non-proliferative diabetic retinopathy.

**Commercial Relationships:** Douglas Matsunaga, Carl Zeiss Meditec (F); Jack Yi, Carl Zeiss Meditec (F); Lisa C. Olmos, Carl Zeiss Meditec (F); John Legarreta, Carl Zeiss Meditec (F); Andrew D. Legarreta, Carl Zeiss Meditec (F); Giovanni Gregori, Carl Zeiss Meditec (F); Utkarsh Sharma, Carl Zeiss Meditec (E); Philip J. Rosenfeld, Carl Zeiss Meditec (F); Carmen A. Puliafito, Carl Zeiss Meditec (F); Amir H. Kashani, Carl Zeiss Meditec (F)

**Support:** An Unrestricted grant from Research to Prevent Blindness, New York, NY 10022

**Program Number:** 3336 **Poster Board Number:** B0119

**Presentation Time:** 11:00 AM–12:45 PM

**OCT-based microangiography of diabetic retinopathy**

*Qinqin Zhang<sup>1</sup>, Cecilia S. Lee<sup>2</sup>, Yanping Huang<sup>1</sup>, Kasra Attaran-Rezaei<sup>2</sup>, Jennifer R. Chao<sup>2</sup>, Richard Munsen<sup>2</sup>, James L. Kinyoun<sup>2</sup>, Ruikang K. Wang<sup>1,2</sup>.* <sup>1</sup>Department of Bioengineering, University of Washington, Seattle, WA; <sup>2</sup>Department of Ophthalmology, University of Washington, Seattle, WA.

**Purpose:** To perform a feasibility study using OCT-based microangiography (OMAG) to generate detailed retinal microvascular maps in human subjects with diabetic retinopathy (DR)

**Methods:** A 67 kHz Cirrus HD-OCT prototype system with motion tracking (Carl Zeiss Meditec, Dublin, CA) was used to generate retinal microvascular maps in 20 eyes of 10 subjects with DR by the use of OMAG algorithms. Phase compensation and cross-correlation methods were used to provide high quality capillary perfusion maps of the retina from the 3D dataset. We also used a segmentation algorithm to separate microvasculature within landmarked physiological depth layers of the retina as well as within the choroid. The layers include ganglion cell layer+ inner plexiform layer (Inner retinal layer), inner nuclear layer + outer plexiform layer (middle retinal layer) and outer nuclear layer (Outer retinal layer). For better visualization, color coding was used for different layers: red — inner retinal layer; green — middle retinal layer and blue — outer retinal layer. Clinical fundus images and fluorescein angiograms (for most subjects) were acquired on the same day as the OCT scan and compared with resulting enface OMAG images

**Results:** Retinal OMAG images generated from the Cirrus-5000 system showed clearer microvascular maps compared to fundus images and FA. In addition, OMAG provides depth-resolved information, allowing visualization of the three landmarked physiological layers. The microvascular features of typical DR observed include microaneurysms, capillary dropout, and dilated or tortuous vessels. The results also demonstrated the ability of OCT-angiography to distinguish different forms of microaneurysms, such as saccular, fusiform and focal bulges. Most of the microaneurysms (green dots) were observed in the deeper retinal capillary plexus, originating from locations between INL and OPL. Tortuous vessels were also observed in the temporal-superior region, which is a significant feature of DR. Fig.1 gives an example of an OMAG depiction of irregular enlargement of the foveal avascular zone, consistent with mild diabetic macular ischemia, compared with the corresponding fundus image

**Conclusions:** The OCT-angiography prototype system demonstrated the capability to generate detailed retinal OMAG microvascular maps that can be valuable in aiding the diagnosis and perhaps treatment of DR

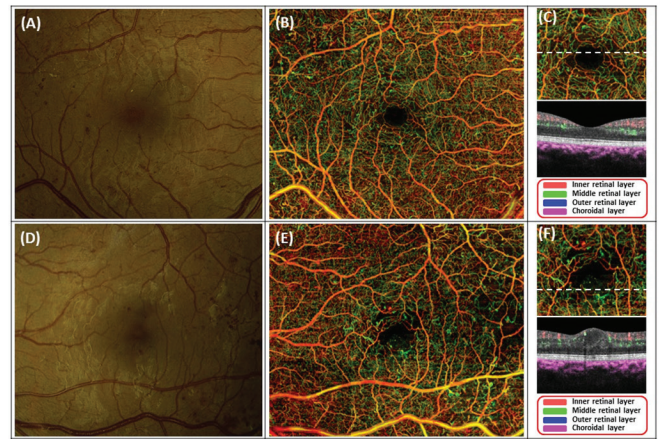


Fig 1 OMAG provides detailed visualization of retinal vasculature in DR patient

**Commercial Relationships:** Qinqin Zhang, Carl Zeiss Meditec (F); Cecilia S. Lee, None; Yanping Huang, None; Kasra Attaran-Rezaei, None; Jennifer R. Chao, None; Richard Munsen, None; James L. Kinyoun, None; Ruikang K. Wang, Carl Zeiss Meditec (F), Carl Zeiss Meditec (P)

**Support:** NEI R01EY024158, Carl Zeiss Meditec Inc, Research to Prevent Blindness.

**Program Number:** 3337 **Poster Board Number:** B0120

**Presentation Time:** 11:00 AM–12:45 PM

**Diagnosis of nonproliferative diabetic retinopathy by microaneurysm detection on swept source optical coherence tomography (SS-OCT)**

*Theodore Leng, Ryan W. Nelson.* Ophthalmology, Byers Eye Institute at Stanford, Stanford University School of Medicine, Palo Alto, CA.

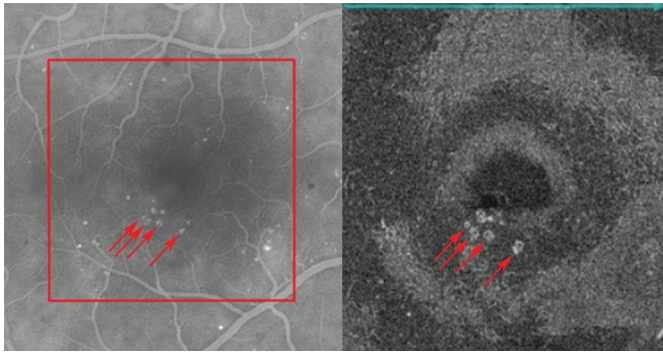
**Purpose:** To describe a novel method of identifying retinal vascular microaneurysms (MAs) in nonproliferative diabetic retinopathy (NPDR) using swept source optical coherence tomography (SS-OCT)

**Methods:** SS-OCT images were acquired in 17 eyes with NPDR using a prototype SS-OCT device with a laser wavelength centered at 1060 nm and an acquisition speed of 100,000 A-scans/sec. 3 x 3 x 3 mm raster scans were obtained centered on the fovea (512 A-scans/B-scan, 512 B-scans/cube, 1500 pixels of depth). Sequential restricted summed voxel projections, or “slabs,” were created with a thickness of 4 μm through the cube and the images registered with intravenous fluorescein angiography (FA) images obtained at the same visit. MAs were identified on SS-OCT slabs and correlated to MAs identified on FA images.

**Results:** MAs were identified in SS-OCT slabs in 15 of 17 eyes, resulting in a NPDR diagnosis rate of 88%.

A mean of 20.9 slabs (SD 3.0) were analyzed in each eye. The mean number of MAs identified on each FA was 11.7 (SD 11.9, range 1-38). The mean number of MAs identified via SS-OCT slabs was 8.1 per cube (SD 9.3, range 0-30); 62.7% (SD 31, range 0-100). The two cases with no SS-OCT MA detection had only one MA identified on FA. Ultimately, 68.84% of MAs were identified via SS-OCT slabs.

**Conclusions:** SS-OCT visualization of MAs could serve as a tool for the diagnosis of NPDR. This technique should be explored in larger studies. It may also be possible to apply this SS-OCT imaging biomarker for population-based diabetic retinopathy screening initiatives.



Fluorescein angiogram (FA) (left) and corresponding SS-OCT slab image (right) of a right eye with nonproliferative diabetic retinopathy. The right image corresponds to the area demarcated with the red box on the FA image. Microaneurysms are noted with arrows on both images.

**Commercial Relationships:** Theodore Leng, Carl Zeiss Meditec, Inc. (C); Ryan W. Nelson, None

**Support:** The prototype SS-OCT device was provided by Carl Zeiss Meditec, Inc. for this study. Institutional review board approval was obtained as this device is not currently FDA certified, but 510K clearance is pending.

**Program Number:** 3338 **Poster Board Number:** B0121

**Presentation Time:** 11:00 AM–12:45 PM

**Diabetic Retinopathy Features Detected with 6x6 mm OCT Angiogram Using SSADA Algorithm**

Thomas S. Hwang, Yali Jia, Simon S. Gao, Andreas K. Lauer, Christina J. Flaxel, Steven Bailey, Phoebe Lin, David J. Wilson, David Huang. Ophthalmology, Casey Eye Institute, Portland, OR.

**Purpose:** Diabetic retinopathy (DR) is a common retinal vascular disease with classic fluorescein angiography (FA) features that are useful for treatment and classification. OCT Angiography is a dye-free alternative to FA. Using a commercially available 70kHz OCT and the split-spectrum amplitude decorrelation angiography (SSADA) algorithm, 6x6 mm images can be obtained in 3.5 seconds. We evaluated the ability of this technique to detect the angiographic features catalogued by the Early Treatment of Diabetic Retinopathy Study (ETDRS).

**Methods:** Four patients with DR were imaged with conventional FA and OCT angiography. The images were evaluated for the ability to detect ETDRS features and other manifestations of vasculopathy.

**Results:** OCT angiography detected enlargement and distortion of the foveal avascular zone, retinal capillary dropout, and pruning of arteriolar branches. Areas of capillary loss obscured by fluorescein leakage on FA were more clearly defined on OCT angiography. Some areas of focal leakage on FA that were thought to be microaneurysms were found to be small tufts of neovascularization that extended above the inner limiting membrane.

**Conclusions:** OCT angiography does not show leakage, but can better delineate areas of capillary dropout and detect early retinal neovascularization. This new noninvasive angiography technology may be useful for routine surveillance of proliferative and ischemic changes in diabetic retinopathy.

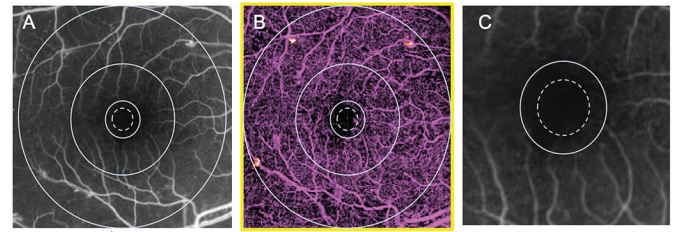


Figure 1 shows 6x6 mm fluorescein angiography (A) OCT angiogram (B) of a patient with diabetic retinopathy with ETDRS grid superposed showing FAZ enlargement inferotemporally and temporally between the 300 (dotted) and 500  $\mu$ m circles. Flow signal detected between retinal pigment epithelium (RPE) and the internal limiting membrane (ILM) is shown in magenta and signal internal to the ILM is displayed in yellow. Magnified FA (C) shows corresponding FAZ enlargement.

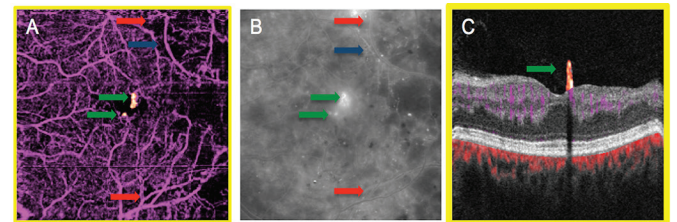


Figure 2: OCT angiogram (A) and FA (B) discloses areas of capillary dropout in the temporal macula with pruning of the arterioles. In the FA, diffuse leakage obscures an area of capillary dropout seen on OCT angiography (red arrows). An arteriole with vessel wall staining and narrowing (blue arrow) in the FA is shown to be a barely visible ghost vessel on OCT angiography. Focal areas of leakage near the fovea thought to be large microaneurysms on FA were shown to be NV on OCT angiography (green arrows).

**Commercial Relationships:** Thomas S. Hwang, None; Yali Jia, Optovue, Inc. (F); Optovue, Inc. (P); Simon S. Gao, None; Andreas K. Lauer, Oxford BioMedica (C); Christina J. Flaxel, None; Steven Bailey, None; Phoebe Lin, None; David J. Wilson, None; David Huang, Carl Zeiss Meditec, Inc. (P), Optovue, Inc. (F), Optovue, Inc. (I), Optovue, Inc. (P)

**Support:** DP3 DK104397, RPB, CTSA grant (UL1TR000128), T32 EY23211

**Program Number:** 3339 **Poster Board Number:** B0122

**Presentation Time:** 11:00 AM–12:45 PM

**Clinical evaluation of vascular lesions in diabetic retinopathy using optical coherence tomography angiography**

Akihiro Ishibazawa, Taiji Nagaoka, Atsushi Takahashi, Tsuneaki Omae, Tomofumi Tani, Kenji Sogawa, Harumasa Yokota, Akitoshi Yoshida. Ophthalmology, Asahikawa Medical University, Asahikawa, Japan.

**Purpose:** To evaluate the ability of optical coherence tomography angiography (OCTA) to visualize clinical fundus findings in patients with diabetic retinopathy (DR).

**Methods:** Forty-seven eyes of 25 patients with DR were scanned using a high-speed 840-nm-wavelength spectral-domain optical coherence tomography (OCT) instrument (RTVue XR Avanti, Optovue Inc., Fremont, CA). Blood flow was detected using the split-spectrum amplitude-decorrelation angiography (SSADA) algorithm, and three-dimensional macular or optic disc angiography was computed. Color fundus and fluorescein angiography (FA) images also were obtained in all eyes and compared to the en-face SSADA

images for the ability to visualize microaneurysms (MAs), retinal nonperfusion (RNP), and neovascularization (NV).

**Results:** Ninety-three percent of MAs detected by FA in 42 eyes appeared as focally dilated saccular or fusiform capillaries in the en-face SSADA images. The MAs were located in the superficial vascular plexus (SVP) (30.3%) or the deep capillary plexus (DCP) (69.7%). The RNP visualized by FA appeared as lesions with no or sparse capillaries in the SSADA images. Measurement of the RNP area near the macula in seven eyes showed that the RNP area in the SVP (mean  $\pm$  standard error of the mean [SEM],  $3.67 \pm 1.69$  mm<sup>2</sup>) was larger than in the DCP (mean  $\pm$  SEM,  $3.02 \pm 1.44$  mm<sup>2</sup>). The NV at the disc seen in four eyes on FA images and had marked fluorescein leakage in the early phase. The vascular structure of the NV was clearly visualized in the SSADA images. NV regression and regeneration were quantified in an eye treated with anti-vascular endothelial growth factor therapy.

**Conclusions:** OCTA can clearly visualize MAs and RNP and enables evaluation of the retinal capillaries layer by layer. Quantitative information on NV also can be obtained. OCTA may be clinically useful to evaluate the microvascular status and therapeutic effect of treatments for DR.

**Commercial Relationships:** Akihiro Ishibazawa, None; Taiji Nagaoka, None; Atsushi Takahashi, None; Tsuneaki Omae, None; Tomofumi Tani, None; Kenji Sogawa, None; Harumasa Yokota, None; Akitoshi Yoshida, None

**Support:** Grant-in-Aid for Young Scientists (B) 25861608

**Program Number:** 3340 **Poster Board Number:** B0123

**Presentation Time:** 11:00 AM–12:45 PM

**Quantitative and qualitative evaluation of Diabetic Retinopathy retinal vasculature with Cirrus-5000 Angiography prototype**

Lin An<sup>1</sup>, Mary K. Durbin<sup>1</sup>, Scott Lee<sup>2</sup>, Patty Chung<sup>2</sup>, Michal Laron<sup>1</sup>, Utkarsh Sharma<sup>3</sup>. <sup>1</sup>Application and Clinical Department, Carl Zeiss Meditec, Walnut Creek, CA; <sup>2</sup>East Bay Retina Consultants, Inc., Oakland, CA; <sup>3</sup>Advanced Development, Carl Zeiss Meditec, Dublin, CA.

**Purpose:** To demonstrate that the new Cirrus-5000 Angio-prototype is capable to achieve both quantitative and qualitative evaluations of retinal vasculature features for human subjects with Diabetic Retinopathy.

**Methods:** A Cirrus-5000 instrument was modified to allow OCT angiography imaging. The system could provide two scanning modes for imaging ocular vasculature, a 6 mm x 6 mm with 350 by 350 A-scans and a 3 mm x 3 mm scan with 245 by 245 A-scans to achieve higher resolution. Both scanning modes could be finished ~ 4 seconds. The microvasculature data obtained from OCT intensity cube were segmented into three layers (superficial, deeper and outer retinal layers) and color encoded into different colors (red, green and blue respectively). The color composite image could be used to indicate the relative depth positions of vasculature features.

A DR subject and a normal subject were recruited and imaged. Fluorescein angiography imaging and OCT angiography imaging were both performed on the DR subject, and the normal was imaged only with OCTA. Visual comparison was performed between the FA and OCTA images and features of interest were correlated. A vessel density calculation method was applied on both DR and normal OCT angiography images.

**Results:** OCT angiography revealed much clearer microvascular details compared to the FA image. Many vasculature features were well observed in the OCT angiography image. Microaneurysm, capillary drop out and capillary tortuosity could be detected through OCT angiography without using imaging dye. Unlike FA images, the OCT angiography image provided depth resolved information.

The vessel density results of normal and DR subjects clearly demonstrate that the vessel density of DR subject is lower than normal subject, which is primarily due to the capillary drop out of DR subject.

**Conclusions:** The Cirrus-5000 Angio-prototype is capable of achieving non-invasive detailed depth resolved microvasculature map for DR retinal vasculature evaluation. The images delivered by Cirrus-5000 Angio-prototype have good correlation with FA images, quantitative analysis is also possible.

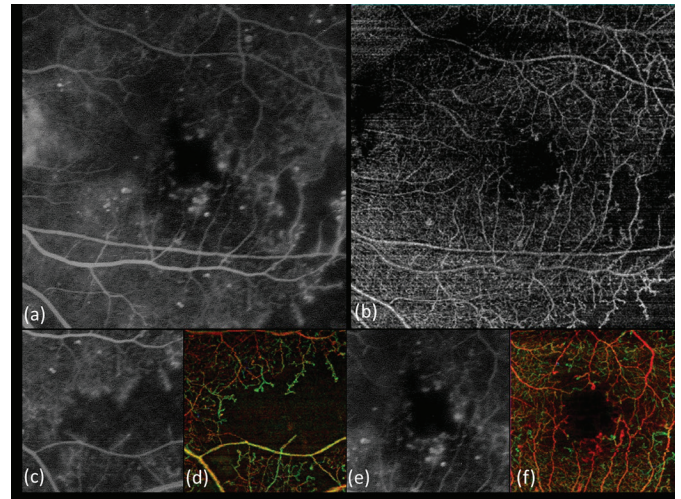


Fig 1. OCT angiography obtained from Cirrus-5000 angio prototype not only has good correlation with FA image but also reveals better details, including the micro-vasculature features and depth resolved information.

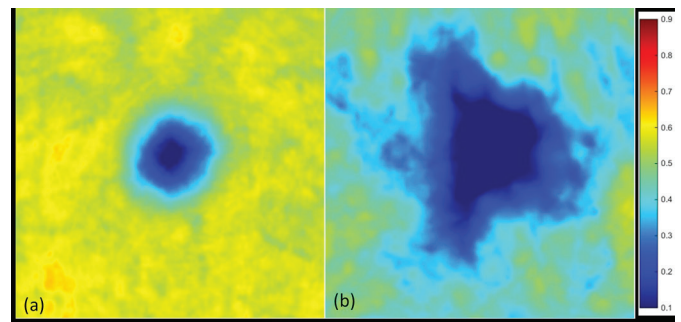


Fig 2. Retinal Vessel density map of the normal (a) and DR subject (b).

**Commercial Relationships:** Lin An, Carl Zeiss Meditec, Inc. (E); Mary K. Durbin, Carl Zeiss Meditec, Inc. (E); Scott Lee, Carl Zeiss Meditec, Inc. (C); Patty Chung, None; Michal Laron, Carl Zeiss Meditec, Inc. (E); Utkarsh Sharma, Carl Zeiss Meditec, Inc. (E)

**Program Number:** 3341 **Poster Board Number:** B0124

**Presentation Time:** 11:00 AM–12:45 PM

**Prototype Ultra-High Speed Swept Source Optical Coherence Tomography Angiography compared with Intravenous Fluorescein Angiography in Diabetic Retinopathy**

David A. Salz<sup>1</sup>, Talisa de Carlo<sup>1,2</sup>, Mehreen Adhi<sup>1,2</sup>, Eric Moul<sup>2</sup>, Woo Jhon Choi<sup>2</sup>, Caroline R. Baumal<sup>1</sup>, Andre J. Witkin<sup>1</sup>, Jay S. Duker<sup>1</sup>, James G. Fujimoto<sup>2</sup>, Nadia K. Waheed<sup>1</sup>. <sup>1</sup>Ophthalmology, Tufts Medical Center, Boston, MA; <sup>2</sup>Department of Electrical Engineering and Computer Science, and Research, MIT, Cambridge, MA.

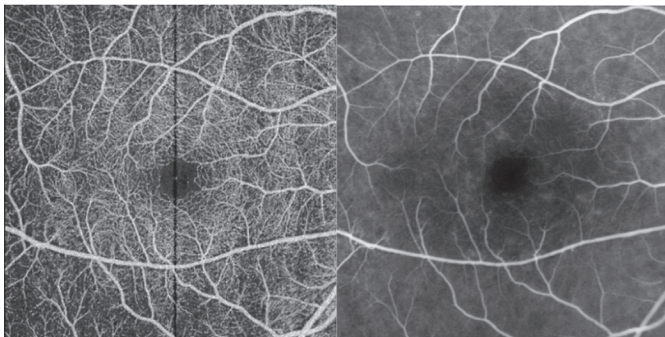
**Purpose:** To compare the utility of a prototype ultrahigh speed swept source optical coherence tomography (OCT) angiography with

intravenous fluorescein angiography (IVFA) in patients with diabetic retinopathy (DR).

**Methods:** This is a prospective observational cross-sectional study. A prototype ultra high speed swept source OCT angiography was performed using 400,000 A scans per second to scan 3mm × 3mm and 6mm × 6mm areas centered at the fovea in 11 normal eyes and 29 eyes in patients with diabetes. IVFA was performed in all patients within 8 weeks of the OCT angiography. Inclusion criteria for diabetic patients included type 1 or type 2 diabetes with a clinical examination by a retinal specialist confirming the presence of DR. Two masked *Boston Image Reading Center* (BIRC) trained readers reviewed both IVFA and OCT angiography images independently on all patients with diabetes to identify microaneurysms and other retinal abnormalities on both images. The size of the foveal avascular zone (FAZ) and the perifoveal intercapillary area was measured in both control and diabetic patients using the BIRC image analysis software. The findings were then compared to determine the clinical utility of OCT angiography compared with IVFA.

**Results:** The FAZ and perifoveal intercapillary area were enlarged in patients with DR compared with controls. Ultra high speed swept source OCT angiography was able to obtain detailed maps of the retinal microvasculature and was able to identify the majority of microaneurysms noted on fluorescein angiography with localization of their exact retinal depth within a specific vascular plexus using en face imaging. OCT angiography also revealed retinal vascular abnormalities and microaneurysms not detected by IVFA.

**Conclusions:** Ultra high speed swept source OCT angiography appears to be of significant utility in patients with DR, and is completely non-invasive as compared with IVFA. It is able to detect the majority of microaneurysms seen by IVFA, and is also able to delineate other areas of retinal vascular abnormalities that were not seen clinically or on IVFA. OCT angiography is also more accurate for determining the FAZ and perifoveal intercapillary area. OCT angiography may be of clinical utility in the evaluation and treatment of diabetic patients.



OCT angiography (left) versus IVFA (right) of the same eye with NPDR.

**Commercial Relationships:** David A. Salz, None; Talisa de Carlo, None; Mehreen Adhi, None; Eric Moul, None; Woo Jhon Choi, None; Caroline R. Baumal, None; Andre J. Witkin, None; Jay S. Duker, Carl Zeiss Meditech Inc. (F), EyeNetra (I), Hemera Biosciences Inc. (I), Ophthotech Corp. (I), Optovue, Inc. (F); James G. Fujimoto, Carl Zeiss Meditech, Inc. (P), Optivue, Inc. (I); Nadia K. Waheed, None

**Support:** This work was supported in part by a Research to Prevent Blindness Unrestricted grant to the New England Eye Center/ Department of Ophthalmology, Tufts University School of Medicine, National Institutes of Health (NIH) contracts R01-EY011289-28, R01-EY013178-12, R01-CA075289-16, Air Force Office of Scientific Research contracts FA9550-10-1-0551 and FA9550-12-1-0499, DFG contracts DFG-HO-1791/11-1, DFG Training Group 1773, DFG-GSC80-SAOT, and Massachusetts Lions Club.

**Program Number:** 3342 **Poster Board Number:** B0125

**Presentation Time:** 11:00 AM–12:45 PM

**Quantitative Analysis of Capillary Network Density in Diabetic Retinopathy Using Optical Coherence Tomography with Split-Spectrum Amplitudinal Decorrelation Angiography**

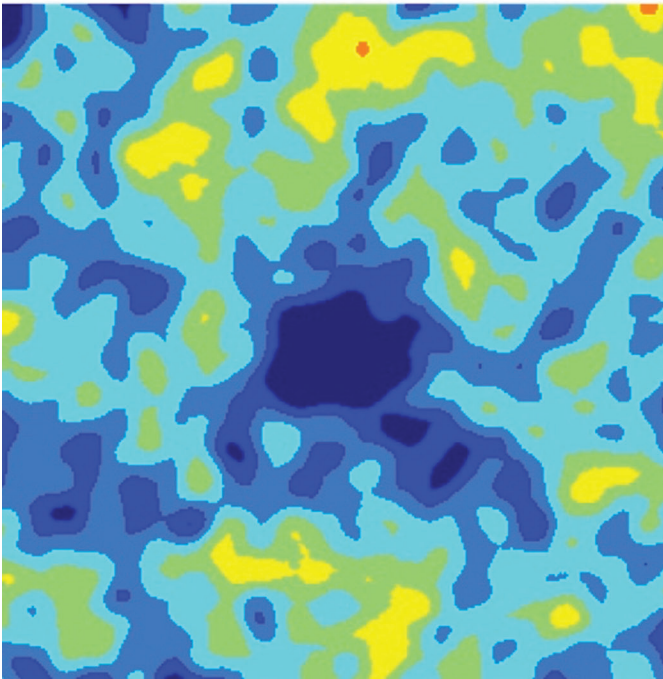
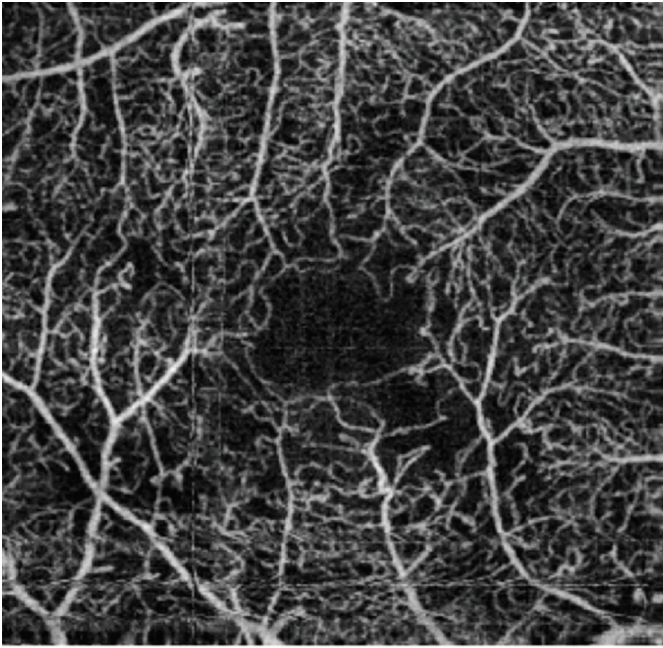
Steven Agemy<sup>1</sup>, Jessica Lee<sup>1</sup>, Patricia Garcia<sup>1</sup>, Yi-Sing Hsiao<sup>2</sup>, Toco Y. Chui<sup>1</sup>, Richard B. Rosen<sup>1</sup>. <sup>1</sup>Ophthalmology, New York Eye & Ear Infirmary of Mount Sinai, New York, NY; <sup>2</sup>Optovue, Inc., Fremont, CA.

**Purpose:** To quantitatively visualize retinal vascular flow in patients with diabetic retinopathy using Optical Coherence Tomography Angiography and a novel perfusion density mapping software.

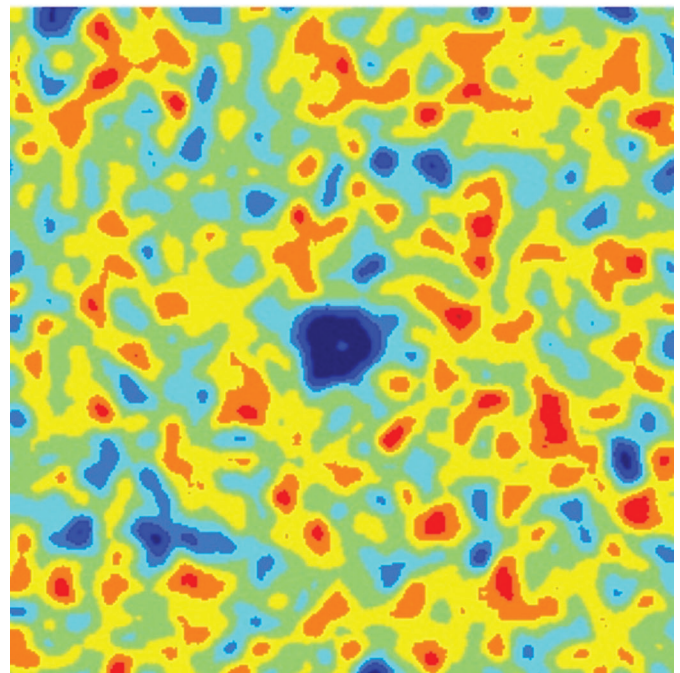
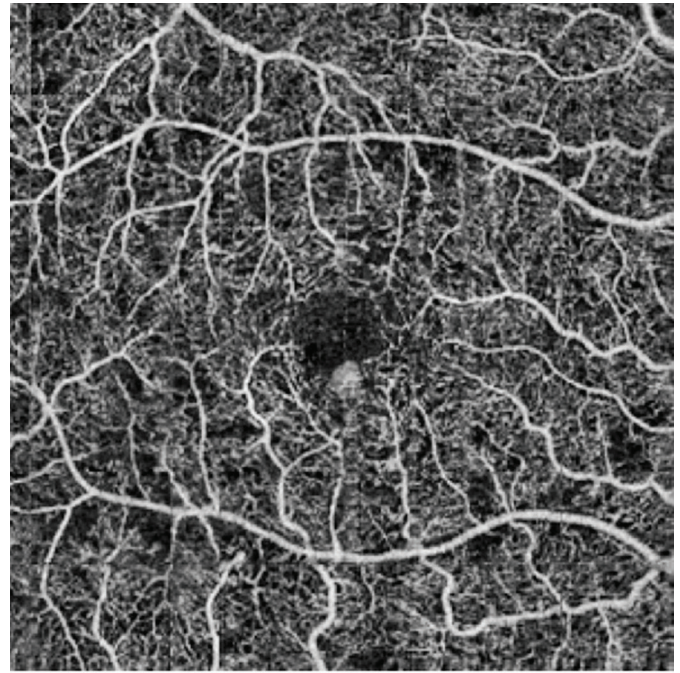
**Methods:** OCT volumetric images of the macula were obtained (3mm x 3mm and 6mm x 6mm) at 70 kHz A-scans per second using the Optovue Avanti XR OCT system (Fremont, CA). Prototype software employing the split-spectrum amplitudinal decorrelational algorithm (SSADA) was used to construct SD-OCT angiograms of the macular microvasculature. These images were then skeletonized using Matlab software and processed to create topographic maps of vascular density. Average perfusion density was also calculated for the whole volumetric image.

**Results:** 18 eyes of 10 subjects with nonproliferative diabetic retinopathy, 18 eyes of 9 subjects with proliferative diabetic retinopathy, and 8 eyes of 4 control subjects were imaged. The average perfusion density for the control group was 0.2477 ± 0.0639 (3x3) and 0.2702 ± 0.1006 (6x6). While the average perfusion density for the NPDR group was significantly reduced at 0.2012 ± 0.0694 (3x3) and 0.2474 ± 0.1048 (6x6). The PDR group appeared further reduced at 0.1944 ± 0.0692 (3x3) and 0.2402 ± 0.1047 (6x6).

**Conclusions:** Topographic perfusion density mapping based upon OCT angiography provides an easily interpretable quantitative picture of retinal vascular flow. Using these novel perfusion density maps, differences between normals and diabetic eyes at various stages of retinopathy were easily recognizable. The ability to derive quantitative values for average volumetric perfusion may also prove useful for detecting progression and anticipating the need for more aggressive interventions.



SD-OCT angiography images (3mm x 3mm) of a 42 year old male with proliferative diabetic retinopathy. **Top:** Enhanced image **Bottom:** Topographic vessel density map with average perfusion density of  $0.1809 \pm 0.0701$  (skeletonized vessel count/total pixel count)



SD-OCT angiography images (6mm x 6mm) of a 61 year old female with nonproliferative diabetic retinopathy. **Top:** Enhanced image **Bottom:** Topographic vessel density map with average perfusion density of  $0.2676 \pm 0.1002$  (skeletonized vessel count/total pixel count)

**Commercial Relationships:** Steven Agemy, None; Jessica Lee, None; Patricia Garcia, None; Yi-Sing Hsiao, OptoVue, Inc. (E); Toco Y. Chui, None; Richard B. Rosen, OptoVue, Inc. (C)



**Program Number:** 3343 **Poster Board Number:** B0126

**Presentation Time:** 11:00 AM–12:45 PM

**Automated Quantification of Macular Ischemia Using Optical Coherence Tomography Angiography in Diabetic Retinopathy**

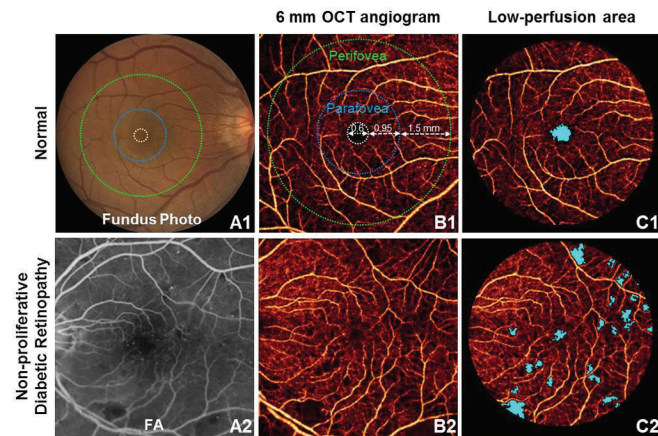
*Yali Jia, Simon S. Gao, Thomas S. Hwang, Andreas K. Lauer, Steven Bailey, Christina J. Flaxel, David J. Wilson, David Huang.* Casey Eye Institute, Oregon Health & Science University, Portland, OR.

**Purpose:** To quantify macular ischemia in diabetic retinopathy (DR) using optical coherence tomography (OCT) angiography.

**Methods:** The macula of 7 eyes of healthy control subjects and 7 eyes with various levels of DR were imaged with a commercially available 70 kHz OCT (RTVue XR, Optovue, Inc). Three dimensional (3D) OCT angiography scans were acquired over 3×3 and 6×6 mm regions by using 5 repeated B-scans at 216 raster positions, each B-scan consisting of 216 A-scans. Flow was detected with the split-spectrum amplitude decorrelation angiography (SSADA) algorithm and motion artifact was removed by 3D orthogonal registration and merging of 2 scans. Retinal angiogram was created by projecting the flow signal internal to the retinal pigment epithelium in *en face* orientation. Parafoveal and perifoveal vessel density were defined as the percentage of pixels with detectable flow in the respective regions (Fig. 1B1). The threshold for detecting flow was set at 2.33 standard deviations above the mean signal within the foveal avascular zone (FAZ) (0.6 mm circle) of the control eyes. An automated algorithm detected the area of macular low-perfusion, defined as the area with flow signal below threshold within 5.5 mm from the foveal center including the FAZ. (Fig. 1C).

**Results:** In 2 cases of DR, 6×6 mm scans were excluded due to failed registration. 3×3 mm scans of these two cases were used for the calculation of parafoveal vessel density. Compared to normal controls, the parafoveal and perifoveal vessel density were significantly reduced, low-perfusion area was significantly greater in eyes with DR. Areas of low perfusion in OCT angiogram corresponded to ischemic areas in fluorescein angiography.

**Conclusions:** OCT angiography can quantify retinal ischemia and offers an objective and rigorous method of grading macular ischemia in diabetic retinopathy.



Automated detection of nonperfusion in normal control (upper panels) and diabetic retinopathy (lower panels). White dashed circle: normal foveal avascular zone (0.6 mm diameter). Area between white and blue dashed circles: parafoveal zone. Area between blue and green dashed circles: perifoveal zone. Low-perfused areas (blue in C) are detected by identifying flow signals lower than a set cutoff point.

	Normal	Diabetic Retinopathy	P-value
Parafoveal Vessel Density (%)	88.14 ± 4.59 (n = 7)	74.72 ± 8.23 (n = 7)	0.006
Perifoveal Vessel Density (%)	90.50 ± 3.48 (n = 7)	79.25 ± 5.33 (n = 5)	0.012
Low-perfusion Area (mm <sup>2</sup> )	0.22 ± 0.06 (n = 7)	0.80 ± 0.10 (n = 5)	0.004

P-value calculated using Mann-Whitney U test.

Comparison of macular perfusion between normal controls and diabetic retinopathy

**Commercial Relationships:** Yali Jia, Optovue, Inc (F), Optovue, Inc (P); Simon S. Gao, None; Thomas S. Hwang, None; Andreas K. Lauer, None; Steven Bailey, None; Christina J. Flaxel, None; David J. Wilson, None; David Huang, Optovue, Inc (F), Optovue, Inc (I), Optovue, Inc (P)

**Support:** DP3 DK104397, R01 EY024544, CTSA grant (UL1TR000128), RPB, T32 EY23211

**Program Number:** 3344 **Poster Board Number:** B0127

**Presentation Time:** 11:00 AM–12:45 PM

**Changes in the Radial Peri-papillary Capillaries with aging: the forgotten vascular bed in glaucoma pathogenesis**

*Tailoi Chan-Ling<sup>1</sup>, Samyoul Ahn<sup>1</sup>, Mark Koina<sup>2</sup>, Samuel J. Adamson<sup>1</sup>, Marconi Barbosa<sup>3</sup>, Louise Baxter<sup>1</sup>, Frank Arfuso<sup>4</sup>, Anthony Logaraj<sup>4</sup>, George Fatseas<sup>1</sup>.* <sup>1</sup>Retinal & Developmental Neurobiology Laboratory, University of Sydney, Sydney, NSW, Australia; <sup>2</sup>ACT Pathology, Canberra Hospital, Garran, ACT, Australia; <sup>3</sup>Diagnostics for Eye Diseases Group, Eccles Institute for Neuroscience, JCSMR, Australian National University, Canberra, ACT, Australia; <sup>4</sup>School of Anatomy, Physiology and Human Biology, The University of Western Australia, Perth, WA, Australia.

**Purpose:** To examine if age-associated changes in the radial peri-papillary capillaries (RPCs) constitute a significant component of glaucoma pathogenesis.

**Methods:** 8 human fetal eyes, (8-40 weeks gestation (WG)), 4 healthy adult eyes (aged 17 to 33), and 12 aged human eyes (aged 40-86 years) were examined using multiple marker immunohistochemistry (wholmounts and transverse sections) with antibodies against CD34, CD39, GFAP, NG2,  $\alpha$ SMA, S100 $\beta$ , and UEA-1 Lectin. Vascular density, astrocyte and pericyte ensheathment, RPC distribution, vascular branching patterns, and CD39 expression were examined using confocal microscopy. RPC ultrastructure was examined using TEM.

**Results:** RPCs were first evident between 18-22WG, in a narrow rim surrounding the optic nerve head and expanded gradually until birth. However, at birth RPC distribution was limited compared to young adult. RPCs showed complete basal lamina and tight junctions between adjacent VECs and were located within a 45 $\mu$ m region from the middle of the NFL and middle of GCL. Pericyte ensheathment was examined ultrastructurally and using NG2 and  $\alpha$ SMA IHC. The frequency of pericyte ensheathment was 75% of that observed in the capillaries of the inner retinal vascular bed. Remarkably, astrocytic ensheathment examined both ultrastructurally and with anti-GFAP and S100 $\beta$  IHC showed a very rare occurrence of astrocytic ensheathment. RPC vascular density index (33% at 32 years compared to 20% at 80 years) and distribution decreased markedly with age. Using threshold intensity analysis, we demonstrated that CD39 expression decreased with age. Importantly, many RPC segments became discontinuous and rheology and blood flow was likely impeded in the most aged specimens.

**Conclusions:** Our novel observation that RPCs have a constitutive paucity of astrocytic ensheathment has implications for their ability

to auto-regulate blood flow in response to neuronal activity. Taken together, our data leads us to suggest that the lack of astrocytic-vascular interactions on the RPCs and their marked atrophy in aging compromises their ability to maintain homeostasis and support neuronal function in 'physiological aging' and contribute to glaucoma pathogenesis. Our findings show a correlation between decreasing RPC vascular perfusion with aging but does not demonstrate causality between vascular changes and GC loss.

**Commercial Relationships:** Tailoi Chan-Ling, None; Samyoul Ahn, None; Mark Koina, None; Samuel J. Adamson, None; Marconi Barbosa, None; Louise Baxter, None; Frank Arfuso, None; Anthony Logaraj, None; George Fatseas, None

**Support:** National Health and Medical Research Council of Australia (Nos. 1005730 & 571100), the Baxter Charitable Foundation, the Alma Hazel Eddy Trust and the Rebecca L. Cooper Medical Research Foundation

**Program Number:** 3345 **Poster Board Number:** B0128

**Presentation Time:** 11:00 AM–12:45 PM

### **Swept-Source OCT Angiography (OCTA) of Subjects with Retinal Vein Occlusions**

Sun Young Lee<sup>1</sup>, Douglas Matsunaga<sup>1</sup>, Jack Yi<sup>1</sup>, Mary K. Durbin<sup>2</sup>, Carmen A. Puliafito<sup>1</sup>, Amir H. Kashani<sup>1</sup>. <sup>1</sup>Ophthalmology, USC Eye Institute, Los Angeles, CA; <sup>2</sup>Advanced Development, Carl Zeiss Meditec, Inc, Dublin, CA.

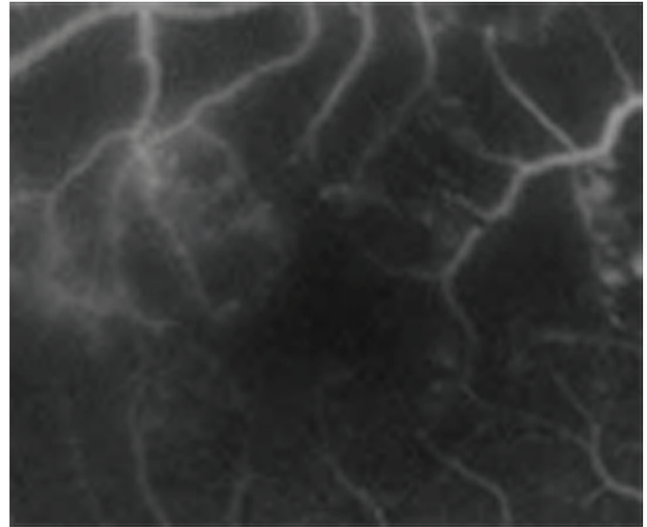
**Purpose:** To assess the retinal vasculature in patients with retinal vein occlusion (RVO) using OCTA.

**Methods:** Cross-sectional, observational study of subjects with RVO. All subjects underwent complete ophthalmic examination and had a confirmed diagnosis of RVO. Data was acquired using a Cirrus high-speed 1050 nm SS-OCT prototype system (100,000 kHz) and a 840 nm SD-OCT prototype system (67,500 kHz)(Carl Zeiss Meditec, Dublin, CA) on 3x3mm sections of the macula and compared to conventional fluorescein angiography (FA). Retinal vasculature was assessed in three retinal slabs consisting of the superficial retina (inner limiting membrane to superficial inner plexiform layer), middle retina (deep inner plexiform layer to superficial outer nuclear layer) and outer retina (deep outer nuclear layer to external limiting membrane). The vasculature was reconstructed using a phase and intensity contrast based algorithm and visualized *en face* for comparison with fluorescein angiograms (FA).

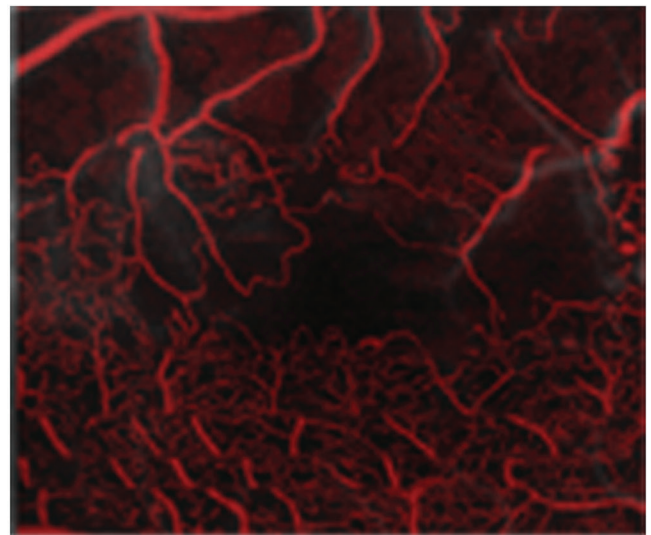
**Results:** OCTA in subjects with RVO (N=5) clearly demonstrates areas of non-perfusion, tortuous or dilated vessels and abnormal capillary morphology. These findings are qualitatively consistent with findings on fluorescein angiography (FA). Dilated and anomalous capillaries were more clearly defined in OCTA than in most frames of fluorescein angiograms. This is particularly evident in late FA images with even mild leakage that tended to washout surrounding capillaries. There were no findings on OCTA that correlated with areas of FA leakage in any case. OCTA demonstrated clear areas of capillary non-perfusion that correlated well with FA findings. Using OCTA, the capillary non-perfusion could be localized to both inner and middle retinal layers in all cases.

**Conclusions:** OCTA provides high-resolution and non-invasive angiograms that correlate well with most findings on fluorescein angiography, except dye leakage. OCTA shows that capillary non-perfusion in RVO involves both inner and middle retinal layers.

## Fluorescein Angiography



## OCT Angiography



**Commercial Relationships:** Sun Young Lee, Carl Zeiss Meditec (F); Douglas Matsunaga, Carl Zeiss Meditec (F); Jack Yi, Carl Zeiss Meditec (F); Mary K. Durbin, Carl Zeiss Meditec (E); Carmen A. Puliafito, Carl Zeiss Meditec (F); Amir H. Kashani, Carl Zeiss Meditec (F)

**Support:** Unrestricted grant from Research to Prevent Blindness, New York, NY 10022

**Program Number:** 3346 **Poster Board Number:** B0129

**Presentation Time:** 11:00 AM–12:45 PM

**Analysis of vessels functionality in retinal vein occlusion treated with intravitreal ranibizumab**

Federico Corvi<sup>1</sup>, Carlo La Spina<sup>1</sup>, Lucia Benatti<sup>1</sup>, Lea Querques<sup>1</sup>, Rosangela Lattanzio<sup>1</sup>, Francesco Bandello<sup>1</sup>, Giuseppe Querques<sup>1,2</sup>.

<sup>1</sup>Ophthalmology, IRCCS, Vita-Salute San Raffaele University, Milan, Italy; <sup>2</sup>University Paris Est Creteil, Centre Hospitalier Intercommunal de Creteil, Creteil, France.

**Purpose:** To investigate the effects of intravitreal injection of ranibizumab on retinal vessels functionality in patients with retinal vein occlusion (RVO).

**Methods:** Consecutive treatment-naïve patients with macular edema secondary to RVO were enrolled in this prospective study. All patients underwent a complete ophthalmic evaluation, including optical coherence tomography and dynamic and static retinal vessel analysis using the Dynamic Vessels Analyzer (DVA) before (baseline), 1 week and 1 month after administration of intravitreal ranibizumab. Investigation of RVO patients were compared to age- and sex-matched control subjects.

**Results:** We included a total of 11 eyes of 11 patients with ME secondary to RVO (10 men; mean age 56.8±13.3 years). In RVO patients, dynamic analysis showed a significant increase of mean venous dilation from +2.46±1.03% at baseline to +3.96±1.3% at 1 week (p=0.001). At 1-week mean maximum venous and arterial dilations did not differ from control subjects. Static analysis showed a mean overall significant decrease of CRAE and CRVE from baseline to 1 week (from 174.8±22.5MU to 167.2±26.7MU [p=0.04], and from 228.4±20.7MU to 217.3±22.8 [p=0.0002]). Mean CRAE in healthy control subjects was 175.9±10.45MU, not significantly different from baseline, week-1 and month-1 of RVO eyes. Conversely, mean CRVE was 195.5±9.91 MU in healthy control subjects, significantly different from baseline, week 1 and month 1 of RVO eyes. By considering only each single occluded quadrant in the 11 RVO eyes (for a total of 29 quadrants), mean CRAE significantly decreased at 1 week (from 102.3±19.7MU to 192.7±21.6MU [p=0.003]). Mean CRVE for occluded quadrants significantly decreased at both 1 week and 1 month (from 136.4±24.5MU to 123.5±24.7MU [p<0.0001]). By considering only the non-occluded quadrants (only BRVO, for a total of 15 quadrants), mean CRAE did not change from baseline to week-1 and month-1 (from 101.8±14.2MU to 100±15.6MU and to 103.2±15MU [p=0.9]). Similarly, mean CRVE for non-occluded quadrants did not change from baseline to week-1 and to month-1 (126.1±12MU to 123.2±13.4MU and to 124.1±10.9MU [p=0.9]).

**Conclusions:** Using DVA in patients with RVO we found that intravitreal ranibizumab increased veins dilation (dynamic analysis), and had a vasoconstrictive effect on both arteries and veins, especially in the occluded quadrants (static analysis).

**Commercial Relationships:** Federico Corvi, None; Carlo La Spina, None; Lucia Benatti, None; Lea Querques, None; Rosangela Lattanzio, None; Francesco Bandello, ALIMERA (C), ALLERGAN (C), BAYER (C), FARMILA-THEA (C), GENETECH (C), HOFFMAN-LAROCHE (C), NOVAGALI PHARMA (C), NOVARTIS (C), SANOFI-AVENTIS (C), SCHERING-PHARMA (C); Giuseppe Querques, ALCON (C), ALIMERA (C), ALLERGAN (C), BAUSCH AND LOMB (C), BAYER (C), NOVARTIS (C), OPHTHOTECH (C)

**Program Number:** 3347 **Poster Board Number:** B0130

**Presentation Time:** 11:00 AM–12:45 PM

**Evaluation of choroidal and retinal vasculature network in patients with retinitis pigmentosa using optical microangiography**

Kasra Attaran-Rezaei<sup>1</sup>, Qinqin Zhang<sup>2</sup>, Jennifer R. Chao<sup>1</sup>, Yanping Huang<sup>2</sup>, Ruikang K. Wang<sup>2</sup>. <sup>1</sup>Ophthalmology, University Of Washington, Seattle, WA; <sup>2</sup>bioengineering, university Of Washington, Seattle, WA.

**Purpose:** Retinitis pigmentosa (RP) is a heterogeneous group of hereditary retinal diseases that result in progressive loss of rod and cone photoreceptors. The ocular blood circulation has been shown to be altered in RP in many experimental and clinical studies. Optical coherence tomography (OCT) based microangiography (OMAG) was recently illustrated for the functional imaging of the microvascular network within the tissue beds. In this study we evaluated the retinal and choroidal microvascular architecture in RP patients using OMAG.

**Methods:** Eight patients (sixteen eyes) with Retinitis Pigmentosa underwent OMAG. OMAG was performed by Zeiss spectral domain OCT-angiography prototype using a 6 mm X 6 mm field of view around macular region. The resulting retinal image was segmented into two layers: the inner retinal layer from the ganglion cell layer to the inner plexiform layer, the deeper retinal layer from the inner nuclear layer to the external limiting membrane. The choroidal image was segmented into choriocapillaris and choroidal layers. The vascular distribution in each layer was depicted as an enface image.

**Results:** In all eyes with RP imaged by OMAG, abnormal microvasculature was detected in both the deeper retinal vasculature layer (from the inner nuclear layer to the external limiting membrane) and choroidal vasculature. A representative result from one patient (left eye) is provided in the figure attached. The OMAG results correlated very well with visual field testing and with reduced choroidal-retina thickness measured by Zeiss SD-OCT-angiography prototype in RP patients.

**Conclusions:** OMAG is a new imaging technique that can evaluate the microvascular network changes in the retina and choroid. OMAG imaging provided detailed, depth-resolved information about the microvasculature changes in Retinitis Pigmentosa patients. OMAG shows loss of normal vessel architecture in the choriocapillaris, choroid and deeper retinal vascular layer. These images corresponded well with published clinical and histological findings.

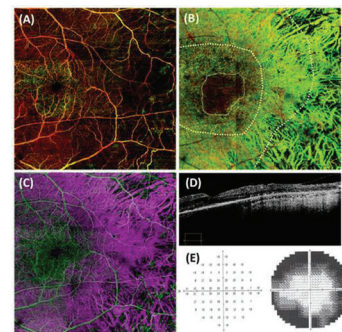


Figure. OMAG visualizes the detailed changes in microvascular architecture within retina and choroid in RP patients. (A) Retinal vasculature showing loss of blood vessels predominately in the deeper retinal layer (inner vessels coded with red, deeper vessels coded with green). (B) Choroidal vasculature showing loss of vessels and pigments in the choriocapillaris and retinal pigment epithelial layers (choriocapillaris vessels coded with red, and choroidal vessels coded with green). (C) Combined enface image of retinal (green) and choroidal (purple) vessels, showing severe loss of peripheral vessels, while the vessels in the central foveal region almost left intact, which correlates very well with (D) OCT structural image and (E) visual field test results.

**Commercial Relationships:** Kasra Attaran-Rezaei, None; Qinqin Zhang, None; Jennifer R. Chao, None; Yanping Huang, None; Ruikang K. Wang, Carl Zeiss Meditec Inc (P)

**Support:** R01EY024158. P30-EY001730. Research to Prevent Blindness Unrestricted Grant.

**Program Number:** 3348 **Poster Board Number:** B0131

**Presentation Time:** 11:00 AM–12:45 PM

**Quantitative optical coherence tomography angiography of the choriocapillaris in central serous chorioretinopathy**

*Scott M. McClintic, Yali Jia, Steven Bailey, Simon S. Gao, David Huang.* Ophthalmology, Casey Eye Institute, Oregon Health & Science University, Portland, OR.

**Purpose:** To determine if optical coherence tomography (OCT) angiography can detect abnormal choriocapillaris blood flow in central serous chorioretinopathy (CSC) compared to a group of normal controls.

**Methods:** Five eyes of 5 study participants with CSC (1 acute, 4 chronic) and 5 eyes of 5 normal controls were scanned with a spectral domain OCT (RTVue XR; 70 kHz scanning speed). Macular angiograms (3x3 mm, 6x6 mm) were obtained using the split-spectrum amplitude decorrelation angiography (SSADA) algorithm, which detects areas of flow in otherwise static tissue. The volumetric angiogram was segmented into inner retinal, outer retinal, and choriocapillaris (10 microns below BM). Color-coded OCT cross sections allowed for representation of both flow and structure (purple = inner retina flow, red = outer retina flow). Vessel density (VD) of the choriocapillaris was the percentage of pixels with detectable flow in the segmented en face choriocapillaris angiogram. Statistical analysis included calculation of mean  $\pm$  standard deviation and the Mann Whitney U test for group comparison.

**Results:** Mean choriocapillaris VD in the 3x3 mm scan was significantly reduced in CSC subjects ( $93.93\% \pm 3.99\%$ ) compared to normals ( $98.64\% \pm 0.61\%$ ),  $P < 0.009$ . *En face* OCT angiograms in normal participants revealed relatively homogenous choriocapillaris flow. CSC subjects had patchy areas of decreased flow, which correlated to regions of hypo-cyanescence on indocyanine green angiography (ICGA). Hyperfluorescent staining and leakage on fluorescein angiography (FA) correlated to most, but not all, areas of reduced choriocapillaris flow.

**Conclusions:** OCT angiography detected reduced choriocapillaris vessel density in CSC subjects compared to normal controls. Patchy areas of reduced flow were visible on *en face* choriocapillaris angiograms. Further study of the choriocapillaris with OCT angiography may improve understanding of CSC pathogenesis.

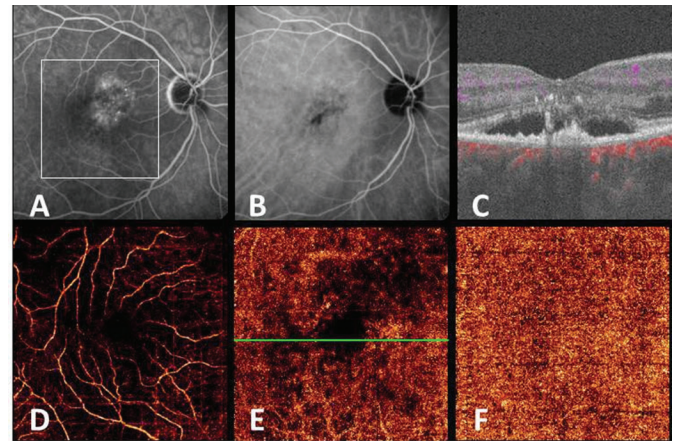


Figure 1. A-E: Chronic CSC participant, including midphase FA (A) and ICGA (B), cross section OCT angiogram at level of green line (C), inner retina OCT angiogram (D), choriocapillaris OCT angiogram (E). F: Choriocapillaris OCT angiogram for normal participant. White box corresponds to sample area of OCT angiogram.

**Commercial Relationships:** Scott M. McClintic, None; Yali Jia, Optovue, Inc. (F), Optovue, Inc. (P); Steven Bailey, None; Simon S. Gao, None; David Huang, Carl Zeiss Meditec, Inc. (P), Optovue, Inc. (F), Optovue, Inc. (I), Optovue, Inc. (P)

**Support:** R01 EY023285, R01 EY024544, DP3 DK104397, RPB, CTSA grant (UL1TR000128), NIH T32 EY23211

**Program Number:** 3349 **Poster Board Number:** B0132

**Presentation Time:** 11:00 AM–12:45 PM

**Optical Coherence Tomography Angiography of chronic central serous chorioretinopathy in elderly patients**

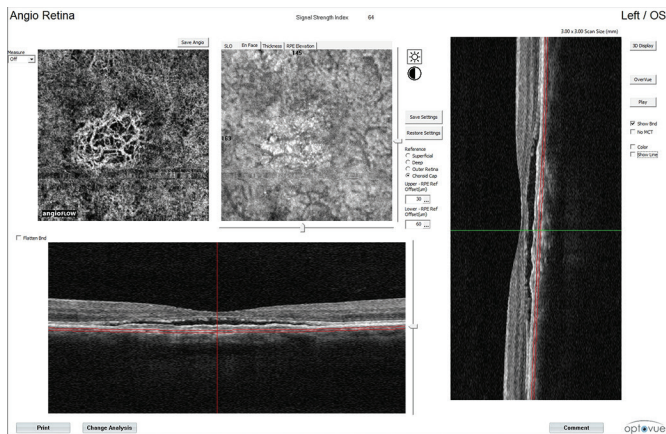
*Mariachiara Morara<sup>2</sup>, Chiara Veronese<sup>2</sup>, Martina Melucci<sup>1</sup>, Filippo Tassi<sup>1</sup>, Nicole Balducci<sup>2</sup>, Antonio Ciardella<sup>2</sup>.* <sup>1</sup>University of Bologna - Policlinico S.Orsola-Malpighi, Bologna, Italy; <sup>2</sup>Policlinico S.Orsola - Malpighi, Bologna, Italy.

**Purpose:** To noninvasively describe the features of retinal and choroidal vascular changes in elderly patients with central serous chorioretinopathy (CSC) with Optical Coherence Tomography Angiography (OCTA).

**Methods:** Cross-sectional, observational study of 10 patients between 55 and 64 years of age with central serous chorioretinopathy. OCTA was performed on 3x3 and 6x6 mm area centered on the fovea. The 3D angiography was segmented in 4 layers: superficial and deep (to show retinal vasculature), outer retina (to identify Choroidal neovascularization) and chorio-capillary.

**Results:** Serous retinal detachment was clearly visualized by OCTA in 10 eyes of 10 patients with CSC. A thin Pigment epithelial detachment (PED), that is difficult to identify with conventional images modalities, was identified in 10 eyes of 10 patients. In 4 patients OCTA detected a distinct choroidal neovascular pattern in chorio-capillary.

**Conclusions:** According to PED morphology in CSC, OCTA allows to detect associated CNV, previously undiagnosed by conventional imaging modalities.



**Commercial Relationships:** Mariachiara Morara, None; Chiara Veronese, None; Martina Melucci, None; Filippo Tassi, None; Nicole Balducci, None; Antonio Ciardella, None

**Program Number:** 3350 **Poster Board Number:** B0133

**Presentation Time:** 11:00 AM–12:45 PM

### Optical coherence tomography angiography (OCTA) detection of choroidal neovascularization (CNV) in chronic central serous chorioretinopathy (CSCR)

Marco A. Bonini<sup>1,2</sup>, Talisa de Carlo<sup>2,3</sup>, Daniela Ferrara<sup>2</sup>, Caroline Bauma<sup>2</sup>, Andre J. Witkin<sup>2</sup>, Elias Reichel<sup>2</sup>, Jay S. Duker<sup>2</sup>, Nadia K. Waheed<sup>2</sup>. <sup>1</sup>Ministry of Education, Brasília, Brazil; <sup>2</sup>Retina, New England Eye Center, Boston, MA; <sup>3</sup>Massachusetts Institute of Technology, Boston, MA.

**Purpose:** To evaluate the sensitivity of spectral-domain OCTA in detecting CNV associated with pigment epithelial detachment (PED) in chronic CSCR

**Methods:** Eyes that were previously diagnosed with chronic CSCR and that were receiving multimodal imaging for suspicion of CNV were prospectively recruited to receive additional ancillary imaging test using the prototype AngioVue OCTA software on a commercially-available spectral-domain OCT (SD-OCT) device to generate en-face images (OCT angiograms) (Optovue, Inc, Fremont, CA). Orthogonal registration and merging of two consecutive image sets is used to obtain 3x3mm and 6x6mm OCT angiograms. The OCTA software was used to delineate a region of interest with an inner boundary at the level of the outer aspect of the outer plexiform layer and an outer boundary at the level of Bruch's membrane. An "artifact removal" function within the software was utilized to subtract retinal vessel shadowing from the OCT angiogram. Qualitative analysis was performed based on OCTA findings of vascular flow representing CNV and CNV appearance. Cross-sectional OCT b-scans were used to determine CNV location relative to the retinal pigment epithelium and Bruch's membrane.

**Results:** Twenty-seven eyes of 23 consecutive CSCR patients demonstrating chronic CSCR and associated PED were enrolled in this study. Dye based angiography showed clear evidence of CNV in all eyes. From the eight eyes with confirmed CNV, five eyes had well-circumscribed vessels in the CNV area and three eyes showed poorly-circumscribed vessels on OCTA. Manual displacement of the outer boundary segmentation line down to the choriocapillaris level on correlating OCT b-scans was performed and allowed delineation of CNV boundaries in 6/8 eyes (75%) and feeder vessel in 2/8 (25%) eyes with CNV.

**Conclusions:** We demonstrated agreement between non-invasive OCTA and dye-based angiography in detecting CNV associated with chronic CSCR. This study suggests that OCTA may be a viable

alternative to dye based angiography in the diagnosis of CNV in patients with chronic CSCR. Since OCTA is completely non-invasive it could at least be considered a first step in establishing the diagnosis. Future studies with larger sample size are needed to improve our understanding of this diagnostic method, and provide further information to validate this imaging technique in clinical practice.

**Commercial Relationships:** Marco A. Bonini, None; Talisa de Carlo, None; Daniela Ferrara, None; Caroline Bauma, None; Andre J. Witkin, None; Elias Reichel, None; Jay S. Duker, Carl Zeiss Meditec (C), Optovue (C); Nadia K. Waheed, None  
**Support:** This work was supported in part by a Research to Prevent Blindness Unrestricted grant to the New England Eye Center/ Department of Ophthalmology, Tufts University School of Medicine, National Institutes of Health (NIH) contracts R01-EY011289-28, R01-EY013178-12, R01-CA075289-16, Air Force Office of Scientific Research contracts FA9550-10-1-0551 and FA9550-12-1-0499, DFG contracts DFG-HO-1791/11-1, DFG Training Group 1773, DFG-GSC80-SAOT, and Massachusetts Lions Club.

**Program Number:** 3351 **Poster Board Number:** B0134

**Presentation Time:** 11:00 AM–12:45 PM

### DYNAMIC AND STATIC VESSELS ANALYSIS IN PATHOLOGIC MYOPIA

Lucia Benatti<sup>1</sup>, Carlo La Spina<sup>1</sup>, Federico Corvi<sup>1</sup>, Giuseppe Querques<sup>1,2</sup>, Francesco Bandello<sup>1</sup>. <sup>1</sup>Ophthalmology, University Vita-Salute San Raffaele, Milan, Italy; <sup>2</sup>Ophthalmology, Centre Hospitalier Intercommunal de Creteil, Creteil, France.

**Purpose:** To investigate retinal vascular anatomy and function in eyes with pathologic myopia by Dynamic Vessel Analyzer (DVA, Imedos, Jena, Germany) in order to explain why these eyes are resistant to diabetes-related changes.

**Methods:** A total of 20 patients with pathologic myopia (20 eyes) were included in the study and compared with 20 eyes of age and sex matched healthy control subjects. Complete ophthalmologic examination, dynamic and static retinal vessels analysis were performed on all participants.

**Results:** The dynamic analysis of eyes stimulated by flickering light highlighted a mean arterial dilation of  $2.44 \pm 1.59\%$  in myopic eyes and  $3.28 \pm 1.76\%$  in healthy eyes ( $p=0.189$ ). Mean venous dilation was  $3.45 \pm 1.82\%$  and  $4.45 \pm 2.72\%$ , respectively ( $p=0.409$ ). In myopic patients, the static retinal analysis showed a mean Central Retinal Artery Equivalent (CRAE) of  $171.6 \pm 24.3$ , a mean Central Retinal Vein Equivalent (CRVE) of  $199.5 \pm 27.73$  and a mean arteriovenous ratio (AVR) of  $0.86 \pm 0.01$ . In control subjects mean CRAE was  $190.3 \pm 11.93$  and mean CRVE  $215.7 \pm 13.30$  (both  $p = 0.0031$  vs respective measurements in myopia) and mean AVR was  $0.88 \pm 0.04$  ( $p=0.913$ ). An inverse relationship between axial length and CRAE and CRVE ( $r^2 = 0.18$ ,  $p=0.0051$  and  $r^2 = 0.18$ ,  $p=0.0165$ , respectively) was evidenced by the linear regression analysis.

**Conclusions:** Static and dynamic vessels analysis showed that myopic eyes have retinal posterior pole vessels with reduced diameter, but with normal function. The vascular network at the posterior pole does not appear to play a key role in determining chronic state of ischemia involved in the relative protection from diabetic retinopathy.

**Commercial Relationships:** Lucia Benatti, None; Carlo La Spina, None; Federico Corvi, None; Giuseppe Querques, ALIMERA (C), ALLERGAN (C), BAUSCH AND LOMB (C), BAYER (C), NOVARTIS (C), OPHTHOTECH (C); Francesco Bandello, ALCON (C), ALIMERA (C), ALLERGAN (C), BAUSCH AND LOMB (C), BAYER (C), FARMILA-THEA (C), GENETECH (C), NOVARTIS (C), PFIZER (C), THROMBOGENICS (C)

**Program Number:** 3352 **Poster Board Number:** B0135

**Presentation Time:** 11:00 AM–12:45 PM

**Optical Coherence Tomography Angiography of Pigment Epithelial Detachment**

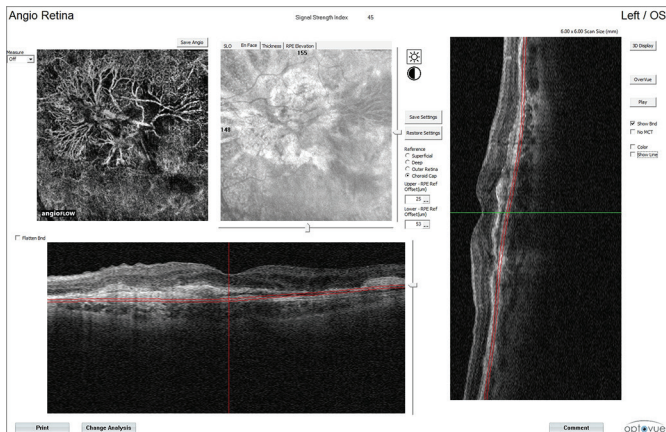
Chiara Veronese<sup>1</sup>, Mariachiara Morara<sup>1</sup>, Martina Melucci<sup>2</sup>, Filippo Tassi<sup>2</sup>, Nicole Balducci<sup>1</sup>, Antonio Ciardella<sup>1</sup>. <sup>1</sup>Policlinico S.Orsola-Malpighi, Bologna, Italy; <sup>2</sup>University of Bologna, Bologna, Italy.

**Purpose:** To noninvasively describe the spectrum of pigment epithelial detachments (PEDs) occurring mainly in age-related macular degeneration (AMD), central serous chorioretinopathy (CSC), inflammatory and iatrogenic retinal disorders with Optical Coherence Tomography Angiography (OCTA).

**Methods:** Observational, cross-sectional study of 34 patients (19 men and 15 women), ranged in age from 50 to 70 years (mean age 63.2 years) with drusenoid, serous, vascularized or mixed PEDs. The instrument used for the OCT images was based on the RTVue XR Avanti (Optovue Inc) and was used to obtain split-spectrum amplitude decorrelation angiography images. OCTA was performed on 3x3 mm and 6x6 mm area centered on the fovea. The 3D angiography was segmented in 4 layers: superficial and deep (to show retinal vasculature), outer retina (to identify Choroidal neovascularization) and chorio-capillary. En face maximum projection was used to obtain 2-dimensional angiograms from the 4 layers.

**Results:** En face OCT angiograms of PEDs showed sizes and locations that were confirmed by fluorescein angiography (FA). OCTA of 34 eyes detected 34 PEDs: vascularized in 21 eyes (61.8%), serous in 7 eyes (20.6%), drusenoid in 4 eyes (11.8%), inflammatory in 1 eye (2.9%) and iatrogenic in 1 eye (2.9%).

**Conclusions:** OCTA provides depth-resolved information and detailed images of PEDs and may offer noninvasive differentiation between various kinds of PEDs.



**Commercial Relationships:** Chiara Veronese, None; Mariachiara Morara, None; Martina Melucci, None; Filippo Tassi, None; Nicole Balducci, None; Antonio Ciardella, None

**Program Number:** 3353 **Poster Board Number:** B0136

**Presentation Time:** 11:00 AM–12:45 PM

**The dark atrophy: an angio-OCT study**

Alessandra Acquistapace, Marco Pellegrini, Marta Oldani, Matteo G. Cereda, Andrea Giani, Vittoria Ravera, Giovanni Staurenghi. Sacco Hospital Eye Clinic, Department of Clinical Science, San Fermo della Battaglia, Italy.

**Purpose:** to evaluate the status of choriocapillaris and choroidal structures using angio-OCT in patients affected by macular atrophy

secondary to age-related macular degeneration (GA) and Stargardt disease (STGDT).

**Methods:** Retrospective study. All the patients underwent a complete ophthalmological examination including blue and green autofluorescence (B-FAF, G-FAF), fluorescein (FA) and indocyanine green (ICGA) angiography, enhanced depth imaging spectral domain optical coherence tomography (SD-EDI OCT) (HRA+OCT Spectralis, Heidelberg Engineering, Heidelberg, Germany) and angio-OCT using AngioVue technologies (Optovue, in).

**Results:** 20 eyes of 10 patients affected by GA and 20 eyes of 10 patients affected by STGDT were included in the study. Mean age was 53,3 for STGDT patients and 76,88 for GA. Atrophy was hypofluorescent in both B-FAF and G-FAF in all the cases. In the early frames FA displayed hyperfluorescence in the atrophic area in 80% of GA and 0% of STGDT patients whereas dark choroid was present in 0% of patients and 90% respectively. ICGA showed, in late frames, hypocyanescence in 95% of STGDT and 16% of GA patients and isocyanescence in 84% of GA patients. At Angio-OCT imaging it was possible to detect a global rarefaction of choroidal layers in 94% of GA patients with no selective loss of choriocapillaris while in STGDT patients loss of choriocapillaris was typically antecedent to the loss of the other layers.

**Conclusions:** SSADA analysis in STGDT patients displayed a selective involvement of choriocapillaris compared to GA population. This finding results in agreement with possible expression of ABCA4 at this level and with previous ICGA studies.

**Commercial Relationships:** Alessandra Acquistapace, None; Marco Pellegrini, Bayer (S); Marta Oldani, None; Matteo G. Cereda, None; Andrea Giani, Novartis Advisory Board (C); Vittoria Ravera, None; Giovanni Staurenghi, Alcon Laboratories, Inc (C), Allergan, Inc (C), Bayer (C), Boehringer (C), Genentech (C), GlaxoSmithKline (C), Heidelberg Engineering (C), Novartis Pharmaceuticals corporation (C), Novartis Pharmaceuticals corporation (S), Optos, Inc (C), Optos, Inc (C), Optovue (S), Roche (C), Zeiss (C), Zeiss (S)

**Program Number:** 3354 **Poster Board Number:** B0137

**Presentation Time:** 11:00 AM–12:45 PM

**OCT angiography provides insights into choroideremia pathology**

Nieraj Jain, Yali Jia, Simon S. Gao, Michael J. Gale, David Huang, Richard G. Weleber, Mark E. Pennesi. Casey Eye Institute, Oregon Health & Science University, Portland, OR.

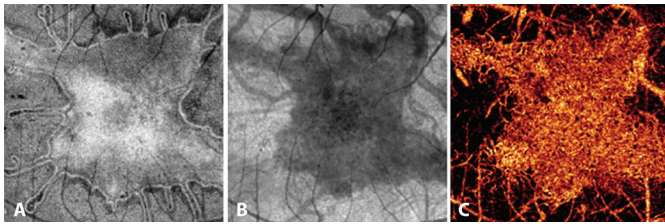
**Purpose:** To explore choriocapillaris (CC) alterations in choroideremia (CHM) with optical coherence tomography (OCT) angiography and to correlate these findings with deficits in retinal structure and visual function.

**Methods:** This is a prospective study of subjects with CHM, CHM carrier state, and normal controls. Subjects underwent imaging with 70 KHz spectral OCT (RTVue-XR) in 3x3mm and 6x6mm macular areas using the split-spectrum amplitude-decorrelation angiography approach. Segmentation of the CC with en face maximal projection provided a 2 dimensional angiogram. Adaptive optics (AO) images were analyzed with custom cone-counting software to provide a cone density map. Additional structural imaging included fundus autofluorescence and color fundus photography. Visual function was assessed through best corrected visual acuity (BCVA) and microperimetry using a custom 101 point testing grid. Image registration was performed to evaluate the spatial relationship between CC density and structural and functional metrics of the retina and retinal pigment epithelium (RPE).

**Results:** 6 subjects with CHM, 2 carriers, and 7 controls were enrolled. BCVA ranged from 20/20 to 20/30 in affected males and 20/20 to 20/60 in carrier females. Mean age amongst affected males

## ARVO 2015 Annual Meeting Abstracts

and carriers was  $44.5 \pm 15.1$  years. OCT angiography demonstrated regions nearly devoid of CC amongst affected males, and patchy areas of reduced CC density amongst carriers. In affected males, there was strong spatial correlation between CC density, retinal and RPE anatomy, and visual function. Subtle discrepancies were noted at transition zones. Amongst carrier females, there were greater discrepancies. In some carrier eyes, reduced CC density and visual function coincided in areas with apparently normal retinal structure. **Conclusions:** OCT angiography permits *in vivo* CC assessment not previously possible, and demonstrates a spectrum of CC pathology in CHM. Structure-function correlations provide new insights into the disease pathology. This technology offers promising new endpoints for upcoming clinical trials in CHM.



Registered *en face* OCT images in a choroideremia patient demonstrate (A) segmented photoreceptor reflectance; (B) total reflectance depicting the region of intact RPE (central dark region); and (C) OCT angiogram with regional variability in choriocapillaris flow (high flow represented by bright gold; no flow represented by black).

**Commercial Relationships:** Nieraj Jain, None; Yali Jia, Opovue, Inc. (F), Opovue, Inc. (P); Simon S. Gao, None; Michael J. Gale, None; David Huang, Carl Zeiss Meditec, Inc. (P), Opovue, Inc. (F), Opovue, Inc. (I), Opovue, Inc. (P); Richard G. Weleber, U.S. patent no. 8657446 (P); Mark E. Pennesi, Sucampo Pharmaceuticals (C)

**Support:** NIH grants R01 EY023285, R01 EY024544, 1K08 EY0231186-01 (Pennesi), DP3 DK104397, T32 EY23211, P30EY010572 core grant, CTSA grant (UL1TR000128); FFB grants CDA CF-CL-0614-0647-OHSU (Jain), Enhanced CDA (Pennesi); RPB CDA (Pennesi)

**Program Number:** 3355 **Poster Board Number:** B0138

**Presentation Time:** 11:00 AM–12:45 PM

### Evaluation of Age-related Macular Degeneration and Polypoidal Choroidal Vasculopathy using OCT-based Microangiography

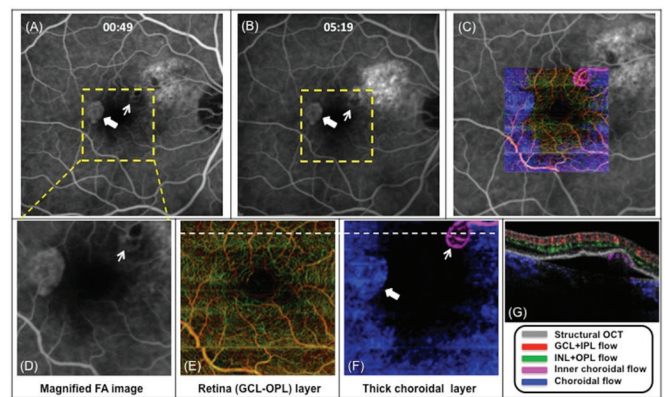
Ruikang K. Wang<sup>1</sup>, Qinqin Zhang<sup>1</sup>, Cecilia Lee<sup>2</sup>, Yanping Huang<sup>1</sup>, Kasra Attaran Rezaei<sup>2</sup>, Richard Munsen<sup>2</sup>, Jennifer R. Chao<sup>2</sup>, James L. Kinyoun<sup>2</sup>. <sup>1</sup>Bioengineering, University of Washington, Seattle, WA; <sup>2</sup>Ophthalmology, University of Washington, Seattle, WA.

**Purpose:** To assess the feasibility and proficiency of OCT-based microangiography (OMAG) in the detection and visualization of vascular involvement at different stages of age-related macular degeneration (AMD).

**Methods:** Twenty patients were recruited, including early stage AMD, geographic atrophy (GA), neovascular AMD and polypoidal choroidal vasculopathy (PCV). Patients were scanned by a Zeiss OCT-angiography prototype with motion tracking. OCT scans centered on the fovea were captured to generate the OMAG images. OMAG images were segmented into 4 layers including the inner (GCL->IPL), deeper (INL->photoreceptor layer) retinal layers, choriocapillaris, and deeper choroidal layer. *En face* images were used to represent angiograms at different layers (coded with different colors for visual purposes).

**Results:** *En face* OMAG images showed overall good agreement with fluorescein angiography (FA). OMAG gave more detailed visualization of vascular networks that were less affected by subretinal hemorrhages. In early stage AMD, small drusen were observed, but retinal vessels seemed the same as for normal subjects. For patients with GA, abnormalities of the RPE layer resulted in the ability to easily observe the choriocapillaris and large choroidal vessels. Feeding and draining vessels were identified in neovascular AMD and PCV. Choroidal neovascularization (CNV) was more demarcated by OMAG as compared to FA due to the late leakage of fluorescein dye which obscures the CNV.

**Conclusions:** OMAG provides depth-resolved and detailed vascular images of AMD. In most cases, proper segmentation is the key to identifying the location of abnormal vessels. Our ongoing studies with OMAG will standardize quantification of the retinal and choroidal vascular layers during the progression of AMD as well as following treatment, particularly with anti-VEGF agents.



PCV of serosanguineous PEDs from 72-year old patient. (A, B) are the early and late phase FA images; (C) The color OMAG image from retina to choroid overlying the FA image; (D) The magnified FA image corresponding to the OMAG images; (E) The vasculature within inner (red) and deeper (green) retinal layer. (F) The vasculature from RPE to choroid layers. (G) The cross-sectional structure image at the position marked by the white line in (E, F) overlying flow image; color coding scheme is shown.

**Commercial Relationships:** Ruikang K. Wang, Carl Zeiss Meditec Inc (F), Carl Zeiss Meditec Inc (P); Qinqin Zhang, Carl Zeiss Meditec (F); Cecilia Lee, None; Yanping Huang, None; Kasra Attaran Rezaei, None; Richard Munsen, None; Jennifer R. Chao, None; James L. Kinyoun, None

**Support:** NEI R01EY024158, Carl Zeiss Meditec Inc, Research to Prevent Blindness.

**Program Number:** 3356 **Poster Board Number:** B0139

**Presentation Time:** 11:00 AM–12:45 PM

### OCT Angiography (OCTA) of Macular Telangiectasia Type 2

John E. Legarreta<sup>1</sup>, Andrew D. Legarreta<sup>1</sup>, Mariana R. Thorell<sup>1</sup>, Qinqin Zhang<sup>2</sup>, Giovanni Gregori<sup>1</sup>, Douglas Matsunaga<sup>3</sup>, Amir H. Kashani<sup>3</sup>, Ruikang K. Wang<sup>2</sup>, Carmen A. Puliafito<sup>3</sup>, Philip J. Rosenfeld<sup>1</sup>. <sup>1</sup>Ophthalmology, Bascom Palmer Eye Institute, University of Miami Miller School of Medicine, Miami, FL; <sup>2</sup>Bioengineering, University of Washington, Seattle, WA; <sup>3</sup>USC Eye Center, Keck School of Medicine, University of Southern California, Los Angeles, CA.

**Purpose:** To evaluate the microvasculature of the central macula in eyes with macular telangiectasis type 2 (MacTel2) using swept-source (SS) and spectral-domain (SD) optical coherence tomography (OCT) angiography.

**Methods:** Subjects were enrolled in a prospective, observational study and evaluated using a high-speed 1050 nm SS-OCT prototype system (100,000 kHz) and a 840 nm SD-OCT prototype system (68,000 kHz). SS-OCT angiography was performed using a 3X3mm raster scan pattern centered on the fovea. In the transverse scanning direction, a single B-scan was comprised of 300 A-scans. Four consecutive B-scans were performed at each fixed position before proceeding to the next transverse position on the retina. A total of 300 B-scan positions located 10 µm apart over a 3 mm distance were sampled. SD-OCT angiography was performed using a 3X3mm and 6X6mm raster scan pattern. In the 3X3 raster scan, four consecutive B-scans, each comprised of 245 A-scans, were performed in the transverse scanning direction. In the 6X6 raster scan pattern, the transverse scanning direction was comprised of two consecutive B-scans, each of 350 A-scans. A total of 245 B-scan positions were located 12.4 µm apart over the 3 mm distance, and a total of 350 B-scan positions were located 17.1 µm apart over the 6 mm distance. Algorithms segmented the retina into three layers; an inner retinal layer, a middle retinal layer, and an outer retinal layer. The vascular distribution in each layer was depicted as an en face image. En face OCT angiographic images were compared to early and late phase fluorescein angiography (FA) images.

**Results:** OCT angiography imaging was performed on 35 subjects (67 eyes) with MacTel2. In all MacTel2 eyes, an abnormal microvasculature was detected. In early stages of MacTel2, these abnormal vessels appeared to reside predominantly in the middle retinal layers or deep capillary plexus. The earliest manifestations included dilation and truncation of the microvasculature in the temporal juxtafoveal location. As the disease progressed, all retinal layers became involved and demonstrated abnormal vascular patterns.

**Conclusions:** OCT angiography can be performed with both SS-OCT and SD-OCT instruments and provides rapid, non-invasive, high-resolution, depth-resolved images comparable to or even better than conventional fluorescein angiography in eyes with MacTel2.

**Commercial Relationships:** John E. Legarreta, Carl Zeiss Meditec, Inc (F); Andrew D. Legarreta, Carl Zeiss Meditec, Inc (F); Mariana R. Thorell, Carl Zeiss Meditec, Inc (F); Qinqin Zhang, Carl Zeiss Meditec, Inc (F); Giovanni Gregori, Carl Zeiss Meditec, Inc (F), Carl Zeiss Meditec, Inc (P); Douglas Matsunaga, Carl Zeiss Meditec, Inc (F); Amir H. Kashani, Carl Zeiss Meditec, Inc (F); Ruikang K. Wang, Carl Zeiss Meditec, Inc (F); Carmen A. Puliafito, Carl Zeiss Meditec, Inc (F); Philip J. Rosenfeld, Carl Zeiss Meditec, Inc (F)

**Support:** Research Support from Carl Zeiss Meditec, Inc

**Program Number:** 3357 **Poster Board Number:** B0140

**Presentation Time:** 11:00 AM–12:45 PM

**Optical Microangiography Imaging in a Patient with Retinal Vasculopathy from Susac's Syndrome**

Raghu C. Mudumbai<sup>1</sup>, Qinqin Zhang<sup>1,2</sup>, Chieh-Li Chen<sup>1,2</sup>, Yanping Huang<sup>1,2</sup>, Ruikang K. Wang<sup>1,2</sup>. <sup>1</sup>Ophthalmology, University of Washington Eye Institute, Seattle, WA; <sup>2</sup>Bioengineering, University of Washington Medical Center, Seattle, WA.

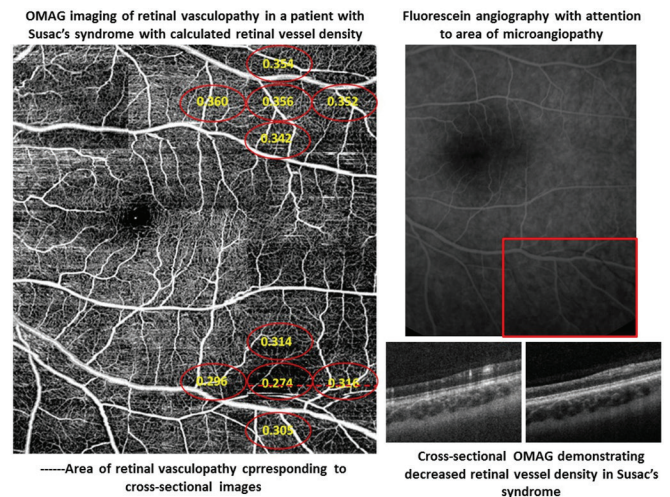
**Purpose:** To investigate the retinal perfusion differences in a patient found to have a focal retinal vasculopathy from Susac's syndrome using optical microangiography (OMAG).

**Methods:** A 22 year old woman was diagnosed with Susac's syndrome based on a triad of intracranial lesions including involvement of the corpus callosum on MRI, hearing loss, and vision loss. Ophthalmic examination showing 2 cotton wool spots along the inferotemporal arcade OS. HVF indicated an area of a deep defect superiorly OS that was symptomatic to the patient. Fluorescein angiography (FA) indicated a corresponding filling defect in the arterioles without signs of pseudo-emboli consistent with Susac's syndrome.

The patient's retina was scanned with a 67 kHz Cirrus 5000 HD-OCT based angiography prototype system with motion tracking (Zeiss, Dublin, CA) with a 6 mm x 6 mm field of view to provide 3D OMAG retinal microvascular maps. Using proprietary semi-automatic segmentation software, retinal OMAG images were segmented into 3 layers including Inner retinal layer (ganglion cell + inner plexiform layer), middle retinal layer (inner nuclear + outer plexiform layer) and outer retinal layer (outer nuclear + photoreceptor layer). Enface maximum projection was used to represent angiograms at different layers (coded with different colors for visual purpose).

**Results:** Results showed strong correlation between OMAG and the area of retinal non-perfusion identified by FA. Quantitative analysis of the retinal vessel density (the ratio of retinal vessel area over the area evaluated) indicated a sharp drop in the retinal perfusion of the effected zone compared to the surrounding retina. Comparison of the retinal hemifields also indicated a significant difference between the effected zone and the corresponding area in the opposite hemifield. Cross sectional analysis of retinal perfusion zones indicated diffuse loss of both the inner and outer retinal layers, slightly more pronounced in the middle retinal vessels. See figure.

**Conclusions:** OMAG is able to provide additional information that cannot be obtained with FA that quantifies the severity of non-perfusion as well as cross sectional analysis of retinal layer vasculature involvement. OMAG may be a useful modality to characterize the retinal vasculopathy of Susac's syndrome.



**Commercial Relationships:** Raghu C. Mudumbai, None; Qinqin Zhang, None; Chieh-Li Chen, None; Yanping Huang, None; Ruikang K. Wang, Carl Zeiss Meditec (F), Carl Zeiss Meditec (P) **Support:** Research To Prevent Blindness



**Program Number:** 3358 **Poster Board Number:** B0141

**Presentation Time:** 11:00 AM–12:45 PM

**Constriction of retinal arterioles by 3 and 12 months after gastric bypass surgery in type 2 diabetic patients with poor glycaemic control**

Troels Brynskov<sup>1,2</sup>, Caroline Schmidt Laugesen<sup>1</sup>, Torben Lykke Sørensen<sup>1,2</sup>. <sup>1</sup>Department of Ophthalmology, Roskilde Hospital, Roskilde, Denmark; <sup>2</sup>Faculty of Health Science, University of Copenhagen, Copenhagen, Denmark.

**Purpose:** Gastric bypass surgery induces large metabolic changes and rapidly normalizes blood glucose levels in type 2 diabetic patients, but the consequences for the retinal vasculature are largely unknown. We hypothesized that gastric bypass surgery could lead to early changes in retinal vessel diameters – a marker of endothelial function previously associated with the development of diabetic retinopathy – in a cohort of patients with type 2 diabetes.

**Methods:** This was a prospective, observational clinical study. A total of 53 eyes of 53 patients underwent thorough ophthalmologic baseline examination 2 weeks before Roux-en-Y gastric bypass surgery. All patients had type 2 diabetes. The examinations were repeated at 3 and 12 months after the surgery. Retinal arterioles and venules were semi-automatically measured using the “big-six”-method on a fundus picture taken of the optic disk. We analyzed the data using paired t-tests. Subgroup analysis was performed using a linear regression model adjusting for sex, age, change in body mass index, change in mean arterial pressure (MAP), baseline HbA1c, and change in HbA1c.

**Results:** Higher HbA1c at baseline led to a decrease in the central retinal artery equivalent (CRAE) of 2.2  $\mu\text{m}$  per % HbA1c ( $\pm 2.0$ ,  $p=0.04$ ) at 3 months and of 3.0  $\mu\text{m}$  per % HbA1c ( $\pm 2.4$ ,  $p=0.01$ ) at 12 months. A fall in blood pressure compared to baseline was associated with a decrease in both CRAE ( $p=0.006$ ) and central retinal vein equivalent (CRVE,  $p=0.01$ ) at 3 months but did not reach significance at 12 months ( $p=0.051$  and  $p=0.12$  respectively). All retinal vessel diameter measures for the whole group were unchanged: at 3 months after surgery CRAE had decreased by a mean of 1.3  $\mu\text{m}$  ( $\pm 1.9$ ,  $p=0.17$ ) while CRVE had increased by a mean of 0.59  $\mu\text{m}$  ( $\pm 2.7$ ,  $p=0.66$ ) and the Arterio-Venous Ratio (AVR) decreased by a mean of 0.0042 ( $\pm 0.011$ ,  $p=0.44$ ). At 12 months CRAE decreased a mean of 0.95  $\mu\text{m}$  ( $\pm 2.2$ ,  $p=0.39$ ), CRVE decreased a mean of 2.2  $\mu\text{m}$  ( $\pm 2.7$ ,  $p=0.12$ ) and AVR increased a mean of 0.0015 ( $\pm 0.011$ ,  $p=0.79$ ).

**Conclusions:** Patients with poorer glycaemic control as measured by HbA1c at baseline experienced an early and sustained constriction of the retinal arterioles in the first year after gastric bypass surgery. This is an encouraging finding, as other longitudinal studies have identified arteriolar constriction as an early marker for improvement in diabetic retinopathy.

**Commercial Relationships:** Troels Brynskov, None; Caroline Schmidt Laugesen, None; Torben Lykke Sørensen, None

**Support:** Fight for Sight, Denmark

**Clinical Trial:** SJ-205

**Program Number:** 3359 **Poster Board Number:** B0142

**Presentation Time:** 11:00 AM–12:45 PM

**Assessment of Macular Circulation in Patients With Retinal Vasculitis using OCT Angiography**

Rasanamar Sandhu, Yali Jia, Liang Liu, Neal V. Palejwala, Eric B. Suhler, Thomas S. Hwang, David Huang, Phoebe Lin. Casey Eye Institute, Oregon Health Sciences University, Portland, OR.

**Purpose:** A feature of OCT angiography is its ability to provide quantitative estimate of retinal blood flow by calculating vessel density. This study examines macular blood flow using OCT

angiography in eyes with angiographically active retinal vasculitis compared to normal eyes.

**Methods:** Adult patient with retinal vasculitis were imaged with fluorescein angiography (FA) and OCT angiography with 70 kHz OCT, using the split-spectrum amplitude decorrelation angiography algorithm (SSADA). A 3 x 3 mm angiogram centered at the fovea was obtained by projecting the flow signal internal to the RPE in the *en face* orientation. Parafoveal vessel density was defined as percentage of pixels with detectable flow signal in a 1mm-wide ring surrounding the fovea (Fig. 1A). The choriocapillaris vessel density was calculated as a percentage of pixels with detectable flow signal within 10 microns external to the RPE in the 3x3mm area.

**Results:** 5 patients (7 eyes) with angiographically active retinal vasculitis were included in the study. Their diagnoses included lupus retinal vasculitis with choroiditis, Behcet's disease, TINU with retinal vasculitis, sarcoidosis, and idiopathic retinal vasculitis. 11 normal eyes were drawn from a previously compiled database. The average vessel density in normal eyes, in a 1mm wide parafoveal ring (Figure 1A), was 87.1% (95% CI 83.9-90.2). In eyes with retinal vasculitis, the average parafoveal vessel density (see Figure 1B for example) was significantly lower, at 79.8% (95% CI 76.3-83.4,  $p=0.006$ ). We also imaged choroidal blood flow in the patient with lupus vasculitis and choroiditis. Her choriocapillaris vessel densities were 83.3% and 83.6% in the right and left eyes, respectively, compared to 96.3% (95%CI 94.0%-98.5%) in normal eyes ( $n=7$ ).

**Conclusions:** Patients with retinal vasculitis have significantly lower parafoveal vessel density compared to normal eyes, as measured by OCT angiography. Lower parafoveal vessel density was noted even in patients who had only peripheral vasculitis on FA. This technique shows promise as a possible biomarker for determining disease activity, and gauging treatment response in patients with retinal vasculitis.

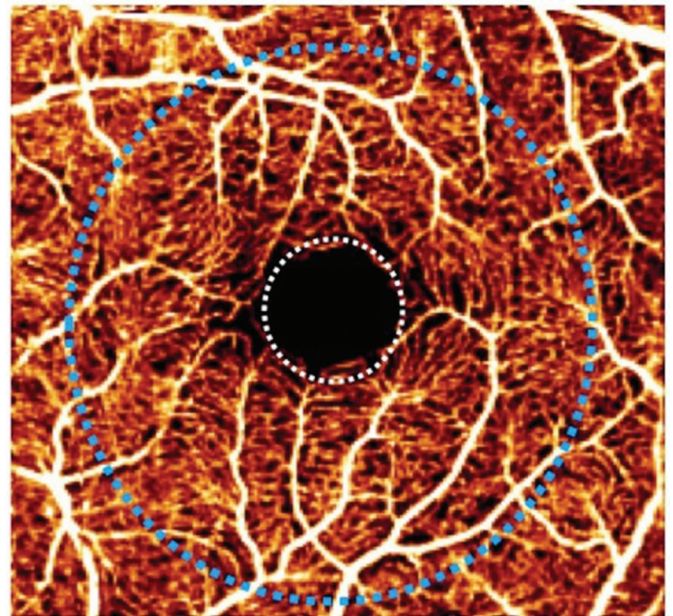


Fig1A: OCT angiography of a normal eye. The circles demarcate the 1mm-wide parafoveal ring where vascular density was measured.

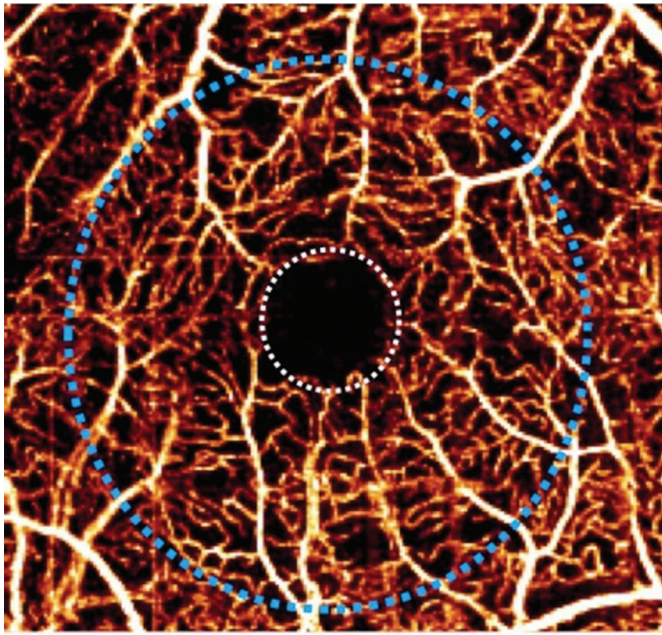


Fig1B: OCT angiography of a patient with lupus retinal vasculitis, displaying lower parafoveal vascular density.

**Commercial Relationships:** Rasanamar Sandhu, None; Yali Jia, Optovue, Inc. (F), Optovue, Inc. (P); Liang Liu, None; Neal V. Palejwala, None; Eric B. Suhler, None; Thomas S. Hwang, None; David Huang, Carl Zeiss Meditec, Inc (P), Optovue, Inc. (F), Optovue, Inc. (I), Optovue, Inc. (P); Phoebe Lin, None  
**Support:** T32EY023211, R01 EY023285, R01 EY024544, DP3 DK104397, RPB, CTSA grant (UL1TR000128)

**Program Number:** 3360 **Poster Board Number:** B0143

**Presentation Time:** 11:00 AM–12:45 PM

#### Angiography of Peripapillary Retina in Retinal Vasculitis with 70 kHz Spectral OCT

Liang Liu<sup>1,2</sup>, Yali Jia<sup>1</sup>, David Huang<sup>1</sup>, Phoebe Lin<sup>1</sup>, Alex D.

Pechauer<sup>1</sup>, Eric B. Suhler<sup>1</sup>. <sup>1</sup>casey eye institute, Oregon Health & Science University, Portland, OR; <sup>2</sup>Ophthalmology, Peking Union Medical College Hospital, Beijing, China.

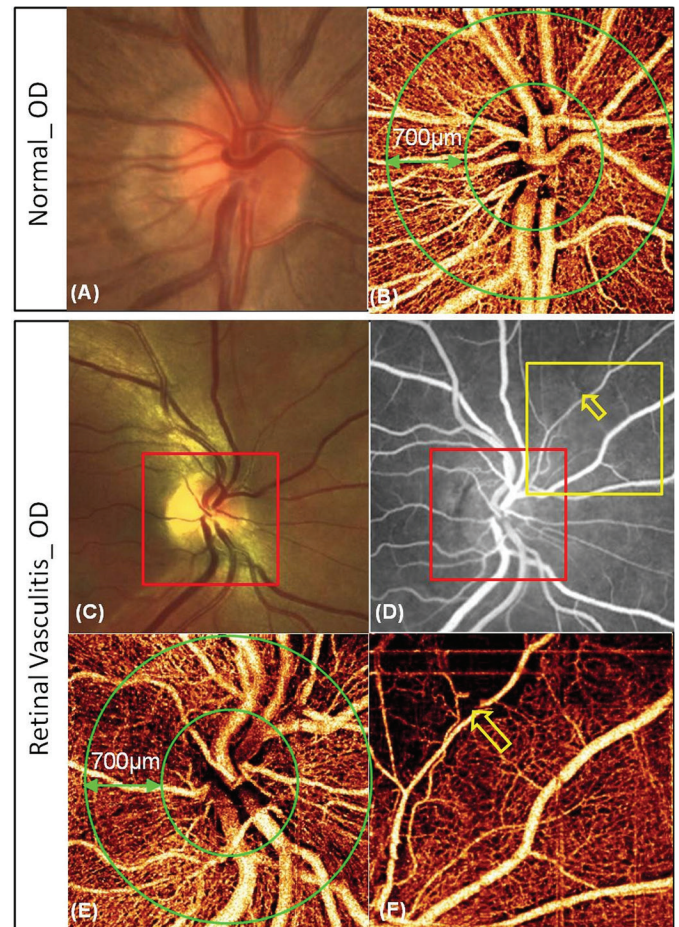
**Purpose:** To compare peripapillary retinal perfusion between normal and retinal vasculitis subjects using a commercially available optical coherence tomography (OCT) system

**Methods:** Each study participant was imaged using a 3x3 mm angiography scan by a high-speed (70 kHz) 840 nm spectrometer-based OCT system. The split-spectrum amplitude decorrelation angiography (SSADA) algorithm was used to compute angiograms. The peripapillary retinal flow index and vessel density were calculated in the 700µm wide annulus extending outward from the optic disc boundary. The flow index was defined as the average decorrelation value on the retinal angiogram in the annulus region. The peripapillary retinal vessel density was defined as the percentage area occupied by vessels. Mann–Whitney test was used to compare these perfusion variables between vasculitis patients and normal subjects

**Results:** The study included 7 normal(7 eyes) and 4 retinal vasculitis patients(5 eyes). In the normal eye, a dense microvascular network around disc was visible on OCT angiography (Fig. B). This network was visibly attenuated in the vasculitis eyes, and focal capillary dropout was detected (Fig. E, F). In normal participants, the population variability of peripapillary retinal flow index and vessel

density was 6.5% and 1.5% coefficient of variation (CV) respectively. In the vasculitis participants, the peripapillary retinal flow index was  $0.085 \pm 0.005$  (mean  $\pm$  SD), which was significantly less ( $P < 0.05$ ) than that of the normal group ( $0.094 \pm 0.006$ ). The vessel density in the vasculitis participants was  $85.2\% \pm 1.3\%$  (mean  $\pm$  SD), which was significantly less ( $P < 0.01$ ) than that of the normal group ( $90.9\% \pm 1.3\%$ )

**Conclusions:** High quality OCT angiograms of peripapillary retina could be obtained in both normal and retinal vasculitis participants. Retinal vasculitis reduction in peripapillary perfusion could be visualized as focal defects and quantified as flow index and vessel density. OCT angiography could be useful in the clinical evaluation of retinal vasculitis.



Results from a normal eye(A, B) and a retinal vasculitis eye(C,D,E,F). The 3x3mm peripapillary *En face* OCT angiogram(E) of the region indicated by the red square in C and D, the microvascular network was reduced compared with normal eye(B). The supranasal OCT angiograms(F) of the region indicated by the yellow square in D, the yellow arrow shows focal capillary dropout in the vasculitis eye(F)

**Commercial Relationships:** Liang Liu, None; Yali Jia, Optovue, Inc (F), Optovue, Inc (P); David Huang, Carl Zeiss Meditec, Inc (P), Optovue, Inc (F), Optovue, Inc (I), Optovue, Inc (P); Phoebe Lin, None; Alex D. Pechauer, None; Eric B. Suhler, None  
**Support:** R01 EY023285, R01 EY024544, DP3 DK104397, RPB, CTSA grant (UL1TR000128).

**Program Number:** 3361 **Poster Board Number:** B0144

**Presentation Time:** 11:00 AM–12:45 PM

**Optical Coherence Tomography Angiography of the Peripapillary in Response to Hyperoxia**

Alex D. Pechauer<sup>1</sup>, Yali Jia<sup>1</sup>, Liang Liu<sup>1</sup>, Simon S. Gao<sup>1</sup>, Chunhui Jiang<sup>2</sup>, David Huang<sup>1</sup>. <sup>1</sup>Ophthalmology, Oregon Health & Science University, Portland, OR; <sup>2</sup>Department of Ophthalmology, Eye and ENT Hospital, Fudan University, Shanghai, China.

**Purpose:** Compare the peripapillary perfusion in healthy subjects before and after hyperoxia using a commercially available optical coherence tomography (OCT) system.

**Methods:** Participants were imaged after a 10 minute exposure to normal and then hyperoxic breathing conditions. One eye of each subject was scanned twice by a high-speed (70 kHz) 830 nm wavelength spectrometer-based OCT system. The optic disc region was scanned using a 3x3 mm volumetric scan. The split-spectrum amplitude decorrelation angiography (SSADA) algorithm was used to compute 3D angiograms. Horizontal and vertical-priority scans were registered and merged to obtain one motion-corrected angiogram (Fig 1). The flow index (FI) was the average decorrelation value of the peripapillary on the *en face* angiogram. The vessel density (VD) was the percent area occupied by vessels in the peripapillary.

**Results:** Six healthy participants were scanned. The FI at baseline was  $0.108 \pm 0.011$  (mean  $\pm$  SD), which was significantly more ( $P = 0.001$ , T-test) than hyperoxia ( $0.099 \pm 0.011$ ). There was a significant difference ( $P = 0.007$ , T-test) in VD between baseline ( $95.9 \pm 2.23$ ) and hyperoxia ( $93.3 \pm 3.43$ ). Repeatability coefficient of variation (CV) for baseline FI was 5.75% and for VD 1.67%. The reproducibility CV for baseline FI and VD was found to be 11.1% and 1.14%, respectively. Each participant had a large variation in between-day autoregulatory response (Fig 2). The hyperoxia induced average percent change relative to the baseline mean had a reproducibility CV of 44.7% for FI and 75% for VD.

**Conclusions:** Using SSADA OCT we have shown that peripapillary microvasculature blood flow can be measured under both normal and hyperoxic conditions using a commercially available OCT system. The decrease in peripapillary perfusion in response to an increase in oxygen partial pressure provides further evidence of retinal autoregulation. The autoregulatory response varied between days.

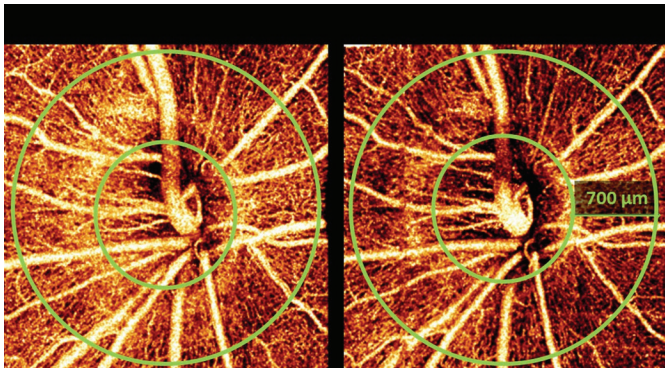


Fig. 1. Angiograms at baseline (A) and hyperoxia (B). Image (B) shows a 17% decrease in flow index and a 4% decrease in vessel density.

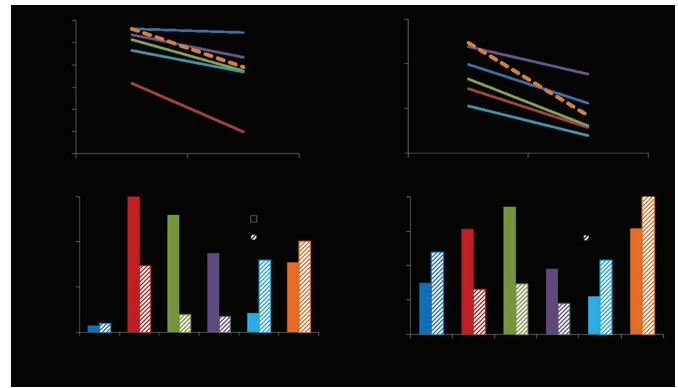


Fig. 2. Vessel density (A) and flow index (B) average from each subject. Percent change in vessel density (C) and flow index (D) during hyperoxia at day one and two.

**Commercial Relationships:** Alex D. Pechauer, None; Yali Jia, Optovue (F), Optovue (P); Liang Liu, None; Simon S. Gao, None; Chunhui Jiang, None; David Huang, Carl Zeiss Meditec (P), Optovue (F), Optovue (I), Optovue (P)

**Support:** R01 EY023285; R01 EY024544; DP3 DK104397; T32 EY23211; CTSA grant (UL1TR000128); RPB

**Program Number:** 3362 **Poster Board Number:** B0145

**Presentation Time:** 11:00 AM–12:45 PM

**Use of ICG-loaded erythrocytes for choroidal angiography in human, pilot study**

Giulia Caminiti<sup>1</sup>, Susanna Maria Carta<sup>1</sup>, Robert Flower<sup>3</sup>, Luigina Rossi<sup>2</sup>, Mauro Magnani<sup>2</sup>, Maurizio Fossarello<sup>1</sup>, Enrico Peiretti<sup>1</sup>. <sup>1</sup>Eye Clinic, University Of Cagliari, Cagliari, Italy; <sup>2</sup>University, Urbino, Italy; <sup>3</sup>Ophthalmology, University school of Medicine, New York, USA Minor Outlying Islands.

**Purpose:** Evaluation of the safety and efficacy of a new methodology of retinal and choroidal dynamic angiography using human erythrocytes preloaded with indocyanine green dye.

**Methods:** A group of 5 patients with different retinal diseases (3 affected by diabetic retinopathy, 1 affected by central serous chorioretinopathy and 1 with exudative age related maculopathy) and a control group from our team of 3 healthy people with no history of eye diseases underwent to an SLO dynamic ICG angiography, using Heidelberg HRA Spectralis (Heidelberg Engineering).

After a withdrawn of 50 ml of autologous blood, red blood cells (RBCs) were processed in a sterile manner using a specific medical device: the Red Cell Loader (EryDel)<sup>®</sup> with the CE approval.

The procedure consisted in the dialysis of erythrocytes at a high hematocrit (about 70-80%) against a hypotonic saline solution (dialysis buffer) to allow the opening of membrane pores of the RBCs; subsequently RBCs were incubated in the presence of the substance to be encapsulated (ICG). The final step of our loading phase was the resealing process by the restoration of physiological isotonicity. The processing time was about 2 hours.

After the preparation of the RBC loaded with ICG, a bolus of these cells was then reinjected in the antecubital vein of the same withdrawn patient. Different concentrations (from 1 ml to 5 ml) of our RBCs loaded were randomly injected before in the healthy controls in order to explore the best quantity for a good angiography. Before and after the angiography with RBCs loaded, the following parameters were measured: blood pressure, hematocrit.

**Results:** High-speed ICG angiography showed the movement of individual and clusters of ICG-loaded erythrocytes in the retinal and the choroidal vessels. The signal was more visible in the early

frames than in the late frames. None of the patients involved in the study showed any ophthalmic or general adverse events after the intravenous injection of ICG-loaded erythrocytes.

**Conclusions:** This pilot trial suggests that the angiography with the ICG-loaded RBCs is safe and well tolerated, meanwhile is very easy to perform. The methodology should be improved on a higher sample of patients in order to verify the rationality and any future clinical applications.

**Commercial Relationships:** Giulia Caminiti, None; Susanna Maria Carta, None; Robert Flower, None; Luigina Rossi, None; Mauro Magnani, None; Maurizio Fossarello, None; Enrico Peiretti, None

**Program Number:** 3363 **Poster Board Number:** B0146

**Presentation Time:** 11:00 AM–12:45 PM

**Imaging the morphology, rheology and flux of single red blood cells in the living mouse eye without contrast agents**

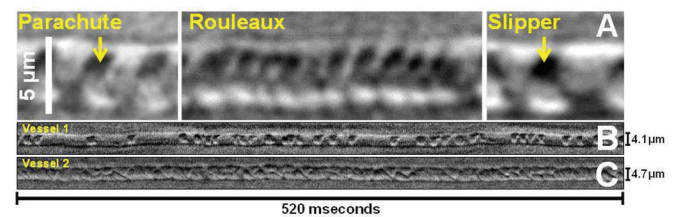
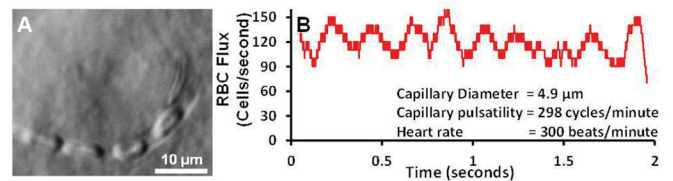
Jesse B. Schallek<sup>1</sup>, Andres Guevara-Torres<sup>2,1</sup>, David R. Williams<sup>1,2</sup>.  
<sup>1</sup>Center for Visual Science, University of Rochester, Rochester, NY;  
<sup>2</sup>The Institute of Optics, University of Rochester, Rochester, NY.

**Purpose:** Adaptive optics scanning light ophthalmoscopy (AOSLO) has been used to measure blood velocity in the living retina by tracking displacement of single blood cells. However, the complex morphology of blood cells has not yet been characterized due to insufficient cell boundary contrast. Here, we use differential imaging to resolve the shape of single red blood cells (RBCs) in the retinal circulation without using contrast agents.

**Methods:** Anesthetized C57BL/6J mice were imaged with an AOSLO using near infrared light. The confocal pinhole in the detection arm was replaced by a split-detector configuration (Scoles et al. 2014 IOVS) where the left and right half of the imaging point spread function was diverted into two, phase-locked photomultiplier tubes (PMT). Differencing the PMT signals provided differential contrast. 2-D point scanning at 25Hz was used to image slow moving RBCs. 1-D point scanning across a vessel at ~31 kHz provided high temporal resolution to image RBCs as they crossed the imaging beam.

**Results:** We observed RBC deformation as cells 6.5 μm in diameter squeezed through the ~4 μm vessel lumen in the smallest capillaries (fig 1a). RBCs maintained a biconcave surface despite a high deformation index (length/diameter) that ranged from 1.55-2.42, similar to those reported in other tissues. 31 kHz 1-D scanning across a vessel imaged a train of erythrocytes that could be counted (RBC flux). Capillaries ranged from 40-161 cells/s (RBC volume of 1.9-7.7 picoliters/s). Capillaries showed robust modulations in RBC flux that corresponded to the heart rate of the anesthetized mouse (~300 beats/minute) demonstrating that pulsatile flow is pervasive in the smallest vessels (fig 1b). The leading and trailing edge of moving RBCs displayed classic “parachute” and “slipper” morphologies (fig 2a) revealing the microscopic rheology of RBC interactions with the vascular endothelium, plasma and glycocalyx. Capillaries showed heterogeneity in RBC packing density despite having similar velocity and size (fig 2bc).

**Conclusions:** This near infrared approach provides new hemodynamic information in capillaries while mitigating phototoxic exposure and obviating the need for blood contrast agents that may alter hemodynamics. Future studies analyzing the shape of moving RBCs have the potential to provide differential diagnosis in a variety of systemic diseases without requiring a blood draw.



**Commercial Relationships:** Jesse B. Schallek, University of Rochester (P); Andres Guevara-Torres, Canon Inc. (F), University of Rochester (P); David R. Williams, Canon Inc. (F), Canon Inc. (R), Polgenix Inc. (F), University of Rochester (P)  
**Support:** Support: F32 EY023496, BRP EY014375. The Schmitt Program on Integrative Brain Research Postdoctoral Fellowship, and Canon Inc.

**Program Number:** 3364 **Poster Board Number:** B0147

**Presentation Time:** 11:00 AM–12:45 PM

**Conjunctival blood flow velocity in patients with retinal vasculitis assessed with the retinal function imager**

Nicole Stuebiger<sup>1</sup>, Aizhu Tao<sup>2,3</sup>, Wen-Hsiang Lee<sup>2</sup>, Sandra Pineda<sup>2</sup>, Hong Jiang<sup>2</sup>, Jianhua Wang<sup>2</sup>, Janet L. Davis<sup>2</sup>, Delia DeBuc<sup>2</sup>.

<sup>1</sup>Department of Ophthalmology, Charite, University Medicine Berlin, Berlin, Germany; <sup>2</sup>Department of Ophthalmology, University of Miami, Bascom Palmer Eye Institute, Miami, FL; <sup>3</sup>Ophthalmology and Optometry, School of Wenzhou Medical College, Wenzhou, China.

**Purpose:** Because studies of the conjunctival microvasculature have provided sensitive indicators of both systemic and CNS vascular diseases we herein present the feasibility and applicability in diagnostic imaging of conjunctival blood flow (BF) velocity in patients with retinal vasculitis using a commercially available Retinal Function Imager (RFI, Optical Imaging Ltd, Rehovot, Israel).

**Methods:** The RFI is a fundus camera-based device and was developed primarily for imaging the retinal BF velocity. To test the feasibility of using the RFI to assess the BF velocity of the conjunctival microvasculature in retinal vasculitis patients, 12 patients (10 patients with Birdshot Chorioretinopathy; 2 patients with retinal vasculitis of unknown origin) (n=21eyes; m:f=3:9, aged 52.4±12.2years) were recruited and compared with a healthy control group (11 individuals; n=11eyes; m:f=3:8; aged 45.5±10.8years). The temporal conjunctiva was imaged in each subject in one or both eyes by RFI and high-resolution, non-invasive capillary perfusion maps (nCPMs) were assessed in addition. The retinal BF of the right eyes (ODs) was imaged for comparison.

**Results:** In the control group the conjunctival blood flow velocity in ODs was 0.80±0.17mm/s and in the left eyes (OSs) 0.77±0.15mm/s. Comparing these data with the conjunctival BF velocities of the study group, we achieved significant differences. The vasculitis patients disclosed conjunctival BF velocity in ODs of 0.71±0.07mm/s (p<0.001) and a BF velocity in OSs of 0.74±0.06mm/s (p<0.05). In the control group BF velocities of the retinal arteries and veins were 3.67 mm/s and 2.32 mm/s, in the study group 2.57 mm/s (p<0.00006) and 1.56mm/s (p<0.00001), respectively. The microvasculature anatomy revealed by the nCPMs appeared unevenly distributed, and lower number of blood vessels along with lower degree of complexity of their branching patterns were evident when compared with a normal healthy eye.

**Conclusions:** With the RFI we could demonstrate for the first time, that in patients with reduced retinal BF velocity due to retinal vasculitis also the conjunctival BF is significantly impaired and mirror the BF velocity changes of retinal microvasculature. Thus, imaging the conjunctival vasculature with the RFI could offer an easily to assess diagnostic tool in retinal vasculitis patients.

**Commercial Relationships:** Nicole Stuebiger, None; Aizhu Tao, None; Wen-Hsiang Lee, None; Sandra Pineda, None; Hong Jiang, None; Jianhua Wang, NIH (F), RBP (F); Janet L. Davis, None; Delia DeBuc, Department of Defense (F), NIH (F), NIH Center Core Grant (F), US 61/139,082 (P)

**Program Number:** 3365 **Poster Board Number:** B0148

**Presentation Time:** 11:00 AM–12:45 PM

**A pilot study of OCT angiography of iris melanomas**

Alison Skalet<sup>1</sup>, Yan Li<sup>1</sup>, Chen D. Lu<sup>2</sup>, Yali Jia<sup>1</sup>, ByungKun Lee<sup>2</sup>, Joachim Hornegger<sup>3</sup>, James G. Fujimoto<sup>3</sup>, David Huang<sup>1</sup>. <sup>1</sup>Casey Eye Institute, Oregon Health and Science University, Portland, OR; <sup>2</sup>Electrical Engineering & Computer Science, Massachusetts Institute of Technology, Cambridge, MA; <sup>3</sup>Pattern Recognition Lab and SAOT, University Erlangen Nuremberg, Erlangen, Germany.

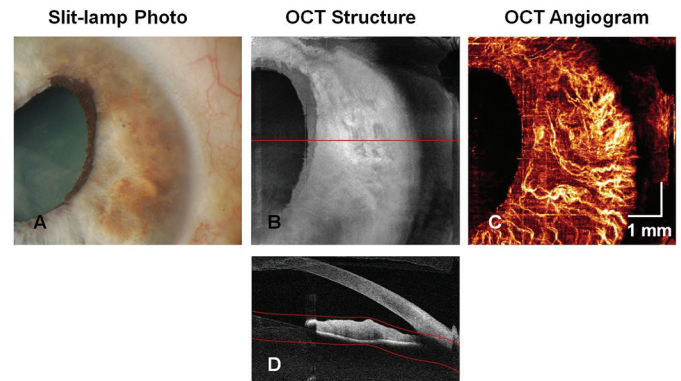
**Purpose:** The purpose of this pilot observational clinical study was to evaluate a new, noninvasive OCT angiography technique in the imaging of iris melanomas.

**Methods:** The eyes of two patients who were diagnosed with iris melanoma were evaluated using a swept-source, anterior segment OCT system operating at 1050 nm wavelength and 100 kHz axial scan repetition rate. Three-dimensional OCT angiography data was acquired over 6 mm x 6 mm regions with scan depth of 5 mm in tissue by using 3 repeated B-scans at 300 raster positions, each B-scan consisting of 300 axial-scans. Horizontal and vertical raster scans were acquired and software motion correction was applied to reduce eye motion and combine the volumes. The split-spectrum amplitude-decorrelation angiography (SSADA) algorithm was used to detect flow and construct angiograms. *En face* OCT angiograms were constructed by maximum flow projection.

**Results:** OCT angiography detected tortuous and disorganized vascular patterns within pigmented iris melanomas in two eyes

(Figure 1). In normal areas of iris outside of the region of tumor involvement, and in normal control eyes, vessels were oriented radially. The tumor vasculature appeared denser than the vessels in unaffected iris areas.

**Conclusions:** OCT angiography at 1050 nm can successfully image vasculature within pigmented iris tumors and may be a less invasive (no injection) alternative to conventional fluorescein angiography for assessing tumors vascularity and monitoring response to treatment. This is the first demonstration of OCT angiography in ocular tumors and further studies are needed.



**Commercial Relationships:** Alison Skalet, None; Yan Li, Carl Zeiss Meditec (P), Optovue (F), Optovue (P); Chen D. Lu, None; Yali Jia, Optovue (F), Optovue (P); ByungKun Lee, None; Joachim Hornegger, Carl Zeiss Meditec (P), Optovue (P); James G. Fujimoto, Carl Zeiss Meditec (P), Optovue (F), Optovue (P); David Huang, Carl Zeiss Meditec (P), Optovue (F), Optovue (I), Optovue (P)

**Support:** Supported by R01EY018184, R01EY023285, UL1TR000128, R01EY011289, a Lloyd Research Endowment Faculty Grant and an unrestricted grant from Research to Prevent Blindness.